On the physical-chemical properties of ceramide C16

and of its mixtures with cholesterol, palmitic acid and cholesteryl oleate

Sofia Leite Souza

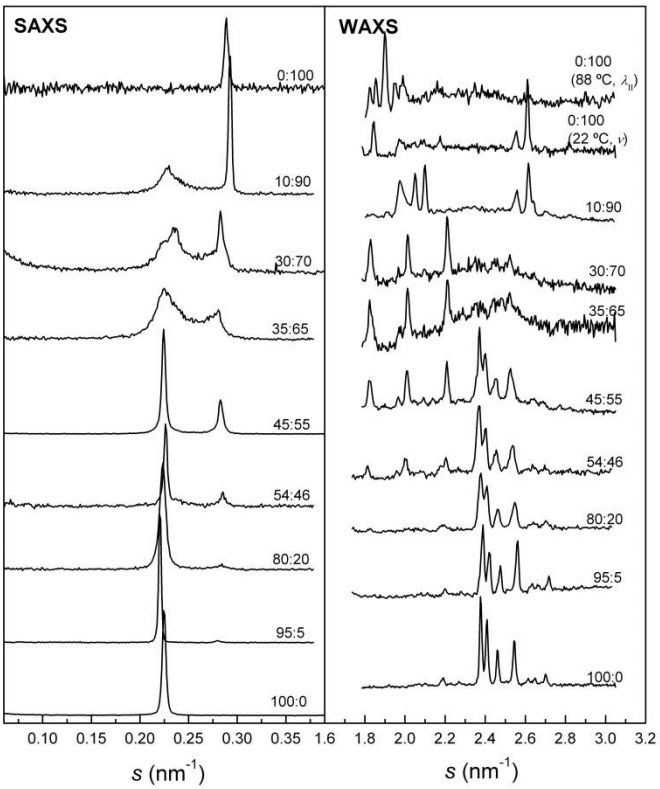

Dissertation presented to obtain the Ph.D degree in Chemistry

Instituto de Tecnologia Química e Biológica | Universidade Nova de Lisboa

Oeiras,
December, 2012

INSTITUTO
DE TECNOLOGIA
QUÍMICA E BIOLÓGICA
/UNL

Knowledge Creation

On the physical-chemical properties of ceramide C16

and of its mixtures with cholesterol, palmitic acid and cholesteryl oleate

Sofia Cristina Fazendas Borges Leite de Souza

Dissertation presented to obtain the Ph.D degree in Chemistry

Instituto de Tecnologia Química e Biológica | Universidade Nova de Lisboa

Oeiras, December, 2012

INSTITUTO
DE TECNOLOGIA
QUÍMICA E BIOLÓGICA
/UNL

Knowledge Creation

Acknowledgements

To the pioneers! To the ITQB and IBET founders. For providing me the infrastructures, equipment, all a complete environment that allowed me to develop this Ph.D. in my country.

To Prof. Eurico, my supervisor, for the opportunity and privilege that he gave me to perform this Ph.D: the laboratory, fully equipped, the financial resources, the culture of the lab. I am grateful for the infinite patience that he had with me. For everything that he taught me. Not only from research, but also, far behind science. Knowledges, culture, treasures that I will carry with me forever.

To Prof. Winchill Vaz, that I had the privilege to meet at the laboratory of Prof. Eurico. For the privilege to have seen such a profound knowledge…For some beautiful scientific discussions.

I tank Prof. James Hamilton for having receiving me at his laboratory in Boston, Massachusetts. For having introduced me to Prof. Donald Small, and Prof. Shipley, to whom I had the privilege of having some discussions. For having stayed there, for all that I have learned.

To Prof. Manuel Carrondo, who gave life to this project, and opened for me the doors of ITQB. To his personal example, and of the team that he had the capacity to build: for the motivation, effort, hard work and enterprise spirit in the attitude towards work.

To my true friend Marta Abrantes, and all my friends and brothers in Christ, for all the help and support.

To my mother, that constantly encouraged me. Without her continuous support, I would have not been able to conclude this Ph.D.

To Josias, my husband. You have always encouraged me to proceed, and have given me your constant support. You have always shared with me the tasks involving the raising of the children, and the house-work. If it was not so, I would have been forced to give up, much time ago…

To my Lord, the God of Abraham, Isaac and Jacob. For continuous support and help. For giving me all the strength that was necessary. For providing, year after year the floaters, that allowed me to not sink.

To Fundação para a Ciência e Tecnologia, for the Ph.D grant BD/6482/2001.

Abstract

Ceramides are known to be involved in cell signalling and are proposed to assist in the formation of laterally segregated membrane domains, known as ceramide rich domains in cell lipid bilayers. The lipid matrix of the *stratum corneum*, the uppermost layer of the skin, which is responsible for its water barrier properties, is mainly composed of ceramides, associated with cholesterol, long chain fatty acids and cholesteryl esters. Despite the importance of ceramides, studies of this lipid class have been relatively neglected, as compared to phosphatidylcolines. In this study both the thermotropism and structure of mixtures of N-palmitoyl-D-*erythro*-sphingosine (C16-Cer) with cholesterol in excess water, were studied by differential scanning calorimetry (DSC) and simultaneous small and wide angle X-ray scattering (SAXS-WAXS). The binary phase diagram of C16-Cer with cholesterol was obtained. One peculiarity observed was the existence of two crystalline compounds of ceramide and cholesterol, one with a lamellar repeat distance of 4.24 nm with a C16-Cer:Cholesterol molar ratio of 1:3, and a second with a lamellar repeat distance of 3.5 nm, with a C16-Cer:Cholesterol molar ratio of 2:3. In subsequent work, the thermotropism and prototropism of ternary C16-Cer, cholesterol and palmitic acid mixtures in excess water were studied, but not to the detail of a phase diagram. Palmitic acid was added in varying molar fractions to a C16-Cer: Cholesterol mixture in the relative molar proportion of 54:46, identical to the *stratum corneum* lipid matrix, and the mixtures were studied at full ionization, pH = 9.0 and full protonation, pH = 4.0. In this study we obtained a general overview of the main phases present, and the phase transformations of the system. Of particular interest, the experimental data also indicated the existence of a third compound, with the attributed stoichiometry of $C16\text{-}Cer_5Cholesterol_4PalmiticAcid_2$. These compounds of C16-Cer, as far as we know, constitute the first direct experimental evidence to date for the existence of laterally organized crystalline structures with amphiphilic lipids able to form bilayers and

cholesterol. This data suggests the existence of the so-called “cholesterol condensed complexes”. The reason for the detection of several lipid-ceramide crystalline aggregates, not observed with other lipids, could be the consequence of the adoption of the L_C state by C16-Cer, in the temperature range of liquid water stability. The solubility of cholesteryl oleate, used as a model cholesterol ester was tested in a mixture of C16-Cer, cholesterol and palmitic acid in excess water, in the same molar proportions of the *stratum corneum* lipid matrix, at the two extreme pH values of 9.0 and 4.0. A combination of several techniques such as DSC, SAXS-WAXS, and magic angle spinning ^{13}C nuclear magnetic resonance, showed that the solubility of cholesteryl oleate in this mixture was negligible at both pH values.

Resumo

As ceramidas são conhecidas por estarem implicadas na sinalização celular, e propostas como sendo funcionais na formação de domínios membranares lateralmente segregados. A matriz lipídica do *stratum corneum*, a camada superficial da pele que é responsável pelas suas propriedades de barreira, é composta maioritariamente por ceramidas, em associação com colesterol, ácidos gordos de cadeia longa e ésteres de colesterol. Apesar da importância das ceramidas, os estudos desta classe lipídica têm sido relativamente negligenciados em comparação com as fosfatidilcolinas. Neste estudo, o termotropismo e a estrutura de misturas de N-palmitoil-D-eritro-esfingosina (C16-Cer) com colesterol em excesso de água, foram estudados por calorimetria diferencial de varrimento (CDV) e difracção de raios X simultaneamente a pequeno e grande ângulo (DXPA-DXGA). Desta forma obtivemos o diagrama de fases binário da C16-Cer com colesterol. Uma peculiaridade observada no sistema, é a existência de dois compostos cristalinos de ceramida e colesterol, um com distância de repetição lamelar de 4.24 nm e com uma razão molar em C16-Cer:Colesterol de 1:3, e um segundo com uma distância de repetição lamelar de 3.5 nm, e uma razão molar em C16-Cer:Colesterol de 2:3. Num trabalho subsequente, foi estudado o termotropismo e o prototropismo de misturas ternárias constituídas por C16-Cer, colesterol e ácido palmítico em excesso de água, mas não com o detalhe necessário para a obtenção de um diagrama de fases. A uma mistura de C16-Cer:Colesterol na proporção molar de 54:46, idêntica à da matriz lipídica do *stratum corneum*, foi adicionado ácido palmítico em proporções molares variáveis, e as misturas foram estudadas em condições de ionização total, pH = 9.0, bem como em condições de protonação total, pH = 4.0. Neste estudo, obtivemos uma visão geral quer das principais fases presentes, quer das transformações de fase do sistema. Entre outras particularidades, os dados experimentais também indicaram a existência de um terceiro composto, para o qual foi obtida a estequiometria de C16-Cer_5Colesterol$_4$ÁcidoPalmítico$_2$.

Estes compostos de C16-Cer constituem, tanto quanto sabemos, a primeira evidência experimental directa da existência de estruturas lateralmente organizadas de natureza cristalina compostas por lípidos anfifílicos formadores de bicamadas e colesterol. Este dado sugere a existência dos chamados “cholesterol condensed complexes”. A razão para a detecção de variados agregados cristalinos lípido-ceramida, não observada com outros lípidos, pode ser uma consequência de a C16-Cer o permitir por se encontrar no estado Lc na gama de temperaturas de estabilidade da água líquida. A solubilidade do oleato de colesterol, usado como éster de colesterol modelo foi testada numa mistura de C16-Cer, colesterol, ácido palmítico em excesso de água, nas mesmas proporções molares da matriz lipídica do *stratum corneum*, aos dois valores de pH extremos de 9.0 e 4.0. A combinação das várias técnicas tais como CDV, DXPA-DXGA, e ressonância magnética nuclear de ^{13}C com rotação da amostra em torno do ângulo mágico, mostraram que a solubilidade do oleato de colesterol nesta mistura era negligenciável a ambos os valores de pH.

Abbreviations

a.u.	arbitrary units
C16-Cer	N-palmitoyl-D-*erythro*-sphingosine
CE	cholesteryl ester
CEs	cholesteryl esters
CER	Ceramide
Ch	Cholesterol
Ch_{aI}	anhydrous cholesterol, polymorph I
Ch_{aII}	anhydrous cholesterol, polymorph II
Ch_{m}	cholesterol monohydrate
ChO	cholesteryl oleate
^{13}C MAS NMR	^{13}C magic angle spinning nuclear magnetic resonance
d	distance between diffracting planes
2D	two-dimensional
3D	three-dimensional
DESY	Deutsches elektronen synchrotron
DPPC	dipalmitoylphosphatidylcholine
DSC	differential scanning calorimetry
egg-Cer	natural ceramide of egg origin
FA	fatty acid
FTIR	fourier transform infrared spectroscopy
GIXD	grazing incidence X-ray diffraction
H_{II}	inverted hexagonal phase
HPLC	High performance liquid chromatography
L_{α}	lamellar liquid crystalline phase
$L_{\alpha1}$	lamellar liquid phase characterized by s = 0.247 nm^{-1}
$L_{\alpha2}$	lamellar liquid phase characterized by s = 0.235 nm^{-1}

L_{β}	lamellar gel phase
$L_{\beta'}$	lamellar gel tilted phase
L_C	lamellar crystalline phase
L_{C1}	pure or almost pure C16 ceramide
L_{C2}	compound phase of C16 ceramide and cholesterol with relative molar proportion 2:3
L_{C3}	compound phase of C16 ceramide, cholesterol and palmitic acid with the relative molar proportion 5:4:2
L_{C4}	compound phase of C16 ceramide and cholesterol with relative molar proportion 1:3
LPP	long periodicity phase
MAS	magic angle spinning
NMR	nuclear magnetic resonance
N-SPHING CER	N-sphingosyl ceramide
PA	palmitic acid
s	reciprocal distance ($s = 1/d$)
SAXS	small angle X-ray scattering
SC	*stratum corneum*
TLC	thin layer chromatography
T_m	temperature of the main phase transition
WAXS	wide angle X-ray scattering

Index

1. Introduction

1.1. Lipids: ceramides, cholesterol, fatty acids and cholesteryl esters

Lipids, together with proteins, nucleic acids, and carbohydrates, are the basic building blocks (molecules) of all living organisms.

Lipid molecules are responsible for numerous biological functions. They are the main constituents of biological barriers forming the cell and the intracellular membranes, are used for storage of cellular energy, and in some living organisms lipids can be found playing roles as biological detergents and as signaling molecules like hormones (for example steroid hormones), prostaglandins, leukotrienes and pheromones.

This thesis will be mainly concerned with one class of lipids, the ceramides (CER), and its mixtures with other lipids. Ceramides have been quite neglected, as compared with other more common amphiphilic lipids, and the work here presented is a contribution for a better understanding of their physical-chemical properties and of the structures adopted by the aggregates formed by ceramides when alone or in mixtures with cholesterol, fatty acids and cholesteryl esters, lipids to which they are often associated in biological systems.

The permeability barriers of virtually all living organisms are obtained with lipids. This can be observed in the root cell membranes, cuticular waxes deposited over the leaf of plants, in the cuticle of insects, in some amphibians, and in the epidermis of the reptiles, birds and mammals[1]. In the context of the present work special attention should be given to the water/xenobiotic barrier property of the epidermis of mammals that is obtained with a mixture of lipids that fills the voids between dead cells, corneocytes, in the uppermost layer of epidermis, the *stratum corneum*. In this mixture, the main lipid classes are

ceramides, cholesterol, long chain fatty acids and cholesteryl esters[2]. If an application is to be found to the work here presented, this will be mainly related to the functions performed by ceramides in the *stratum corneum* (SC) lipid matrix, due to the fact that the systems studied were constituted by a large amount of ceramides, and eventually because some of the ternary mixtures studied present a similarity in the relative molar proportion of cholesterol and long chain fatty acid, that were additionally added.

Ceramides are a subclass of sphingolipids, and are composed of the amino alcohols D-*erythro* sphingosine, dihydrosphingosine or phytosphingosine (including also their C_{16}, C_{17}, C_{19}, and C_{20} homologs), esterified to a long chain fatty acid. In the dihydrosphingosine backbone, the unsaturation is absent, and in phytosphingosine is replaced by a hydroxyl group located at C^4. Ceramides containing additional hydroxyl groups in the fatty acid moiety are also detected in tissue extracts. More complex sphingolipids are obtained from ceramides, such as sphingomyelin, or cerebrosides, by the respective addition of a phosphocholine group or a sugar molecule.

The ceramide used in most studies that compose this thesis is a sphingosine derived ceramide, N-palmitoyl-D-*erythro*-sphingosine, (C16-Cer). The basic structure of this ceramide is presented in Figure 1.1.

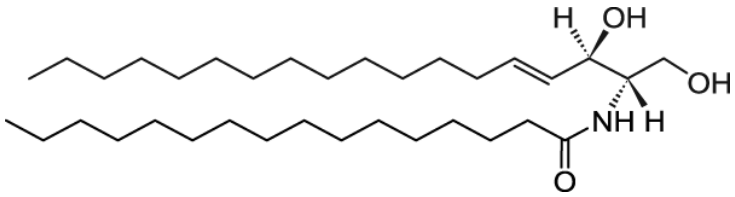

Figure 1.1. - Molecular structure of N-palmitoyl-D-*erythro*-sphingosine.

Cholesterol, 5-cholesten-3β-ol (Ch), (Figure 1.2.), is the major sterol found in mammalian organisms. This lipid is the second most abundant constituent of the SC lipid matrix. Cholesterol is also present in relatively high molecular

fractions in cell membranes[3]. The solubility of Ch in bilayers of glycerophospholipids range from 50 to 66 mol %[4]. This lipid performs important functions in the cell membranes, being essential for viability and cell proliferation[3]. Cholesterol is also a precursor of steroid hormones, bile acids and the active form of vitamin D.

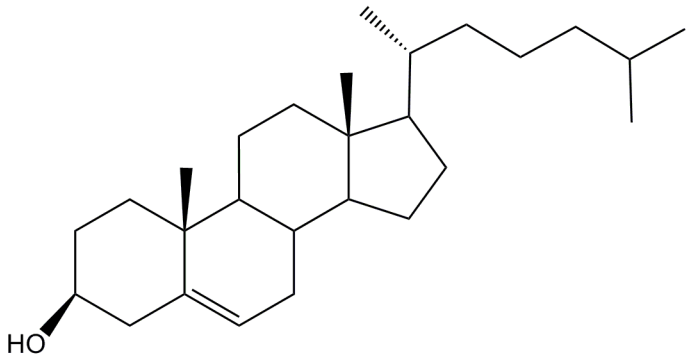

Figure 1.2. - Molecular structure of cholesterol (5-cholesten-3β-ol).

Long chain fatty acids are the third most abundant component of the SC lipid matrix[2]. This lipid class is also present in the plasma and other intracellular membranes, and is frequently found bound to albumin and to lipoproteins. Fatty acids (FA), are the primary energy source in well oxygenated heart, act as second messengers, K^+ channel activators, inhibitors of the binding of plasma low density lipoproteins to receptors, and are uncouplers of oxidative phosphorylation[5]. Since *trans*-membrane translocation ("flip-flop") of long chain fatty acids in phospholipid bilayers occurs rapidly, with a $t_{1/2} \leq 2$ s for un-ionized FA, complex mechanisms (e.g. transport proteins) may not be required for translocation of FA in biological membranes[5]. As predictable, the physical properties of long chain fatty acids and its phase-behavior in the presence of water is strongly dependent on its ionization state (refer to section 1.9 in this chapter).

Cholesteryl esters, (CE), are ubiquitous in biological systems. In higher mammals, they are the form of both cholesterol transport in the blood-stream, and storage in living cells.

1.2. Ceramides: localization and biological function

Ceramides: the main lipid component of the skin barrier

The epidermis of mammals is responsible for their skin water barrier properties. The barrier is located in the SC layer, as become established in the 1950s[6]. Experimental data accumulated during the 80s and 90s of the last century, evidences that the SC lipid matrix plays the major role in this barrier function. This became evident with an experiment in which SC lipid removal with organic solvents, increased transepidermal water loss, TEWL[7], and by the observation that inhibition of enzymes involved in the synthesis of CER, cholesterol and free fatty acid leads to impaired barrier function[8,9]. In the SC lipid matrix, ceramides are the most abundant lipid class[2], performing a key role in this water barrier system.

Ceramides in plasma membrane and the ceramide-rich-domains

In the plasma membrane, ceramides have been established as a second messenger, involved in the induction of cell differentiation, inhibition of cell proliferation, regulation of inflammatory responses, and induction of apoptosis[10].

Studies in model bilayers indicate that lateral phase separation is predominant in mixtures of CER with phospholipids[11]. The involvement of ceramides in cell

signaling in association with the tendency of mixtures of ceramide and phospholipid to form co-existing CER-enriched phase domains, lead to suggestions that CER signaling could occur in specific regions of the cell membrane, like “rafts” and caveolae[12]. In these regions, shingomyelinase would hydrolyze sphingomyelin, generating the CER domains. Additionally, it is claimed by some authors to have evidence for the formation of these CER-enriched membrane domains in cells[13].

Ceramide formation is also known to induce protein-protein contacts, which can modify the activity of the proteins[12], and could be relevant for the signaling function attributed to the CER enriched domains.

In addition, ceramides induce budding of vesicles in model membranes[14], and this ability has also been confirmed in cells, what seems to indicate a functional role in the endocytic pathway[12]. Lateral phase separation of ceramide-rich domains seems to be involved in pathogen internalization and virus budding[13].

1.3. The composition and structural characteristics of stratum corneum

The skin can be divided in several layers, the hypodermis, the dermis, and above it the epidermis (Figure 1.3.), and contains several appendices such as hair follicles, sebaceous and sweat glands. The uppermost layer of the epidermis is called *stratum corneum*. This layer has a thickness of 10-15 μm and is composed of 18 to 21 cell layers[15].

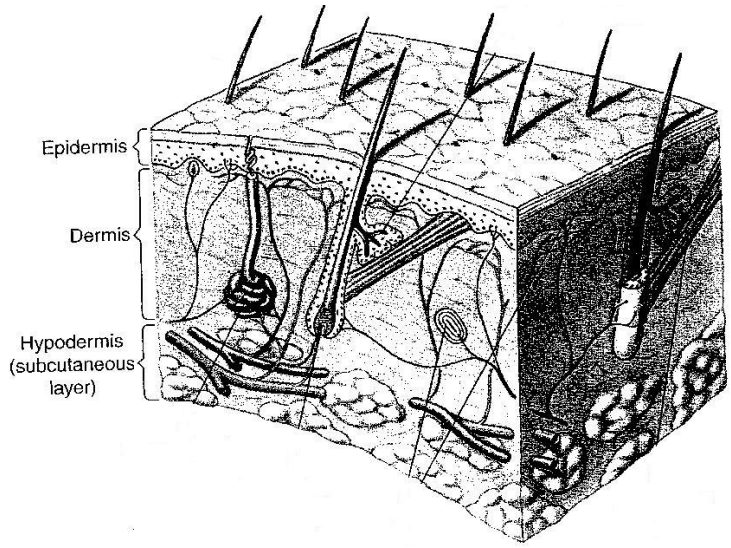

Figure 1.3. - Structure of human skin. *Adapted from ref. 16.*

Stratum corneum, the final product of epidermal differentiation

The SC is the final product of epidermis differentiation. At the basal layer of epidermis, keratinocytes undergo a continuous differentiation program that is completed when these cells finally die, and are called corneocytes. Along the epidermis several layers can be observed, illustrating the steps of keratinocyte differentiation (Figure 1.4.). These layers are respectively, from the deeper to the uppermost: *stratum basale*, *stratum spinosum*, *stratum granulosum*, *stratum lucidum* and finally, the SC[17].

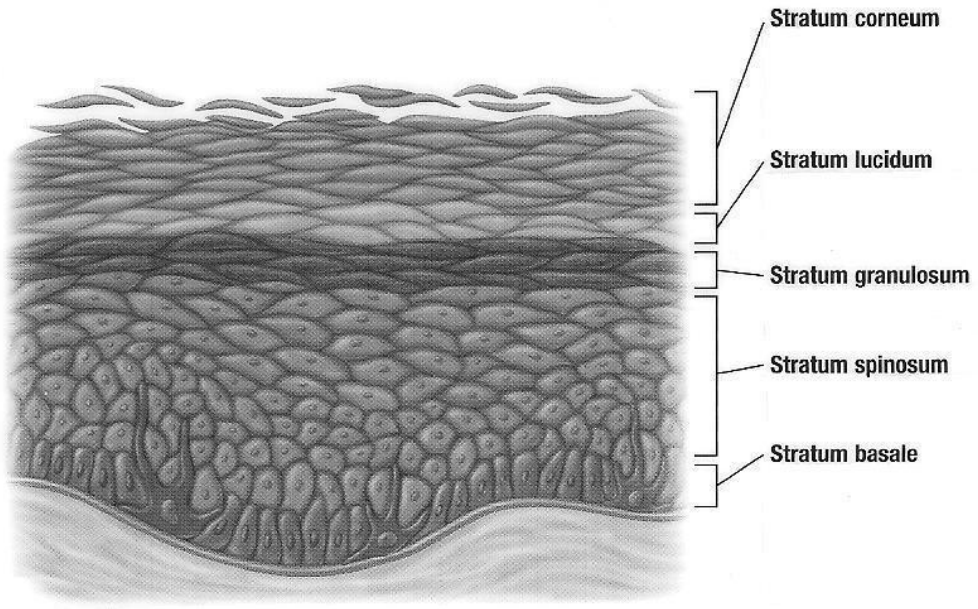

Figure 1.4. - Layers of the epidermis (cross section), evidencing the SC as the uppermost layer. *Adapted from ref. 18.*

This differentiation process is continuously occurring in the body, and layers of "old" SC are continuously shed away from our skin, in a process known as desquamation. It is estimated that a complete cycle of the epidermis, from the basal layer to the SC comprises 20 to 30 days[17].

Along the differentiation process, the keratinocytes will develop cytoplasmatic bundles of tonofilaments and keratin filaments. These cells will start to produce two types of granules: the basophile granules, constituted by keratohyaline, and the lamellar granules, filled with lipid *lamellae*, which are round to ovoid, with a typical diameter ranging from 100 to 400 nm. The lipid content of the lamellar granules will give origin to the SC lipids. At a certain point, their content is released to the extra-cellular space, being composed mainly of phospholipids, glucosylceramides and cholesterol, together with hydrolytic enzymes[2]. The enzymes will process the extruded lipids, which results in a

final lipid composition constituted mainly by ceramides, long chain fatty acids and cholesterol.

Additionally, the keratinocytes will develop in the inner part of the plasma membrane what is identified in electron microscopy as an electron-dense proteic layer with about 10 nm thickness. This membrane is known as the cornified envelope[19]. A covalently bound layer of lipids composed of long chain ω-hydroxyceramides will surround the extra-cellular surface of the corneocytes[20,21]. This layer is known as the lipid envelope.

The result of this differentiation program is the formation of a network of flat dead cells without nuclei, with the cytoplasm filled with keratin, surrounded by a lipid matrix, now constituting the skin uppermost layer, the SC.

pH of the stratum corneum

The *stratum corneum* exhibits an acidic surface pH, while at its base in the inner layer, the pH approaches neutrality[22]. The acidic pH of the SC is essential for the activation of several pH-sensitive enzymes like β-glucocerebrosidase and sphingomyelinase that process some of the lipids extruded by the lamellar granules, to ceramides. Another function proposed for the acidity of the SC, has been to provide antimicrobial properties to the skin. The origin of the SC pH has been attributed to the supply of protons by NHE1, a sodium-proton exchanger expressed by keratinocytes[22] and also to several other mechanisms, such as byproducts of microbial metabolism, lactic acid and lactate from the sweat, the free fatty acids that compose the SC lipid matrix, the progressive desiccation of the SC and/or the generation of *cis*-urocanic acid from filaggrin[22].

Lipid composition of the stratum corneum matrix

The published reports of *stratum corneum* lipid composition are extremely abundant; nevertheless, the proposed amounts for each lipid class are not coincident.

From the determinations in the literature it is reasonable to consider that the SC lipid matrix is composed of ca. 44 mol % of ceramides, 38 mol % of cholesterol and 18 mol % of long chain fatty acids, calculated considering only these three main lipid classes. We have obtained this composition by selecting the three more coincident determinations obtained by three independent research groups using two different experimental techniques, among all the SC lipid determinations published in the literature collected by Wertz and Norlen[23] (Table 1.1.). We chose the determination of Norlen *et al.*[24], in which the relative proportions are reported in weight, and converted to molar composition by using the molecular mass of a C24 ceramide for the ceramide fraction. Some of the more recent SC lipid determinations that appeared after the cited review are also presented in Table 1.1. As can be appreciated, those determinations do not change our conclusions.

Cholesteryl esters are the fourth most abundant lipid class, and small amounts of cholesterol sulfate are also present. This is an unusual composition for a biological membrane. Ceramide occurs in cell membranes only in residual amounts and fatty acids are often present but in much smaller quantities. From these lipids only cholesterol is a common component of cell membranes.

Table 1.1. - Selected *stratum corneum* lipid determinations. The first three determinations are the more similar determinations selected from the compilation of Wertz and Norlen[23]. More recent determinations are also presented. CAD – charged aerosol detector; HPTLC – high performance thin layer chromatography; LSD – light Scattering detector.

Study	Cer (mol%) base $MM_{(cer\ 24)}$ = 650	Ch (mol%) MM = 387	FA (mol%) base $MM_{(C24)}$ = 368	Method
Norlen *et al.,* 1999	44	38	18	HPLC/LSD
Wertz *et al.*, 1987	41	45	15	TLC
Bonté *et al.*, 1997 (a)	41	38	21	TLC
De Paepe *et al.,* 2004	17	49	34	HPTLC
Pappanien *et al.,* 2008	38	34	28	TLC
Merle *et al.*, 2010	48	22	30	HPLC/LSD-CAD

(a) If we discard the unsaturated FA as a contamination, as proposed by Wertz and Norlen[23]

When the ceramides extracted from SC are analyzed by thin layer chromatography (TLC)[25], several chromatographic bands are detected. Figure 1.5. illustrates representative structures of the CER type that constitute each TLC band.

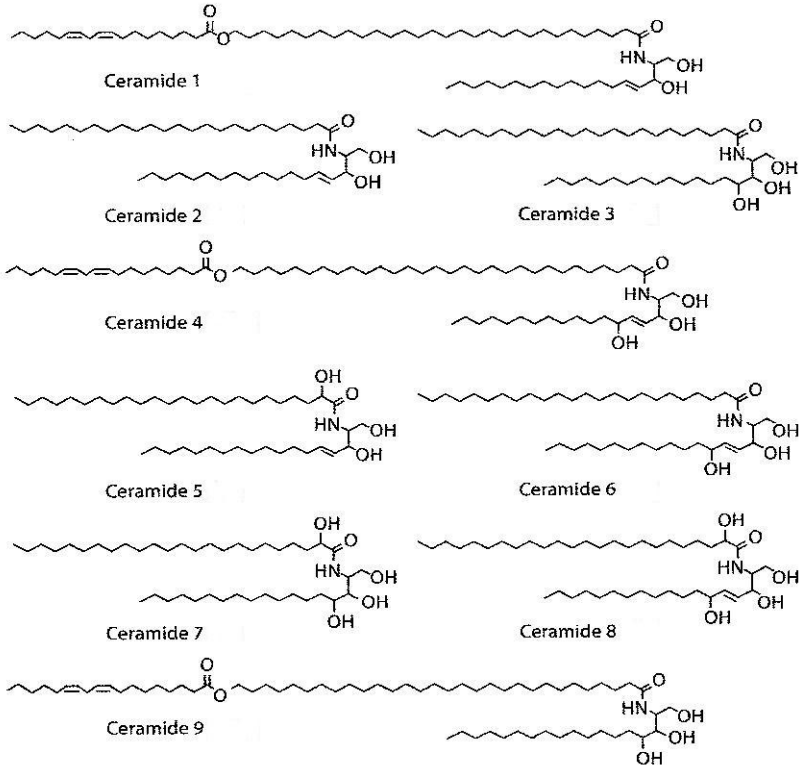

Figure 1.5. - Structures of the ceramides of the *stratum corneum*. *Adapted from ref. 25.*

As can be observed, each fraction contains one structural type of CER. There are combinations of sphingosines or phytosphingosines with amide linked normal or α-hydroxy acids. Within each fraction, there is considerable heterogeneity in aliphatic chain length.

Note the structure of fraction 1, called ceramide [EOS] or acylceramide. In porcine SC, this unusual lipid is composed by a ω-hydroxy-acid containing 30 to 34 carbons, amide linked to sphingosine or dihydrosphingosine. A fatty acid, most often oleic acid, is ester linked to the ω-hydroxyl group. This very long and unusual lipid has attracted much attention, in order to elucidate its biological function. Some authors propose that this CER plays a key role in determining the formation of the *stratum corneum* lamellar phase with 13 nm

thickness[26,27], a long periodicity phase (LPP) detected in SAXS characterizations of intact SC[28,29]. In some studies, the authors only find the 13 nm phase when ceramide 1 is added to certain lipid mixtures, what they interpret as ceramide 1 being necessary for the LPP phase[30,27]. This long chain ceramide has a clearly established role in the formation of the corneocyte lipid envelope[31,32], and the linoleic moiety seems to be required for the transglutaminase 1 enzyme to attach this lipid to the cornified envelope[32].

The long chain fatty acids of the SC, are straight-chain and saturated. The most abundant chain length ranges from C_{24}, C_{26} and C_{28}[2].

Cholesteryl esters are also detected. The amounts reported in the literature range from 2%[19] to 18%[24], depending on the study. This variability is frequent in lipid determinations of tissues, due to contamination. In a study conducted by Wertz and colleagues[33], the lipid composition of the SC was determined in epidermal cysts. Epidermal cysts are isolated structures where the SC grows inside a capsule. Consequently, as no contamination occurs, this lipid determination can correspond more precisely to the true lipid composition of the SC. In this study, a 10 wt % in CEs was obtained, which makes cholesteryl esters as the fourth most abundant lipid class in the SC. Further confirming the relevance of CEs is a study in which the lipid determination of the SC of a reconstructed skin growth *in vitro* has been performed. This SC is obtained from keratinocytes that are growth over a collagen substrate, therefore without subcutaneous or sebaceous contamination, and cholesteryl esters were clearly detected[34].

Organization of the stratum corneum lipids

Electron microscopy following fixation with the stronger oxidizing agent ruthenium tetroxide, shows that the lipids are arranged in defined lamellar layers[35]. Powder diffraction X-ray diffraction studies[28,29], detected in human SC, the presence of two crystalline lamellar phases at 25 ºC. The lamellar repeat distances obtained are 6.4 nm, and 13.4 nm, an unusual thickness for

conventional bilayers. Several theoretical models explaining the molecular arrangement of lipids that give origin to this 13 nm large lamellar phase have been proposed in the literature[36]. Nevertheless, the existence of this LPP phase in native SC is not accepted by all authors, being currently a matter of debate[37,38].

An X-ray signal with lipid origin, located at 4.6 Å, which is characteristic of lipids in the fluid state, is also detected[28], co-existing with the 6.4 and 13.4 nm crystalline lamellar structures.

Empirical approach to the study of the stratum corneum lipid matrix

Several research groups have been studying complex *in vitro* lipid mixtures. These mixtures are designed to mimic the composition, and in some cases the structure of the SC lipid matrix. Recently, these studies have been reviewed in detail by Neubert and colleagues[39]. In a very short resume, we can say that, the lipid compositions used by each group are not exactly the same. Some use skin-extracted ceramides, whereas others opt for natural or synthetic commercially available CER. Some include an additional lipid such as cholesterol sulfate to the three major components, ceramide, cholesterol and saturated fatty acids. Despite these differences and also the diverse preparation methodologies, important information can be derived. It is now clear that using exclusively lipid molecules it is possible to obtain *in vitro* the main structural features of intact SC lipid matrix, discarding the initial proposal by White *et al.*[28], that another component, such as a protein, could be necessary to control the arrangement of the intercellular lipid domains. Several authors have described the presence in their mixtures of the two characteristic lamellar phases, with about 6 nm and 13 nm[40,30]. Also, the rigid organization of the SC lipid matrix at the skin temperature, has been observed in these mixtures by a variety of techniques such as ^{1}H nuclear magnetic resonance (^{1}H-NMR)[41], fourier transform infrared (FTIR)[42,43], and wide angle X-ray scattering[44]. The rigidity of the lipids observed for ternary simpler mixtures

containing only CER, cholesterol and long chain fatty acids has been confirmed in more complex mixtures[45].

Note that the focus of most of these studies has been to replicate *in vitro* the properties of the SC lipid matrix and determine which components, from its complex composition, are the key structural lipids, and not to characterize the physical-chemical properties of the individual lipids, and their mixtures.

In this thesis the thermotropic phase behavior of well-defined binary (containing cholesterol) and ternary (with additional long chain fatty acid) N-sphingosyl ceramide mixtures has been studied. For the binary C16-Cer, cholesterol mixture, a phase diagram in excess water has been obtained. The structural studies by SAXS-WAXS allowed the identification of three stoichiometric aggregates in the mixtures studied, and to our knowledge, this constitutes the first direct experimental evidence of the existence of such structures in lipid bilayers. The miscibility of a model cholesteryl ester, cholesteryl oleate was also accessed, in a ternary mixture of C16-Cer, cholesterol, and long chain fatty acid.

1.4. Thermodynamic properties of pure lipids in water

An important component of the physical-chemical characterization of amphiphilic lipids in excess water is the study of their thermotropic phase behavior.

The main phase transition

A typical heating scan of phosphatidylcholine bilayers in excess water, the amphiphilic lipid for which systematized knowledge was acquired in first place, obtained by differential scanning calorimetry (DSC), is presented in Figure 1.6. This specific lipid type forms bilayers when dispersed in water. As can be appreciated, the main phase transition of an amphiphilic lipid in excess water

is a sharp peak. It corresponds to a phase transition from a state where the lipid chains are more ordered, with a high *trans-gauche* configurational ratio, to a "liquid-crystalline", "fluid" phase[46], in which the hydrocarbon chain configuration is characterized by a lower *trans-gauche* configurational ratio. In this specific example, a first small endotherm is also detected, which corresponds to a pre-transition to the ripped phase, $P_{\beta'}$. This pre-transition is only observed for saturated phosphatidylcholine water mixtures. The maximum temperature of this peak, T_m, is used to characterize the transition, associated with the enthalpy of the transition.

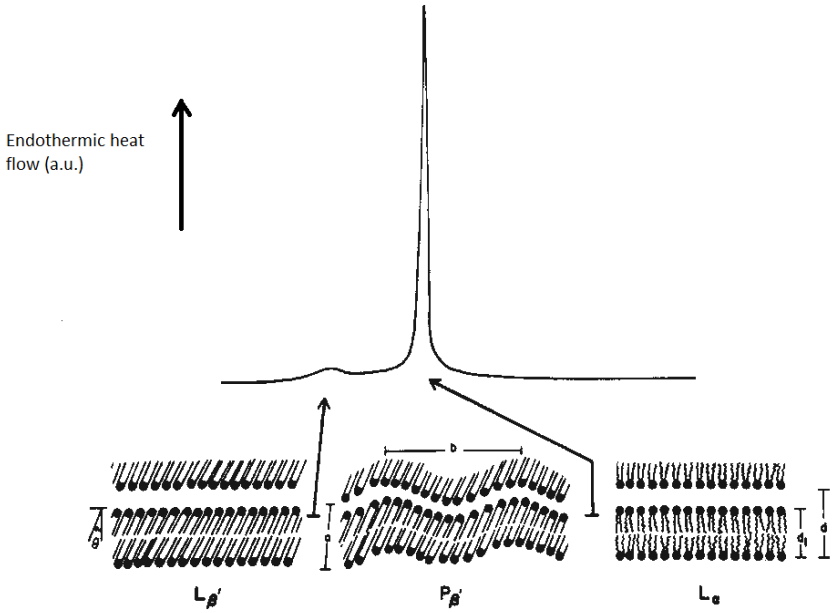

Figure 1.6. - Typical differential scanning calorimetry heating scan of saturated chain phosphatidylcholine bilayers in excess water. The lipid organization correspondent to each temperature region is depicted in the lower portion. $L_{\beta'}$ - Lamellar gel tilted; $P_{\beta'}$ - Rippled gel; L_α - Lamellar liquid crystalline. *Adapted from ref. 84.*

Compilation of T_m, ΔH^o and ΔS, for several lipid types is available[47]. The phase transition temperature is markedly dependent on the hydrocarbon chain length, the nature of the polar head-group, the presence, number and position of double bounds in the hydrocarbon chains, and ionic composition[48].

The main phase transition in lipid bilayers is the result of hydrocarbon chain melting[49]. This has been concluded from two experimental facts. First, the wide angle powder diffraction pattern of saturated phosphatidylcholine bilayers below the temperature of the main phase transition is composed by one or several sharp lines and above T_m by a diffuse line at 4.5 Å, very similar to the profile of fluid long chain alkanes. Additionally, systematic studies of the dependence of T_m with acyl chain length, performed for saturated phosphatidylcholines, showed a systematic increase of the T_m with the increase in acyl chain length.

The phase transition in lipid bilayers has a non-zero transition enthalpy ($\Delta H^o \neq 0$). Nevertheless it occurs in an appreciable range of temperatures. Impurities, and packing imperfections in the solid state, introduce artifact broadening of transition temperatures. With the measurements on purer dipalmitoylphosphatidylcholine (DPPC) samples[50], it become clear that the main lipid bilayer transition is truly first order.

1.5. Structural properties of amphiphilic lipids in water

The amount of water influences the phase behavior of phospholipids. The transition temperature decreases with increasing water content, up to a limit value. The phase behavior of the lipid with variable water amounts can be represented in a diagram as presented in Figure 1.7.

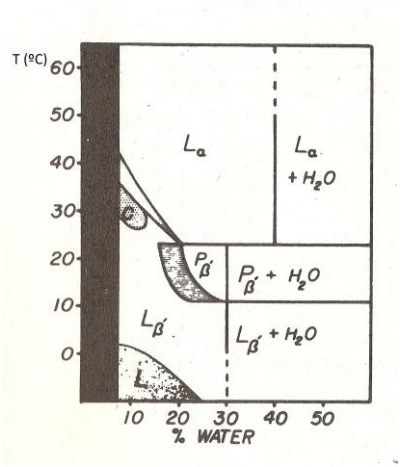

Figure 1.7. - Phase diagram of dimyristoyl phosphatidylcholine as a function of water content. Refer to Figure 1.6., for the meaning of $L_{\beta'}$, $P_{\beta'}$ and L_α. *Adapted from ref. 51.*

Structures formed by amphiphilic lipids in excess water

In mixtures with water, amphiphilic lipids display polymorphism. Several types of lamellar phases have been observed (Figure 1.8.).

The type of structure formed is dependent on the lipid characteristics - headgroup, acyl chain length, presence and position of unsaturations in the hydrocarbon chain - and on other factors, such as temperature, water content, pH, ionic strength and pressure.

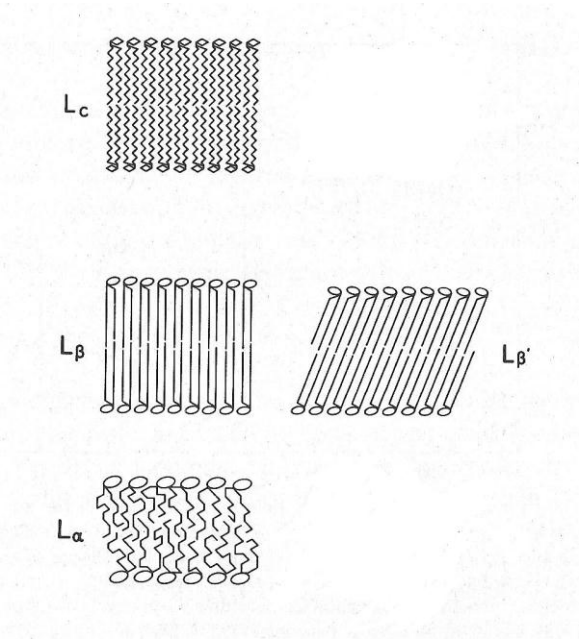

Figure 1.8. – Several lamellar forms of amphiphilic lipids in excess water. L_C - Lamellar crystalline, L_β - Lamellar gel. Refer to Figure 1.6., for the meaning of $L_{\beta'}$ and L_α. *Adapted from ref. 51.*

Lipid-water systems may arrange in a wide range of different structures in addition to the lamellar phases which are the most common in biological systems. Examples of these are the hexagonal phases, in which the lipid molecules form cylinders, either with the polar groups facing outside, H_I, or inside, H_{II}, packed in a hexagonal pattern, and phases of cubic symmetry. Figure 1.9., illustrates both an inverted hexagonal (H_{II}) phase, and an example of a bilayer cubic phase, in which both the lipid and the aqueous phase are continuous (bicontinuous).

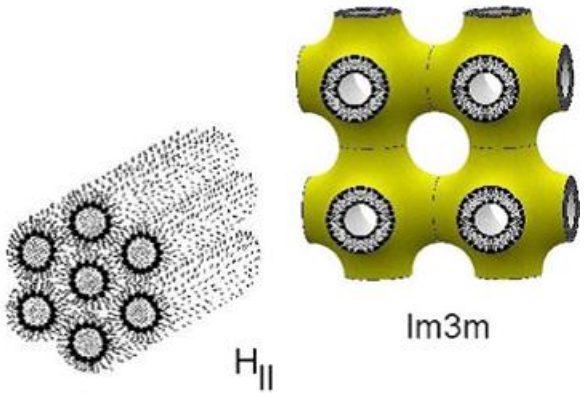

Figure 1.9. - Structure of an inverted hexagonal phase and a bilayer cubic phase. *Adapted from ref. 52.*

A very simplistic but useful model taking only into account geometric considerations can be used to predict and understand the structures formed by the amphiphilic molecules[53]. A surfactant parameter:

$$Ns = \frac{V}{lao} \qquad (1)$$

can be derived in which, V is the volume of the hydrocarbon portion, a_o is the effective area per head group, and l is the length of the hydrocarbon chains. Bilayers may be formed for amphiphilic molecules with a surfactant parameter = 1. Inverted structures, such as inverted hexagonal phases, are formed for surfactant parameter › 1.

Lamellar phases

The nomenclature of lamellar lipid mesophases is composed by a first letter referring to the form of arrangement, and a second describing the acyl chain packing mode (Figure 1.8.).

Lamellar crystalline state: L_C. The molecular lateral packing properties of lipids in this phase are similar to those observed from single crystal X-ray studies of lipids in their anhydrous crystals[51]. Note that this L_C state is not a three dimensional crystal. The several powder pattern wide angle reflections observed in the L_C state, evidence order that propagates only within each bilayer, and not to adjacent bilayers[103].

When the hydrocarbon chains are packed in a precise, crystalline arrangement, each methylene group in the hydrocarbon chain occupies a specific position. As a result, a series of peaks are observed in the X-ray wide angle region that can be indexed in a variety of different cell types. To characterize the amphiphilic lipid mesophase, a specific subcell describing the form of hydrocarbon chain packing is determined. In this acyl chain packing subcell, *a* and *b* describe the two-dimensional lattice perpendicular to the chain axis. Examples of such subcells observed for several lipids are triclinic, orthorhombic and hexagonal[54] (Figure 1.10.). For phospholipids and sphingolipids, were the two hydrocarbon chains are linked to the same molecule, the packing possibilities are restricted. In this case, hybrid subcells have been proposed[55].

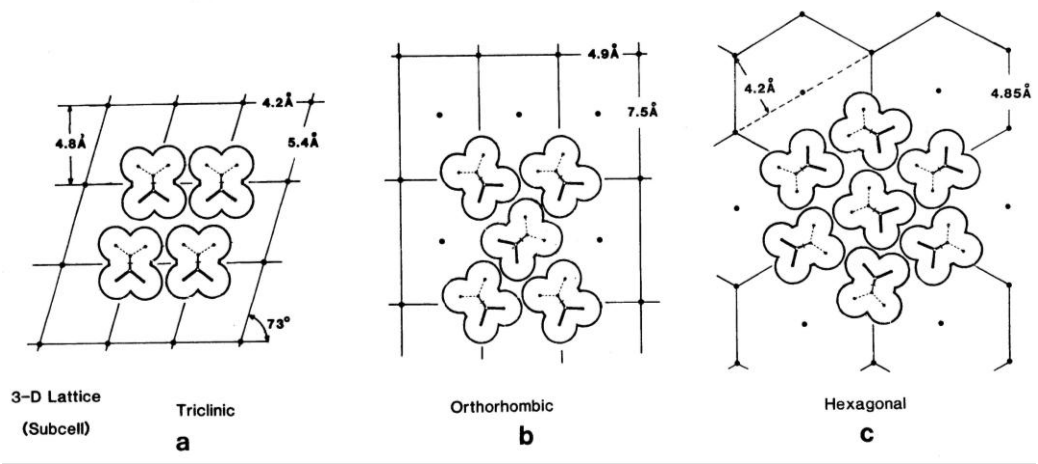

Figure 1.10. - Examples of acyl chain packing modes for several lattices. *Adapted from ref. 54.*

Lamellar gel phase: L_β and $L_{\beta'}$. X-ray powder diffraction of lipid bilayers in the L_β state show a hexagonal or orthorhombic hybrid subcell packing of the hydrocarbon chains. In this state, the molecules are less tightly packed than in the lamellar crystalline phase, and this phase is more hydrated than the L_C. In the $L_{\beta'}$ phase, the acyl chain axes are tilted relative to the normal to the bilayer plane. This tilting is rationalized as resulting from the differences in the in-plane area occupied by the head groups, which is slightly larger than the sum of the in-plane area of the two acyl chains.

Lamellar liquid crystalline state: L_α. In the lamellar liquid crystalline state, the acyl chain configuration is characterized by a low *trans/gauche* configurational ratio. By X-ray powder diffraction, a diffuse broad band centered at 4.5 Å is detected similar to what is observed for fluid aliphatic hydrocarbons. Nevertheless, as become established by ^{2}H NMR, the initial segment of the acyl chains near the interface is relatively ordered. In the L_α state, the bilayer thickness is smaller than in the lamellar gel, and crystalline states, which results from the distortions of the hydrocarbon chains not extended at maximum in the all-*trans* configuration. Most biological

membranes are in the L_α state. The crystalline *lamellae* of the *SC* constitute an exception[28].

1.6. Thermotropism of mixtures of lipids: binary phase diagrams

A phase diagram indicates the phases present in mixtures of all possible combinations of the components, at all temperatures, and the information presented always represents the phase relationships that occur under equilibrium conditions. With a phase diagram we are able to predict, for a given temperature, pressure and chemical composition of the system, which phases are present, their composition and how they interconvert with changes in pressure, temperature or composition. For a system with *C* components the Gibbs phase rule relates the maximum number of phases present at equilibrium, *P*, with the degrees of freedom of the system, *F*:

$$F + P = C + 2 \qquad (2)$$

In the regions of the phase diagram were phase co-existence is observed, it should be noted that there are some specificities in the topology of the mesophases of the two-dimensional (2D) amphiphilic lipid bilayers systems, as compared to three-dimensional (3D) systems. A fundamental difference between lipid bilayers systems and the usual 3D systems is the way in which the phases are dispersed. While to minimize the contribution of the surface tension for the enthalpy of the system the 3D systems tend to decrease the area of interface between the phases in presence this is not the case in lipid bilayers, at least in many of the systems studied[56]. In fact, the size of the distinct patches of lipids is small[56]. In this manner, the two phases do not

occupy separate regions in space, meaning that interfacial effects are expected to be significant.

Types of phase diagrams

The properties of mixtures of substances give origin to different types of phase diagrams. Figure 1.11 illustrates some of the basic types.

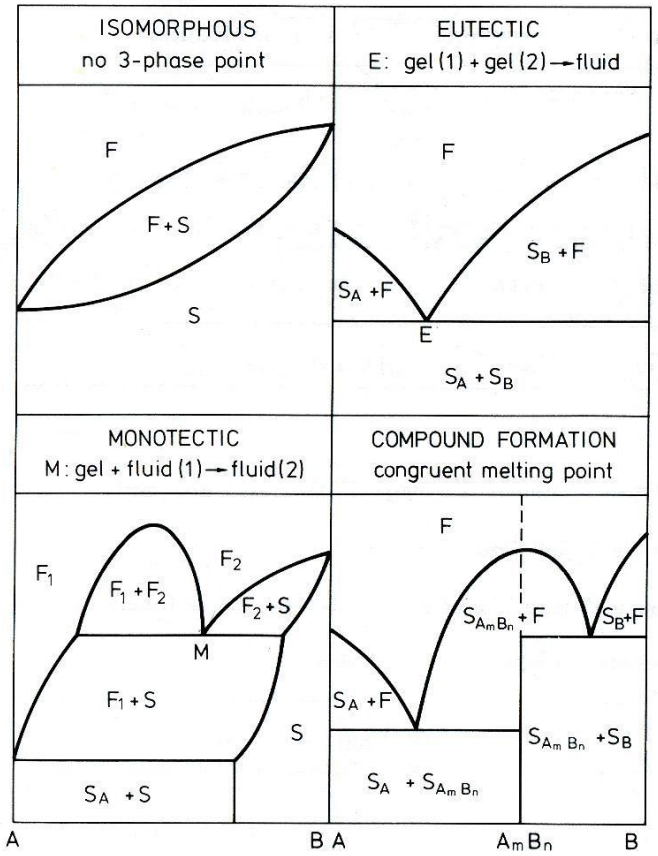

Figure 1.11. - Main types of phase diagrams. F – Fluid; S – Solid; E – Eutectic point; M – monotectic point. *Adapted from ref. 47.*

An isomorphous phase diagram occurs in mixtures where the two components are mutually soluble. The components are soluble in all proportions, both in the liquid and in the solid state. This complete miscibility is only possible if the structure of the pure components is virtually identical[57]. In eutectic systems, the mixture of the two components induces a lowering of the melting point, relative to the melting temperature of each component. The *liquidus* curve passes through a minimum temperature, known as the eutectic point. For this specific composition, the solid mixture melts in a narrow temperature range, in the same manner as a pure compound. In eutectic systems, the components in the liquid state are miscible in all proportions, but miscibility in the solid state is limited. The binary monotectic phase diagrams are included in the eutectic class. The difference relies in the fact that during cooling, two co-existing immiscible liquids give origin to one solid immiscible with another liquid phase whereas in eutectic systems, the liquid melt originates two immiscible solids. Other types of more complex phase diagrams have been described namely the binary peritectic and the binary syntectic.

Congruent transformation

In some phase diagrams a congruent transformation is observed. For a certain specific composition, the mixture melts in an extremely narrow temperature range, and this composition is maintained during the transformation. The mixture behaves exactly as a pure component. When this phenomenon is observed in a phase diagram, the diagram can be separated in two distinct parts, taking the congruent mixture as a single component. In compound phases the molecules are not randomly distributed (solid solution) but each molecular species has a specific position in the crystal lattice. In our thesis work, we have detected several compounds phases, namely for the C16-Cer, cholesterol, and the palmitic acid mixture.

1.7. N-sphingosyl ceramides

The melting point of dry N-24:0-sphingosylceramide and N-16:0-sphingosylceramide is respectively 93-95 ºC[58] and 95.4 ºC[59]. Although the data are only available for two chain lengths, it seems to indicate that for dry ceramides the variation in the melting point with chain length is small. A similar behavior has been observed for other amphiphilic lipids such as phosphatidylcholines, phosphatidylethanolamines, and N-acyl sphingosyl sphingomyelins with saturated acyl chains[47].

To the best of our knowledge there are no single crystal structure models for N-sphingosyl ceramides (N-SPHING CER) in the scientific literature, but there are determinations concerning hydroxylated ceramides. It is not straightforward that the structure of hydroxylated ceramides can be compared to that of N-sphingosyl ceramides. Nevertheless, due to the importance of the structural data obtained from single crystal studies and its possible implication for our work, this information is presented in the following section.

Single crystal structures of hydroxylated ceramides

The single crystal structure of two ceramides, N-tetracosanoyl-phytosphingosine, and N-(2D,3D-dihydroxyoctadecanoyl)-phytosphingosine, a CER with the maximum number of hydroxyl functions, has been determined[60,61]. In those crystals, the ceramides are not packed with parallel-stacked chains, forming a bilayer, but with extended conformations, in single layers, Figure 1.12. This constitutes an exception for amphiphilic double chain lipids, which are organized in bilayers[62].

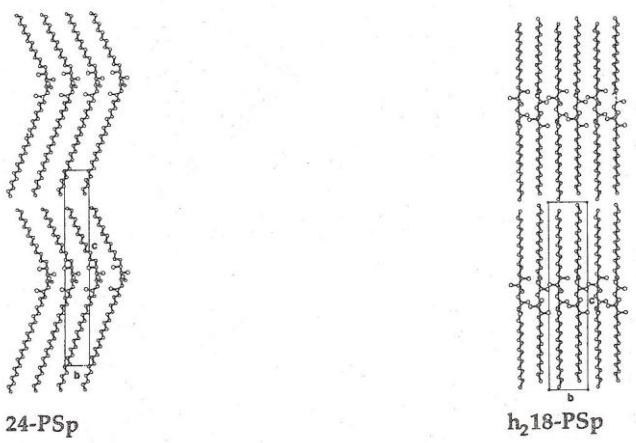

Figure 1.12. - Solid state packing arrangements of two hydroxylated ceramides. The ceramides are 24-PSp - N-tetracosanoyl-phytosphingosine; $h_2$18-PSp - N-(2D,3D-dihydroxyoctadecanoyl)-phytosphingosine. *Adapted from ref. 62*.

In the crystal of N-tetracosanoyl-phytosphingosine[60], the CER molecules are packed with extended chains in single layers, with the molecules adopting a V-shaped conformation (Figure 1.12). The molecules are connected by three intermolecular and one intramolecular hydrogen bond in the polar part of the molecule. The hydrocarbon chains are pointing out in opposite directions, adopting the V-shaped form, to allow space for the hydroxyl groups in the polar part of the molecule. This lipid also forms regular interdigitated bilayers, depending on the protocol of crystallization[63].

In the N-(2D,3D-dihydroxyoctadecanoyl)-phytosphingosine crystal[61], the polar groups are also located in the central region of the monolayers, involved in an extensive network of hydrogen bonds. The amide nitrogen and carbonyl function, and all the four hydroxyl groups are involved in two hydrogen bond systems, such that each molecule establishes six lateral interactions with four neighbor molecules. The hydrocarbon chains are tilted by 46 º with respect to the layer normal. Laterally the chains pack according to the orthorhombic perpendicular chain packing mode. The subcell dimensions are *a* = 5.03, *b* =

7.39 and *c* = 2.53 Å, with α = 90.1 β = 91.4 and γ = 89.6 º. The packing cross-section of the chains perpendicular to their long axis is 18.6 Å.

Pascher and Sundell[61] interpret the reluctance of hydroxylated ceramides to adopt a bilayer structure has the result of a network of hydrogen bonds that is established at the monolayer center. This network of interactions seems to be more favorable than an alternative network in a bilayer arrangement.

Structure in monolayers at the air-water interface

The structure of synthetic N-C18:0-sphingosyl ceramide films at the air-water interface has been studied by X-ray reflectivity and grazing incidence X-ray diffraction[64].

In this study, the authors find evidence for an arrangement of the CER film in two co-existing phases. One with hexagonal acyl chain packing (lattice constant *a* = 4.81 Å), and another with an orthorhombic arrangement (lattice constants *a* = 5.30 Å, *b* = 7.84 Å). At higher compressions, the hexagonal acyl chain packing is predominant. Without compression, both arrangements are detected, and a two dimensional gas phase also co-exists. In another work, Scheffer and colleagues studied monolayers of N-palmitoyl-D-*erythro*-sphingosine, also by grazing incidence X-ray diffraction measurements (GIXD)[65]. For uncompressed monolayers at the air-water interface, they have obtained four overlapping peaks at q_{xy} = 1.45, 1.49, 1.53 and a small one at 1.62 Å $^{-1}$. From their diffraction data they derive a near rectangular unit cell with *a* = 5.02, *b* = 8.17 Å, and γ = 91.9º. At high pressures, approximately 20 mN.m^{-1}, sharper peaks are obtained at q_{xy} = 1.43, 1.48, and at 1.62 Å $^{-1}$ interpreted as a near-rectangular unit cell, with *a* = 5.18 Å, *b* = 7.74 Å and γ = 92.2º. Both phases have a monolayer thickness of 20 Å, derived from the full width at half maximum of the Bragg rods along q_z.

Monolayers of ceramide, cholesterol mixtures

In the above mentioned study of Scheffer and colleagues, several mixtures of N-palmitoyl-D-*erythro*-sphingosine with cholesterol were also characterized by GIXD. At a CER:Ch ratio ranging from 100:0 to 70:30, they detect only crystalline CER. From 70:30 to 50:50 a crystalline mixed phase composed of ceramide and cholesterol is observed, co-existing with the pure CER phase. And from a CER:Ch ration of 33:77 up to 10:90, only the mixed phase is present. They observe continuous miscibility of cholesterol with CER, even at high cholesterol concentrations.

Thermotropic phase behavior

Shah *et al.*[59] have characterized the phase behavior of anhydrous synthetic CER with a non-hydroxy fatty acyl palmitoyl chain, the C16-Cer. A single thermal transition at 95.4 ºC, with a ΔH^{o} = 43.5 kJ.mol^{-1} is observed. By powder pattern X-ray diffraction, it was established that the low temperature organization is a lamellar phase with d = 4.21 nm, and four sharp reflections in the wide angle region located at 0.48, 0.43, 0.41 and 0.37 nm. At 92 ºC, a single broad reflection with a repeat distance of 2.75 nm with a diffuse band in the wide angle region at 0.47 nm, which is indicative of melted acyl chains, is observed.

Hydrated systems of C16-Cer display a broad exothermic transition at 50-70 ºC, followed by an endothermic transition at 90 ºC with a ΔH^{o} of 13.8 kcal/mol[59]. The low temperature metastable phase is lamellar with d = 4.69 nm, and a broad wide angle peak at 0.41 nm. After the exothermic transition, the lamellar phase has a repeat distance of 4.18 nm, and four main wide angle reflections at 0.45, 0.41, 0.40 and 0.38 nm. Finally, at 90 ºC the diffraction pattern is composed by a single broad reflection at 2.99 nm, and a wide angle diffuse reflection at 0.46 nm, which is characteristic of melted chains.

The C16-Cer thermotropism and phase behavior has also been characterized by FTIR[66]. At 63 ºC, a solid-solid phase transition, interpreted as an orthorhombic to hexagonal chain packing transition is observed. With further increase in temperature, at 90 ºC a transition to a phase with conformationally disordered chains is observed.

Ceramides establish strong hydrogen-bonds

In the characterization of N-sphingosyl ceramides, (bovine brain derived) prepared in excess water by FTIR, the presence of strong hydrogen bonds to the CER amide group is clearly detected[67]. This conclusion was derived from the reduction in amide I frequency, generally located at approximately 1650 cm^{-1}, and mostly originated by C=O stretch, and the increase in amide II frequency, generally located at approximately 1550 cm^{-1}, mostly resultant from C-N stretch and N-H in plane bending. This result has also been confirmed for synthetic N-C18:0-sphingosyl-ceramide[68].

Dependence of T_m with acyl chain length

In a study conducted by Hui-Chen Chen and colleagues[66], the main transition temperature of a series of ceramides prepared in excess water has been determined. The ceramides are synthetic N-sphingosyl ceramides with chain lengths C14, C16, C18 and C20. The main transition temperatures are respectively: 86.3, 94.1, 92.7 and 92.9 ºC, evidencing a reduced dependence of T_m on the fatty acid chain length, as compared with hydrated phospholipids bilayers. The authors propose that this effect results from a reduced hydration of ceramides.

Hydration behavior

In our experience N-SPHING CER do not behave as the most thoroughly studied phosphatidylcholines that can be observed to spontaneously hydrate in the presence of water, originating turbid, homogeneous dispersions. On the contrary, when N-sphingosyl ceramides water dispersions are prepared, their macroscopic aspect can be described as a clear fluid containing some “solid like” white plates floating at the water surface. This observation raise concerns related with the capacity of N-SPHING CER to hydrate. Additionally, Jendrasiak and Smith[69], predict that ceramides obtained from hydrolysis of egg and brain sphingomyelin are weak water adsorbers. These natural sphingomyelins have N-sphingosyl architecture. The authors measured the amount of water vapor adsorbed by a monolayer of CER along increasing water vapor pressure.

In opposition, and suggesting that N-sphingosyl ceramides are able to hydrate, a study of the thermotropism of this CER type with increasing water content, evidence a clear reduction in the main phase transition temperature with increasing water amount[59]. Dry synthetic N-C16:0-sphingosyl ceramide has a T_m = 95.4 ºC with ΔH^o = 43.5 kJ.mol^{-1}. The main transition temperature decreases until a limiting water amount of 9.3 weight %, with a T_m = 90.2 ºC, and ΔH^o = 58.5 kJ.mol^{-1}.

Phase diagrams of ceramide with other lipids

The relatively recent interest in the function of ceramides in a number of cellular functions originated several studies involving N-sphingosyl ceramide in the presence of phospholipids namely the construction of partial phase

diagrams. Several phase diagrams have been obtained such as of N-sphingosyl ceramide (bovine brain derived) with DPPC[70], N-sphingosyl ceramide C16:0 with 1-palmitoyl-2-oleoyl phosphatidylcholine, POPC[71], with dimyristoylphosphatidylcholine, DMPC[72] and with dielaidoyl phosphatidylethanolamine, DEPE[73]. The overall picture that results from those diagrams[74] evidences that the miscibility of CER with phospholipids in the gel state is reduced. In the liquid crystalline state, phase separation is already observed at very low ceramide concentrations. The studies were only performed in the region of low ceramide content, up to approximately 20%[74]. Only one study[71] explored the phase diagram at high CER concentrations.
To our knowledge, all the phase diagrams of CER with cholesterol and with fatty acids published in the literature have used phytosphingosine derived ceramides. These CER have distinct physical properties, and therefore are not directly comparable with the ceramide used in our studies, N-sphingosyl ceramide.

1.8. Cholesterol

Structure in the solid state

The crystal structure of cholesterol monohydrate, which is the stable form of cholesterol in water, was studied by Craven[75]. He proposed a structure in which the molecules are organized forming a stacking of bilayers of thickness 3.39 nm. The single crystal structure of the anhydrous form of Ch was determined in 1977 by Shieh *et al.*[76]. The structure proposed was also a stacking of bilayers with a thickness of 3.39 nm. In fact, crystals of 3-hydroxy steroids and their hydrates show a tendency to form bilayer structures[76].

Thermotropic phase-behavior in water

The phase behavior of cholesterol in the presence of water was studied by Loomis *et al.*, in 1979[77]. With the increase in temperature of anhydrous cholesterol:water mixtures, two major transitions are observed, at 39 ºC, with ΔH^o = 0.91 ± 0.5 kcal/mol, and at 151 ºC, with 6.59 ± 0.25 kcal/mole (Figure 1.13. lower trace). The powder pattern X-ray diffraction of the lower temperature polymorph is similar to the phase that is formed above 39 ºC, except for differences in peak intensities. In addition, a new peak at 0.54 nm is detected for the polymorph stable above 39 ºC. Above 151 ºC, an isotropic liquid is formed, with an X-ray diffraction pattern containing two broad maxima centered at 0.6 and 2.1 nm. When the system is cooled, a hysteresis of 35 ºC was observed for the first crystallization. The lower transition also presents some hysteresis.

For cholesterol monohydrate in water (Figure 1.13. upper trace) when the temperature is increased, three thermal transitions are observed. The first occurs at 86.4 ºC, with an ΔH^o of 2.35 kcal/mol, and corresponds to the transition to the anhydrous state. The second is observed at 123.4 ºC, with a ΔH^o of 3.42 kcal/mol, and represents the formation of the hydrated smectic liquid crystalline phase of Ch. Finally, a third transition is observed at 156.8 ºC with an ΔH^o of 2.29 kcal/mol, which corresponds to a transition to a isotropic liquid.

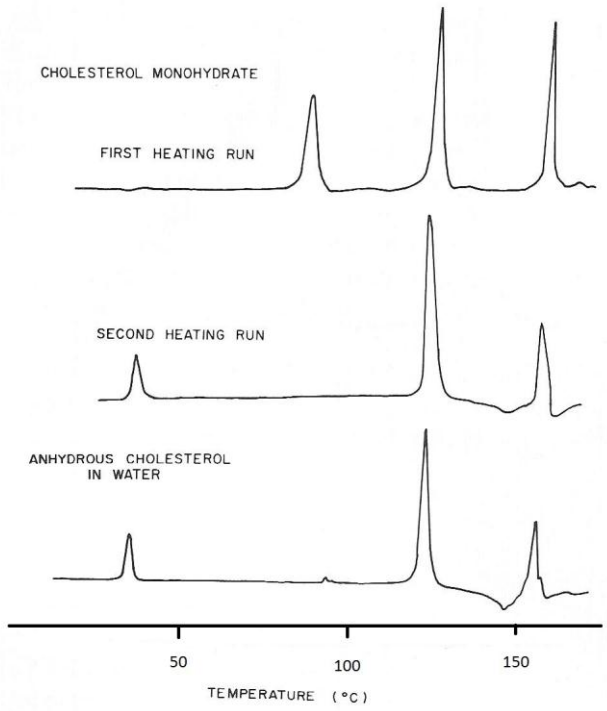

Figure 1.13. - Phase transitions of cholesterol in water both in the monohydrate and anhydrous forms. The differential scanning calorimetry heating scans where acquired at 5 ºC/min. *Adapted from ref. 77.*

Models for phospholipids/cholesterol mixtures: the "condensed complex" formation proposal

The hypothesis that cholesterol forms "complexes" with phospholipids has been raised since the 60s, to explain the non-ideal physical properties of mixtures of Ch with phospholipids[78]. More recently, Mc Connell and co-workers have become defenders of these cholesterol/phospholipid aggregates that they name "condensed complexes", and performed a series of systematic studies on the subject[79].

In their studies of phospholipids mixtures containing cholesterol, in monolayers at the air-water interface, an unusual phase diagram with two upper immiscibility critical points is obtained. They interpret their data as evidencing the formation of stoichiometric aggregates between the phospholipid and Ch. A thermodynamic model assuming the formation of those aggregates that simulates the phase diagram experimental data has been developed. With this quantitative model it was possible to predict and interpret several properties of phospholipids mixtures with cholesterol, such as the Ch chemical activity and average molecular area. All these properties change rapidly near the composition for which cholesterol phospholipid stoichiometric aggregates are thought to be more abundant, which correspond to the position of the sharp cusp in between the two liquid immiscibility areas shown in Figure 1.14. The stoichiometry of the hypothetical aggregates can also be derived from this experimental point.

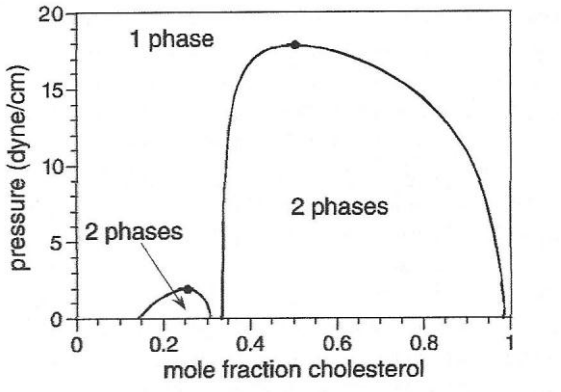

Figure1.14. - An unusual phase diagram with two upper immiscibility critical points. The lipids are egg-sphingomyelin and cholesterol. *Adapted from ref. 78.*

McConnell and co-workers, suggest that the *liquid ordered* phase observed for cholesterol and some phospholipids mixtures can be constituted by stoichiometric aggregates of phospholipid and Ch[78]. They also defend that the "lipid rafts", lipid assemblies that provide laterally segregated platforms, proposed to exist in cell membranes, and to be involved in several cellular functions such as protein and lipid trafficking and signal transduction[80], can be composed of those aggregates[78].

In alternative, several authors propose models for phospholipids mixtures containing Ch without making use of a special mechanism such as the formation of aggregates. Ipsen and colleagues[81] propose that in the liquid phase, cholesterol tends to promote conformationally ordered acyl chains. They have developed a thermodynamic and a microscopic model that is able to explain the typical phospholipids cholesterol phase diagram. However, the formation of regular arrangements as also been advanced by some authors[82]. In regular distributions, the guest molecules are maximally separated in the lipid matrix, as a result of a repulsive interaction. This specific separation originates an ordered arrangement of the positions of the guest molecules in the lipid matrix. With this model, that results in cholesterol molecules being arranged in a hexagonal superlattice[82], the authors are able to explain a series of breaks in the fluorescence intensity of probes incorporated in bilayers of phosphatidylcholines with Ch. A regular arrangement can be responsible for dramatic alterations both at the thermodynamic and structural level, at certain specific Ch molar fractions, and would simply result from a repulsive cholesterol-cholesterol interaction. The physical fundament proposed for the Ch/Ch repulsion is an unfavorable interaction between the bulky, rigid ring structure of sterol molecules. Huang and Feigenson have also proposed a model, the "umbrella model", which predicts that at certain cholesterol molar fractions, highly regular lipid distributions are formed[83]. The experimental data explained by their model is the maximum cholesterol solubility in several model lipid bilayers. The physical origin of the increase in energy associated with the cholesterol-cholesterol contacts is proposed to derive from the incapacity of

the phopholipid head-group “umbrella” to provide shielding of the nonpolar part of cholesterol from exposure to water with further addition of cholesterol.

1.9. Long chain fatty acids

Structure and thermotropic phase behavior in water

The structure and thermotropic phase behavior of long chain fatty acids is influenced by their liotropism[84]. When mixed with water, the FAs can become neutral, ionized, or in a mixture of both forms depending on the surrounding media pH. As a consequence, an additional phase, the so-called fatty acid soap, has to be considered. Fatty acid soaps are the salts of mono, di, or trivalent metals with aliphatic carboxylic acids[84].

The thermotropic phase behavior of long chain fatty acids in excess water has been systematized[84]. As a general rule, a neutral long chain fatty acid melts directly to an isotropic liquid. For the correspondent soap, thermotropic mesomorphism is observed, with formation of several liquid crystalline states before a final transformation to the liquid state. The main phase transition temperatures are considerably higher for the soap, as compared to the respective acid form. In Figure 1.15., a simplified summary of the thermotropic phase behavior of long chain fatty acids in excess water is presented.

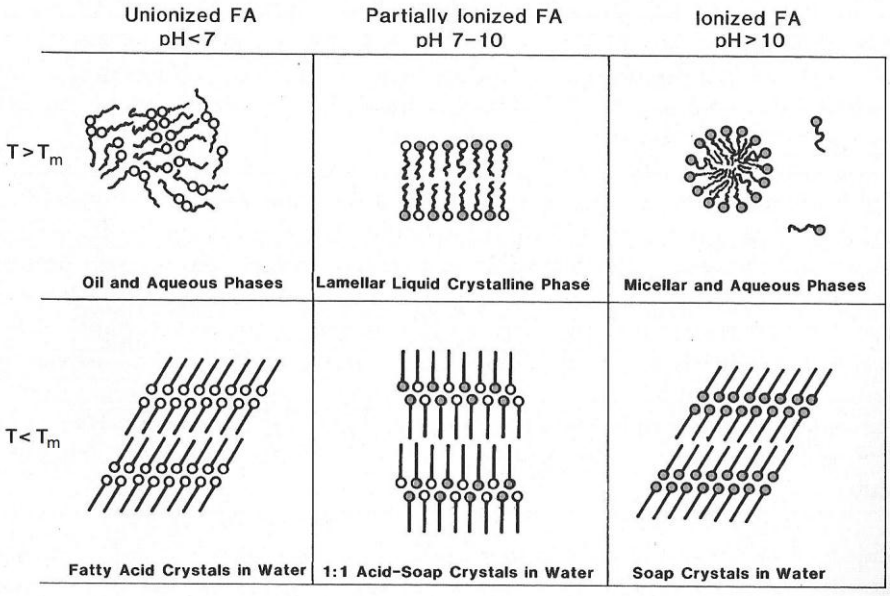

Figure 1.15. - Summary of long chain fatty acids phase behavior in excess water as a function of pH and the state of acyl chain. FA – Fatty acid; T_m – main phase transition temperature. *Adapted from ref. 84.*

In excess water, the neutral form of the FA is arranged in crystals below the main phase transition temperature (T_m). When the temperature is increased, melting to liquid oil in the aqueous phase occurs. The ionized form is organized in soap crystals in water, for temperatures below the T_m, and when the temperature is increased, the crystals melt originating micelles dispersed in water. At intermediate pH values, both the fatty acid neutral and ionized forms are present. In this case, the system is arranged in acid-soap crystals at temperatures below the main phase transition temperature. With increasing temperature, a lamellar liquid crystalline phase is formed. Note that long chain fatty acids behave as amphiphilic lipids at intermediate pH values. The mixture of neutral and ionized forms has the appropriate geometry for bilayer formation, instead of oil droplets or micelles.

This is a simplified summary of long chain fatty acids thermotropic phase behavior, which is highly complex, and is also dependent on FA concentration, type of cation, concentration, and chain length[84].

Induction of inverted hexagonal phases

When a neutral fatty acid is added to phosphatidylcholines, an inverted hexagonal phase is induced upon melting of the system[85,86]. This phenomenon occurs for FA with a chain length equal or superior to C16. This observation is rationalized in the following manner. The inverted structure is favored due to an excess in the acyl chain cross section when the FA is inserted, when compared to the choline head-group area. The formation of hexagonal phases in mixtures of ceramide, cholesterol and fatty acid is also reported by several authors[87,88,41], and in our studies, refer to chapter 3, we have also observed inverted hexagonal phases when the fatty acid was added to a binary CER/Ch mixture.

Phase-behavior of mixtures of palmitic acid and cholesterol in excess water

The thermotropic phase behaviour of some palmitic acid, Ch mixtures in excess water has been studied by Ouimet *et al.*[89]. Mixtures of palmitic acid with cholesterol, both at relative molar proportions of 50:50 and 25:75 at pH = 8.5, form fluid bilayers with a repeat distance of 4.9 nm between 25 ºC and 70 ºC.

At pH = 5.4 and below 50 ºC palmitic acid and Ch are immiscible and phase separate, being in the crystalline form. Between 50 and 55 ºC a transition to a liquid lamellar phase, with d = 3.9 nm is observed. When the amount of

palmitic acid is increased above the eutectic point located between 50 and 70 mol% cholesterol, a co-existing phase rich in palmitic acid melts at 58 ºC[89].

1.10. Cholesteryl Esters

Structural arrangements of cholesteryl esters

The phase behavior of cholesteryl esters is dependent on the fatty acid that is linked to the cholesterol moiety being saturated or unsaturated, and of its chain length. Cholesteryl esters display polymorphism organizing in several types of liquid crystalline states besides the solid and liquid states. In the solid state they can be arranged in three basic types of structures: bilayer, monolayer type II and monolayer type I.

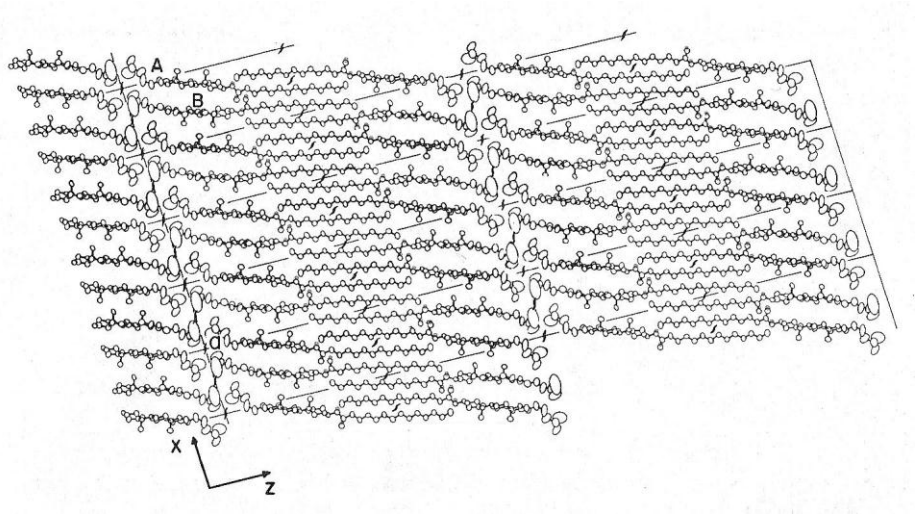

Figure 1.16. - Solid state organization of cholesteryl myristate illustrating the bilayer arrangement. *Adapted from ref. 84.*

For example, cholesteryl myristate in the solid state forms bilayers[84], Figure 1.16. An almost regular packing of alkanoate chains, with a recognizable subcell structure is observed at the center of the bilayer. The cholesteryl rings are parallel closely packed, with projecting cholesteryl tails forming the interface region between bilayers.

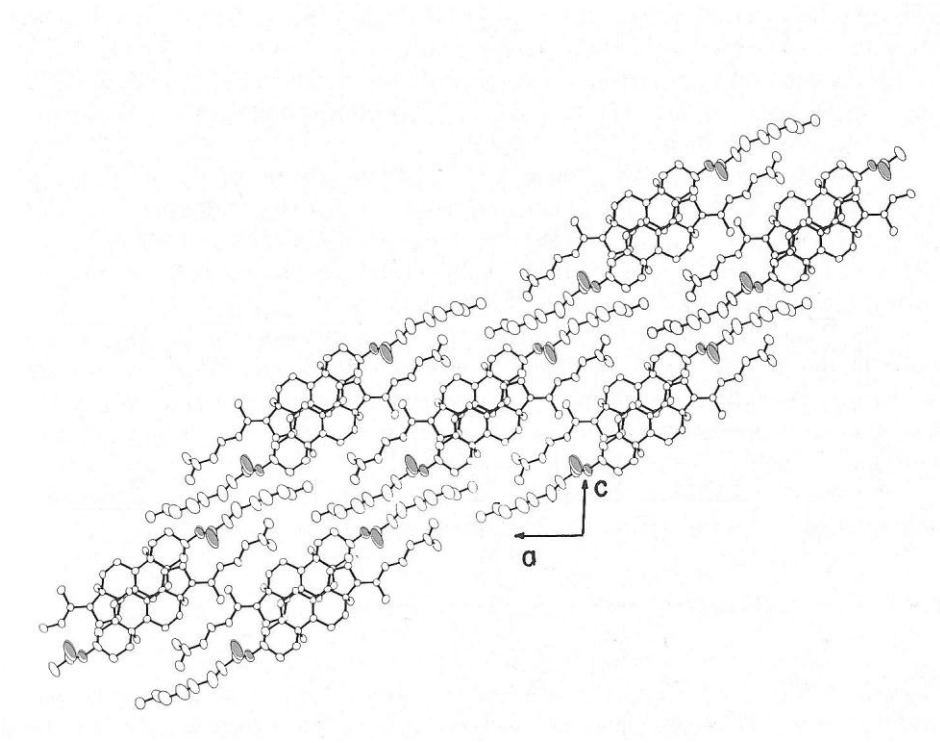

Figure 1.17. - Solid state organization of cholesteryl oleate, illustrating the monolayer type II arrangement. *Adapted from ref. 84.*

Figure 1.17., represents the solid state structure of cholesteryl oleate, organized in a monolayer type II. In this structure molecules are antiparallel, with long axes severely tilted (~30º) with respect to the layer planes. At the center of the monolayer there is efficient packing of cholesteryl ring systems that result from cholesteryl/cholesteryl interactions. These interactions are very important in this type of organization. The ester chains are not very well packed, and can present thermal motion.

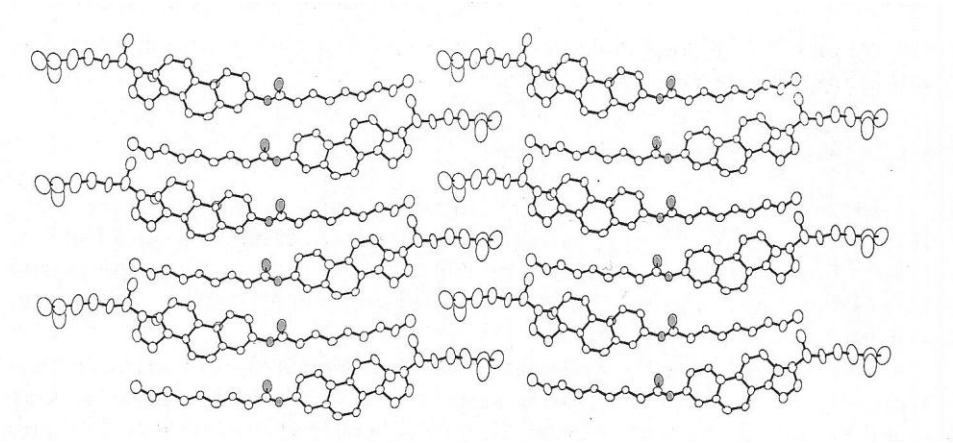

Figure 1.18. - Solid state organization of a cholesteryl nonanoate, illustrating the monolayer type I arrangement. *Adapted from ref. 84.*

Cholesteryl nonanoate, cholesteryl decanoate and laurate may also be arranged in monolayers type I, Figure 1.18. Each tetracyclic system is almost perpendicular to the next. However, this form of organization is less stable than the previously shown monolayer type II.

With increasing temperature, some cholesteryl esters melt to preliminary liquid crystalline states that subsequently originate the liquid isotropic state. These liquid crystalline states are stable. In other esters, the liquid crystalline organizations can only be observed during cooling of the melted state. In this case, the liquid crystalline phases are metastable.

In the liquid crystalline state cholesteryl esters may adopt either the smectic or the cholesteric structure, a type of arrangement that was first observed with cholesteryl esters. The smectic state (Figure 1.19.), has long range order in the direction of the long axis of the molecule, and the molecules are arranged in layers. In the cholesteric state, the molecules are organized in layers, but within each layer, the long axis of the molecules is parallel to the plane of the layers. In each adjacent layer, the direction of molecular orientation rotates slightly with respect to the previous layer, forming a helical pattern, refer to

Figure 1.19. These liquid crystalline arrangements are observed in other molecular classes and acquired relevance in technological applications.

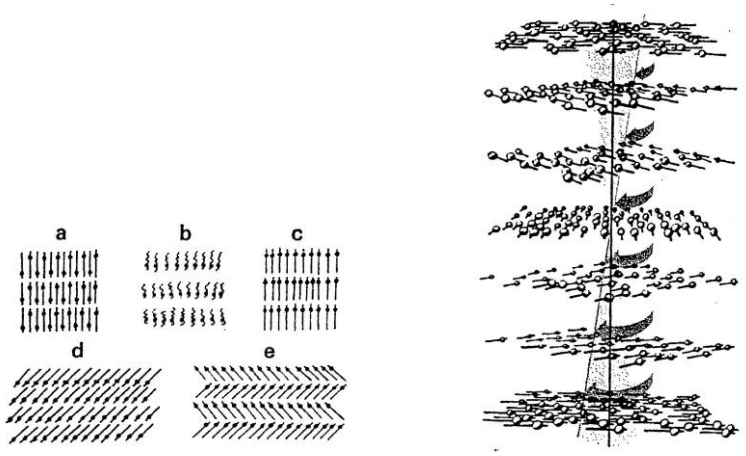

Figure 1.19. - Schematic arrangement of smectic and cholesteric states. Left side – several examples (a-e) of smectic phases, right side– cholesteric phase. *Adapted from ref. 84.*

Cholesteryl oleate structure and thermotropic phase-behavior

In the work contained in this thesis, refer to chapter 4, cholesteryl oleate (ChO), was used as the model CE. This ester was elected, because it corresponds to the most abundant cholesteryl ester found in SC[33].

In the solid state, cholesteryl oleate is organized in monolayer type II[90] and when the temperature is increased, a transition to a isotropic liquid is observed at 51 ºC[91]. Cooling the isotropic liquid, originates the cholesteric state at 47.5 ºC and with further cooling, the smectic state is obtained at 41 ºC. The liquid crystalline states of cholesteryl oleate are metastable, and can only be obtained from an undercooled melt. The original solid monolayer type II arrangement can be obtained from the isotropic liquid or from one of the liquid crystalline metastable states (for a more detailed description please see Chapter 4).

In the literature concerning this particular ester, X-ray data relative to the long spacing reports *d* = 1.88 nm for the solid monolayer type II crystal, and *d* = 3.60 nm for the smectic state[90].

Solubility of cholesteryl esters in amphiphilic lipids

The solubility of CEs in phosphatidylcholine bilayers is very low, only occurring in the liquid crystalline state[92], and in the presence of cholesterol this solubility is further reduced[93]. In sphingomyelin bilayers, the solubility of cholesteryl esters is also very low, and decreases by an order of magnitude, less than 0.1 mol % in the presence of 50 mol % cholesterol[94]. This behaviour contrasts markedly with Ch, which is able to incorporate in lipid bilayers up to 2:1 molar ratio.

The residual miscibility of CEs in the amphiphilic lipids studied, does not exclude the evaluation of their solubility in CER containing mixtures. In fact, there are reports in the literature of high miscibility of CEs in monomolecular films of a phosphatidylcholine[95].

The studies presented in the thesis involve the use of experimental techniques that are shortly described in the next sections.

1.11. Powder pattern X-ray diffraction of lipid-water systems

The first scientists that applied powder pattern X-ray diffraction systematically to obtain structural information for lipid-water systems were Luzzati and colleagues[96], mostly in the 60s.

Hydrated lipid systems, produce a diffraction pattern characterized by several Bragg diffractions at small angles, together with a set of reflections in the wide angle region. These diffraction data, although not permitting a precise atomic level structural characterization, provide important structural information.

The reflections observed at small angles, in our set-up ranging from 0.1 to 0.390 nm^{-1}, permit the deduction of the type of long range organization of the lipid aggregate. These reflections are attempted to fit to several equations, and the symmetry of the phase, whether lamellar, hexagonal or cubic among others is derived. Subsequently, from the parameters of the equation that fitted the data, the dimensions of the lattice are obtained such as for example the lamellar repeat distance in lipid bilayers. The wide angle reflections, in our set-up ranging from 1.78 to 3.05 nm^{-1}, provide information about the acyl chain packing mode (refer to section 1.5). In lipid bilayers in the L_α state, a single broad reflection at 4.5 Å is observed. This reflection indicates a hexagonal lattice. When a single sharp reflection located at 4.2 Å is detected, the bilayer is in the L_β state, with acyl chains packed in a hexagonal lattice with a comparatively smaller inter-chain distance. For the L_C bilayers several reflections are observed, the number and pattern being determined by the crystalline structure. It is important to refer that for bilayers in the rigid states L_β and Lc, the area per head-group can also be derived from this wide angle lattice.

Synchrotron radiation provides an X-ray source with high intensity, when compared with conventional X-ray sources. As a result, appropriate quality diffraction patterns can be obtained with reduced exposure times as short as milliseconds. Several diffraction patterns can be obtained along increasing temperatures, as in the example in Figure 1.20.

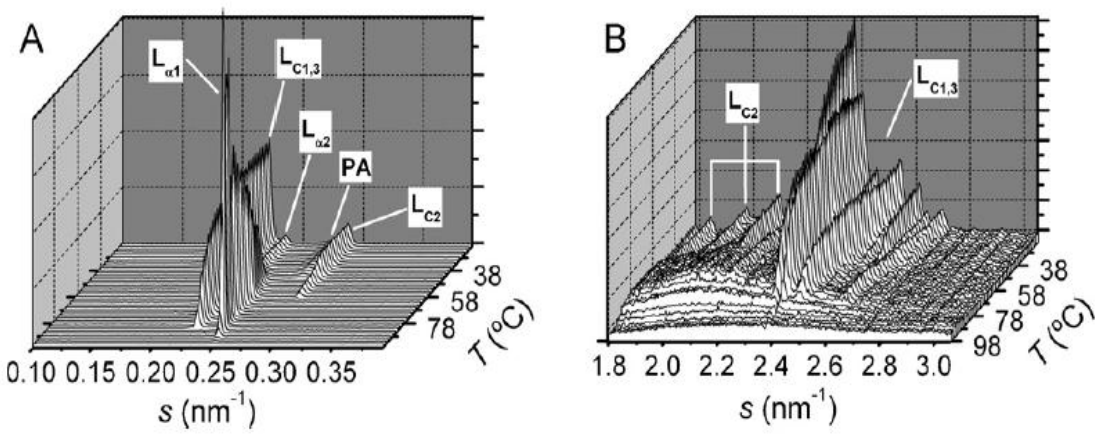

Figure 1.20. - Assembly of successive powder pattern X-ray diffraction profiles along increasing temperatures. The diffraction patterns were obtained at small angles, panel A, and wide angles, panel B, every two minutes, along increasing temperatures at a rate of 1 ºC/min, for a sample composed of C16-Cer:Ch:PalmiticAcid 44:38:18 molar ratio in excess water at pH = 4.0.

In the setup used in our studies, at the Soft Condensed Matter beamline A2 of Hasylab, it is still possible to simultaneously detect the small and the wide angle regions, which in the case of samples of amphiphilic lipids, is essential for both the determination of the type of long range organization of the lipid aggregate and the correspondent acyl chain packing.

1.12. ^{13}C-magic angle spinning-nuclear magnetic resonance applied to lipid bilayers

Probing cholesteryl ester environment

^{13}C NMR can be applied to answer a question as how cholesteryl ester, molecules are positioned in the lipid bilayer, either interdigitated parallel to the chains of the phospholipids in a folded conformation, or in the center of the bilayer[97].

If CEs molecules are positioned in the bilayers exposing the carbonyl group to water, the folded interdigitated parallel hypothesis, the formation of hydrogen bonds with water at the surface of the bilayer, would result in a downfield shift of the ^{13}C carbonyl resonance peak. In this manner ^{13}C NMR can be used as a direct method to study the localization of carbonyl containing lipids in bilayers, taking advantage of a chemical shift change originated by a different surrounding environment. The localization of CEs in two different environments, one inserted and other coexisting outside the bilayer can be observed by the detection of two distinct ^{13}C carbonyl peaks in the spectra, refer to Figure 1.21., at different positions[97].

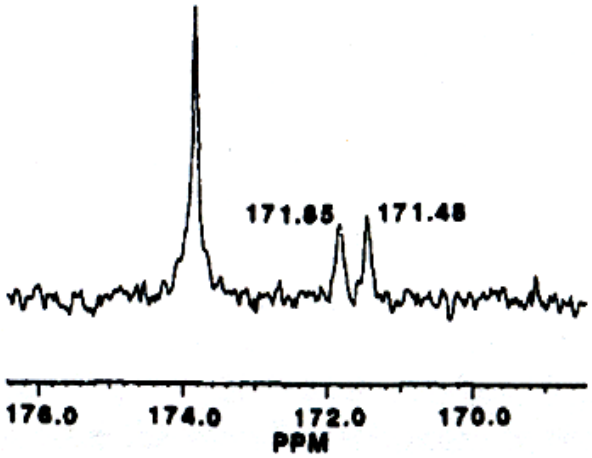

Figure 1.21. - ^{13}C MAS NMR spectra (carbonyl region) of phosphatidylcholine bilayers with 1% ^{13}C carbonyl cholesteryl oleate (ChO). The peaks at 171.85 ppm and 171.48 ppm correspond respectively to ChO inserted in the bilayer and coexisting segregated in oily drops. *Adapted from ref. 98.*

Simple ^{13}C NMR experiments can only be performed in sonicated lipid dispersions, which due to the ultrasound treatment contain only small unilamellar vesicles, SUVs. The size of these liposomes is in the nanometer range, which results in membranes with high curvature. Due to the small size of the vesicles, these samples give conventional NMR spectra with adequate

resolution. Nevertheless, this imposes a limitation to the type of lipid mixtures able to be studied, narrowing its scope to high curvature lipid membranes. This might not be appropriate for certain purposes. In fact, a high curvature imposes a different acyl chain packing as compared with the nearly flat biologic lipid membranes. Solid state NMR provides high resolution spectra of turbid lipid dispersions[98]. The study of lipid dispersions of all types is made possible, including multilamellar lipid bilayers, MLVs, the nearly flat bilayers formed spontaneously by amphiphilic lipids. It is also possible to study mixtures of CER, cholesterol and fatty acid, with or without cholesteryl oleate, which are composed of solid lumps floating in the buffer.

Solid State NMR techniques

The conventional NMR spectra of solid samples display very broad featureless lines. This effect has its origin mainly in dipole-dipole interactions and chemical shift anisotropy[99]. These phenomena are also present in liquid samples, but as the molecules are tumbling rapidly, those directional effects average to zero.

High resolution spectra in solid samples can be obtained, by associating several techniques, including a variety of radiofrequency irradiation patterns and magic angle spinning (MAS).

Decoupling procedures are applied to minimized dipole-dipole interactions. Continuous irradiation of one nucleus effectively decouples it from the other. Following this treatment the NMR spectrum still present broadening, which is caused by chemical shift anisotropy.

It can be deducted mathematically, that, if during the course of an NMR experiment, a sample is put to spin, and bended at the specific precise angle of 54.7º, the so called magic angle, the chemical shift anisotropy of the signals is eliminated. The result of this procedure is a substantial enhancement of spectral resolution.

Another radio-frequency pulse sequence frequently used in solid-state NMR is Cross-polarization, CP[100], a technique developed by Alex Pines in 1973[101], in

which the repeatedly transference of polarization from a more abundant species, generally protons, to the less abundant nuclei is performed. In this manner, the sensitivity problem associated with solid state NMR, which becomes more critical for natural abundance ^{13}C NMR can be overcome.

1.13. References

(1) Menon, G., Ghadially, R. (1997). Morphology of lipid alterations in the epidermis: a review. *Microscop. Res. and Techniq.*, 37, 180-192.

(2) Wertz, P.W. (2000). Lipids and barrier function of the skin. *Acta Derm Venereol. Supp,* 208, 7-11.

(3) Ohvo-Rekila, H., Ramstedt, B., Leppimaki, P., Slotte, J.P. (2002). Cholesterol interactions with phospholipids in membranes. *Progr. Lipid Res.*, 41, 66-97.

(4) Huang, J.H., Buboltz, J.T., Feigenson, G.W. (1999). Maximum solubility of cholesterol in phosphatidylcholine and phosphatidylethanolamine bilayers. *Biochim. Biophys. Acta,* 1417, 89-100.

(5) Kamp, F., Hamilton, J.A. (1992). pH gradients across phospholipids membranes caused by fast flip-flop of un-ionized fatty acids. *Proc. Natl. Acad. Sci USA*, 89, 11367-11370.

(6) Kligman, A.M. (1983). A biological brief on percutaneous absorption. *Drug Develop. and Indust. Pharmacy*, 9, 521-560.

(7) Grubauer, G., Feingold, K.R., Harris, R.M., Elias, P.M. (1989). Lipid content and lipid type as determinants of the epidermal permeability barrier. *J. Lipid Res.*, 30, 89-96.

(8) Feingold, K., Mao-Qiang, M., Menon, G.K., Cho, S.S., Brown, B.E., Elias P.M. (1990). Cholesterol synthesis is required for cutaneous barrier function in mice. *J Clin. Invest.*, 86, 1738-1745.

(9) Holleran, W.M., Man, M.Q., Gao, W.N., Menun, G.K., Elias, P.M., Feingold, K.R. (1991). Sphingolipids are required for mammalian epidermal barrier function. Inhibition of sphingolipid synthesis delays barrier recovery after acute perturbation. *J. Clin. Invest.*, 88, 1338-1345.

(10) Hannun, Y.A., Obeid, L.M. (1995). Ceramide: an intracellular signal for apoptosis. *Trends Biol. Science*, 20, 73-77.

(11) Goni, F.M., Alonso, A. (2006). Biophysics of sphingolipids I. Membrane properties of sphingosine, ceramides and other simple sphingolipids. *Biochim. Biophys. Acta*, 1758, 1902-1921.

(12) Kolesnick, R.N., Goni, F.M., Alonso, A. (2000). Compartmentalization of ceramide signaling: physical foundations and biological effects. *J. Cell Physiol.*, 184, 285-300.

(13) Stancevic, B., Kolesnick, R. (2010). Ceramide-rich platforms in transmembrane signaling. *FEBS Letters*, 584, 1728-1740.

(14) Holopainen, J.M., Angelova, M.I., Kinninen, P.K.J. (2000). Vectorial budding of vesicles by asymmetrical enzymatic formation of ceramide in giant liposomes. *Biophys. J.*, 78, 830-838.

(15) Menon, G.K. (2002). New insights into skin structure: scratching the surface. *Adv. Drug Deliv. Rev.,* 54, S3-S17.

(16) Hickman, J., Roberts, L., Larson, A. (2001). Integrated principles of zoology. 11th edition. McGrawHill, London.

(17) Junqueira, L.C., Carneiro, J., Kelley, R.O. (1992). Basic Histology. Prentice Hall International, London.

(18) Harris, M.A. (1999). The Skin. Permachart Quick Reference Guide. Papertech, Ontario.

(19) Downing, D.T. (1992). Lipid and protein structures in the permeability barrier of mammalian epidermis. *J. Lipid Res.*, 33, 301-313.

(20) Swartzendruber D.C., Wertz, P.W., Madison, K.C., Downing, D.T. (1987). Evidence that the corneocyte has a chemically bound lipid envelope. *J. Invest. Dermatol.*, 88, 709-713.

(21) Wertz, P.W., Downing, D.T. (1987). Covalently bound omega-hydroxyacylsphingosine in the *stratum corneum*. *Biochim. Biophys.*, *Acta,* 917, 108-111.

(22) Behne, M.J., Meyer, J., Hanson, K.M., Barry, N.P., Murata, S., Crumrine, D., Clegg, R.W., Gratton, E., Holleran, W.M., Elias, P.M., Mauro, T.M. (2002). NHE1 regulates the *stratum corneum* permeability barrier homeostasis: microenvironment acidification assessed with FLIM. *J. Biol. Chem*., 277, 47399-47406.

(23) Wertz, P., Norlén, L. (2004). “Confidence intervals” for the “true” lipid composition of the human skin barrier? In Skin, Hair and Nails. Forslin, B., Lindberg, M., Eds., Marcel Dekker, New York, pp. 85-106.

(24) Norlen, L., Nicander, I., Lundh Rozell, L.B., Ullmar, S., Forstind, B. (1999). Inter and intra individual differences in human *stratum corneum* lipid content related to physical parameters of skin barrier function *in vivo*. *J. Invest. Dermatol.*, 112, 72-77.

(25) Madison, K.C. (2003). Barrier function of the skin: “La raison d’être” of epidermis. *J. Invest. Dermatol.*, 121, 231-241.

(26) Bouwstra, J.A., Gooris, G.S., Dubbelaar, F.E., Weerheim, A.M., Ijzerman, A.P., Ponec, M. (1998). Role of ceramide 1 in the molecular organization of the *stratum corneum* lipids. *J. Lipid Res.*, 39, 186-196.

(27) Kuempel, D., Swartzendruber, D.C., Squier, C.A., Wertz, P.W. (1998). *In vitro* reconstitution of *stratum corneum* lipid *lamellae*. *Biochim. Biophys*, *Acta*, 1372, 135-140.

(28) White, S.H., Mirejovsky, D., King, G.I. (1988). Structure of lamellar lipid domains and corneocyte envelopes of murine *stratum corneum*. An X-ray diffraction study. *Biochemistry*, 27, 3725-3732.

(29) Bouwstra, J.A., Gooris, G.S., van der Spek, J.A., Bras, W. (1991). Structural investigations of human *stratum corneum* by small-angle X-ray scattering. *J. Invest. Dematol.*, 6, 1005-1012.

(30) Bouwstra, J.A., Gooris, G.S., Cheng, K., Weerheim, A., Bras, W., Ponec, M. (1996). Phase behavior of isolated skin lipids. *J. Lipid Res.*, 37, 999-1011.

(31) Wertz, P.W., Madison, K.C., Downing, D.T. (1989). Covalently bound lipids of human *stratum corneum*. *J. Invest. Dermat*., 92, 109-111.

(32) Kalinin, A.E., Kajava, A.V., Steinert, P.M. (2002). Epithelial barrier function: assembly and structural features of the cornified cell envelope. *BioEssays*, 24, 789-800.

(33) Wertz, P.W., Schwartzendruber, D.C., Madison, K.C., Downing, D.T. (1987). Composition and morphology of epidermal cyst lipids. *J. Invest. Dermatol.*, 89, 419-425.

(34) Pappinen, S., Hermansson, M., Kuntsche, J., Somerharjn, P., Wertz, P., Urtti, A., Suhonen, M. (2008). Comparison of rat epidermal keratinocyte organotypic culture (ROC) with intact human skin: lipid composition and thermal phase behavior of the *stratum corneum*. *Biochim. Biophys. Acta*, 1778, 824-834.

(35) Madison, K.C., Swartzendruber, D.C., Wertz, P.M., Downing, D.T. (1987). Presence of intact intercellular *lamellae* in the upper layers of the *stratum corneum*. *J. Invest. Dermatol.*, 88, 714-718.

(36) Hill, J., Wertz, P. (2003). Molecular models of the intercellular lipid *lamellae* from epidermal *stratum corneum*. *Biochim. Biophys.*, Acta, 1616, 121-126.

(37) Plasencia, I., Norlen, L., Bagatolli, L.A. (2007). Direct visualization of lipid domains in human skin *stratum corneum´*s lipid membranes: effect of pH and temperature. *Biophys. J.*, 93, 3142-3155.

(38) Kessner, D., Kiselev, M., Dante, S., Hauβ, T., Lersch, P., Wartewig, S., Neubert, R.H.H. (2008). Arrangement of ceramide [EOS] in a *stratum corneum* lipid model matrix: new aspects revealed by neutron diffraction studies. *Eur. Biophys. J. with Biophys. Lett*., 37, 989-999.

(39) Kessner, D., Kiselev, M., Dante, S., Hauβ, T., Lersch, P., Wartewig, S., Neubert, R.H.H. (2008). Properties of ceramides and their impact on the *stratum corneum* structure: a review. *Skin Pharmacol. Physiol.*, 21, 58-74.

(40) McIntosh, T.J., Stewart, M.E., Downing, D.T. (1996). X-ray diffraction analysis of isolated skin lipids: reconstitution of intercellular lipid domains. *Biochemistry*, 35, 3649-3653.

(41) Kitson, N., Thewalt, J., Lafleur, M., Bloom, M. (1994). A model membrane approach to the epidermal permeability barrier. *Biochemistry*, 33, 6707-6715.

(42) Moore, D.J., Rerek, M.E., Mendelsohn, R. (1997). Lipid domains and orthorhombic phases in model *stratum corneum*: evidence from Fourier transform infrared spectroscopy studies. *Biochem. Biophys. Res. Commu.*, 231, 797-801.

(43) Lafleur, M. (1998). Phase behaviour of model *stratum corneum* lipid mixtures: an infrared spectroscopy investigation. *Can. J. Chem.*, 76, 1501-1511.

(44) Bouwstra, J.A., Thewalt, J., Gooris, G.J., Kitson, N. (1997). A model membrane approach to the epidermal permeability barrier: an X-ray diffraction study. *Biochemistry*, 36, 7717-7725.

(45) Bouwstra, J., Gooris, G.S., Dubbelaar, F.E., Weerheim, A.M., Ijzerman, A.P., Ponec, M. (1998). Role of ceramide 1 in the molecular organization of the *stratum corneum* lipids. *J. Lipid Res.*, 39, 186-196.

(46) Vaz, W. (2008). Lipid Bilayer Properties. In Wiley Encyclopedia of Chemical Biology. John Wiley & Sons, New York.

(47) Marsh, D. (1990). Handbook of Lipid Bilayers. CRC Press, Boca Raton.

(48) Gennis, R.B. (1988). Biomembranes, Molecular Structure and Function. Springer-Verlag, New York.

(49) Nagle, J.F. (1980) Theory of the main lipid bilayer phase transition. *Ann. Rev. Phys. Chem.*, 31,157-195.

(50) Albon, N., Sturtevant, J.M. (1978). Nature of the gel to liquid crystal transition of synthetic phosphatidylcholines. *Proc. Nat. Acad. Sci. USA*, 75, 2258-2260.

(51) Cevc, G., Marsh, D. (1987). Phospholipid bilayers, physical principles and models. John Wiley & Sons, New York.

(52) Tenchov, B., Koynova, R. (2012). Cubic phases in membrane lipids. *Eur. Biophys. J.*, 41, 841-850.

(53) Evans, D.F., Wennerström, H. (1994). The colloidal domain. Where physics, chemistry, biology, and technology meet. VCH Publishers, New York.

(54) Small, D.M. (1984). Lateral chain packing in lipids and membranes. *J. Lipid Res.*, 25, 1490-1500.

(55) Abrahamsson, S., Dahlen, B., Lofgren, H., Pascher, I. (1978). Lateral packing of hydrocarbon chains. *Prog. Chem. Fats other Lipids*, 16, 125-143.

(56) Coelho, F.P., Vaz, W.L.C., Melo, E. (1997). Phase topology and percolation in two-component lipid bilayers: a Monte Carlo approach. *Biophysical J.*, 72, 1501-1511.

(57) Rhines, F.N. (1956). Phase Diagrams in metallurgy, their development and application. McGraw-hill Book Company, New York.

(58) Shapiro, D., Flowers, H.M. (1961). Synthetic studies on sphingolipids.6. Total synthesis of cerasine and phrenosine. *J. Am. Chem. Soc.*, 83, 3327-3332.

(59) Shah, J., Atienza, J.M., Duclos, R.I.Jr., Rawlings, A.V., Dong, Z., Shipley, G.G. (1995). Structural and thermotropic properties of synthetic C16:0 (palmitoyl) ceramide: effect of hydration. *J. Lipid Res.*, 36, 1936-1944.

(60) Dahlén, B., Pascher, I. (1972). Molecular arrangements in sphingolipids: crystal structure of N-tetracosanoylphytosphingosine. *Acta Crystallogr. B*, 28, 2396-2404.

(61) Pascher, I., Sundell, S. (1992). Molecular arrangements in sphingolipids: crystal structure of the ceramide N-(2D,3D-dihydroxyoctadecanoyl)-phytosphingosine. *Chem. Phys. Lipids*, 61, 79-86.

(62) Pascher, I., Lundmark, M., Nyholm, P.G., Sundell, S. (1992). Crystal structures of membrane lipids. *Biochim. Biophys. Acta*, 1113, 339-373.

(63) Dahlen, B., Pascher, I. (1979). Molecular arrangements in sphingolipids. Thermotropic phase behavior of tetracosanoylphytosphingosine. *Chem. Phys. Lipids*, 24,119-133.

(64) Vaknin, S.K., Kelley, M. (2000). The structure of D-*erythro*-C18 ceramide at the air-water interface. *Biophys. J.*, 79, 2616-2623.

(65) Scheffer, L., Solomonov, I., Weygand, M.J., Kjaer, K., Leiserowitz, L., Addedi, L. (2005). Structure of cholesterol/ceramide monolayer mixtures: implications to the molecular organization of lipid rafts. *Biophys. J.*, 88, 3381-3391.

(66) Chen, H., Mendelsohn, R., Rerek, M., Moore, D.J. (2000). Fourier transform infrared spectroscopy and differential scanning calorimetry studies of fatty acid homogeneous ceramide 2. *Biochim. Biophys.*, *Acta,* 1468, 293-303.

(67) Moore, D., Rerek, M. (1997). FTIR Spectroscopy studies of the conformational order and phase behaviour of ceramides. *J. Phys. Chem. B*, 101, 8933-8940.

(68) Rerek, M., Chen, H.C., Markon, C.B., van Wych, D., Garidel, P., Mendelsohn, R., Moore, D.J., (2001). Phytosphingosine and sphingosine ceramide headgroup hydrogen bonding: structural insights through thermotropic hydrogen/deuterium exchange. *J. Phys. Chem. B*, 105, 9355-9362.

(69) Jendrasiak, G., Smith, R. (2001). The effect of the choline head group on phospholipids hydration. *Chem. Phys. Lipids*, 113, 55-66.

(70) Carrer, D.C., Maggio, B. (1999). Phase behavior and molecular interactions in mixtures of ceramide with dipalmitoylphosphatidylcholine. *J. Lipid Res.*, 40, 1978-1989.

(71) Silva, L., de Almeida, R.F., Fedorov, A., Matos, A.P., Prieto, M. (2006). Ceramide-platform formation and induced biophysical changes in a fluid phospholipid membrane. *Mol. Membrane Biol*., 23, 137-148.

(72) Holopainen, J.M., Lemmich, J., Richter, F., Mouritsen, O.G., Rapp, G., Kinnunen, P.K. (2000). Dimyristoylphosphatidylcholine/C16:0-ceramide binary liposomes studied by differential scanning calorimetry and wide- and small-angle X-ray scattering. *Biophys. J.*, 78, 2459-2469.

(73) Sot, J., Arandi, F.J., Collado, M.I., Goni, F.M., Alonso, A. (2005). Different effects of long- and short-chain ceramides on the gel-fluid and lamellar-hexagonal transitions of phospholipids: a calorimetric, NMR, and X-ray diffraction study. *Biophys. J.*, 88, 3368-3380.

(74) Goni, F.M., Alonso, A. (2006). Biophysics of sphingolipids I. Membrane properties of sphingosine, ceramides and other simple sphingolipids. *Biochim. Biophys. Acta,* 1758, 1902-1921.

(75) Craven, B.M. (1976). Crystal structure of cholesterol monohydrate. *Nature*, 260, 727-729.

(76) Shieh, H., Hoard, L., Nordman, C. (1977). Crystal structure of anhydrous cholesterol. *Nature*, 267, 287-289.

(77) Loomis, C., Shipley, G., Small, D. (1979). The phase behavior of hydrated cholesterol. *J. Lipid Res.*, 20, 525-535.

(78) McConnell, H., Vrljic, M. (2003). Liquid-liquid immiscibility in membranes. *Annu. Rev. Biophys. Biomol. Struct.*, 32, 469-92.

(79) McConnell, H., Radhakrishnan, A. (2003). Condensed complexes of cholesterol and phospholipids. *Biochim. Biophys. Acta,* 1610, 159-173.

(80) Simons, K., Vaz, W.L.C. (2004). Model systems, lipid rafts, and cell membranes. *Annu. Rev.Biophys. Biomol. Struct.*, 33, 269-295.

(81) Ipsen, J.H., Karlstrom, G., Mouritsen, O.G., Wennerstrom, H., Zuckermann, M.J. (1987). Phase equilibria in the phosphatidylcholine-cholesterol system. *Biochim. Biophys. Acta*, 905, 162-172.

(82) Chong, P.L. (1994). Evidence for regular distribution of sterols in liquid crystalline phosphatidylcholine bilayers. *Proc. Natl. Acad. Sci. USA*, 91, 10069-10073.

(83) Huang, J. Feigenson, G. (1999). A microscopic interaction model of maximum solubility of cholesterol in lipid bilayers. *Biophys. J.*, 76, 2142-2157.

(84) Small, D.M. (1986). Handbook of lipid research. Vol.4 The physical chemistry of lipids, Plenum Press, New York.

(85) Koynova, R., Tenchov, B. (2001). Interactions of surfactants and fatty acids with lipids. *Curr. Opin. Colloid Interface Sci.*, 6, 277-286.

(86) Seddon, J.M., Templer, R.H., Warrender, N.A., Huang, Z., Cevc, G., Marsh, D. (1997). Phosphatidylcholine-fatty acid membranes: effects of headgroup hydration on the phase behaviour and structural parameters of the

gel and inverted hexagonal (H_{II}) phases. *Biochem. Biophys. Acta,* 1327, 131-147.

(87) Abraham, W., Downing, D.T. (1991). Deuterium NMR investigation of polymorphism in *stratum-corneum* lipids. *Biochim. Biophys. Acta,* 1068, 189-194.

(88) Bouwstra, J.A., Gooris, G.S., Dubbelaar, F.E.R., Ponec, M. (2000). Phase behavior of skin barrier model membranes at pH 7.4. *Cell.Mol.Biol.*, 46, 979-992.

(89) Ouimet, J., Croft, S., Pare, C., Katsaras, J., Lafleur, M. (2003). Modulation of the polymorphism of the palmitic acid/cholesterol system by the pH. *Langmuir*, 19, 1089-1097.

(90) Ginsburg, G.S., Small, D.M., Hamilton, J.A. (1982). Temperature-dependent molecular motions of cholesterol esters: a ^{13}C NMR study. *Biochemistry*, 21, 6857-6867.

(91) Small, D.M. (1970). The physical state of lipids of biological importance: cholesterol esters, cholesterol triglyceride. In Surface chemistry of biological systems. Blank, M., Ed., Plenum Press, New York, pp. 55-80.

(92) Janiak, M., Small, D., Shipley, G. (1979). Interactions of cholesterol esters with phospholipids: cholesteryl myristate and dimyristoyl lecithin. *J. Lipid Res.*, 20, 183-199.

(93) Spooner, P., Hamilton, J.A., Grantz, D.L., Small, D.M. (1986). The effect of free-cholesterol on the solubilization of cholesteryl oleate in phosphatidylcholine bilayers – a ^{13}C- NMR study. *Biochim. Biophys. Acta*, 860, 345-353.

(94) Mackay, A., Wassall, S.R., Valic, M.I., Gorrissen, H., Cushley, R.J. (1980). ^{2}H and ^{31}P-NMR studies of cholesteryl palmitate in sphingomyelin dispersions. *Biochim. Biophys. Acta*, 601, 22-33.

(95) Smaby, J., Brockman, H. (1987). Acyl unsaturation and cholesteryl ester miscibility in surfaces – formation of lecithin-cholesteryl esters complexes. *J. Lipid Res.*, 28, 1078-1087.

(96) Luzzati, V. (1968). X-ray diffraction studies of lipid-water systems. In Biological membranes. Chapman, D., Ed., vol.1, Academic Press, New York, pp. 71-123.

(97) Hamilton, J.A., Small, D.M. (1982). Solubilization and localization of cholesteryl oleate in egg phosphatidylcholine vesicles – a C-13 NMR-study. *J. Biol. Chem.*, 257, 7318-7321.

(98) Hamilton, J.A., Fujito, D.T., Hammer, C.F. (1991). Solubilization and localization of weakly polar lipids in unsonicated egg phosphatidylcholine – a C-13 MAS NMR- study. *Biochemistry*, 30, 2894-2902.

(99) Rattle, H. (1995). An NMR primer for life scientists. Partnership Press, Great Britain.

(100) Beckmann, N. (1995). Carbon-13 NMR spectroscopy of biological systems. Academic press. New York.

(101) Pines, A., Gibby, M.G., Waugh, J.S. (1973). Proton-enhanced NMR of dilute spins in solids. *J. Chem. Phys.*, 59, 569-590.

(102) Nagle, J.F., Tristram-Nagle, S. (2000). Structure of lipid bilayers. *Biochem. Biophys. Acta*, 1469, 159-195.

2. Phase behavior of aqueous dispersions of mixtures of N-palmitoyl ceramide and cholesterol: a lipid system with ceramide-cholesterol crystalline lamellar phases

The co-authors of the work presented in this Chapter had the following contributions:

-M.J. Capitán and J. Álvarez analyzed the WAXS data and deduced the crystal structures,

- S. Funari is the beamline scientist of A2 of Hasylab at DESY, optimized the experimental setup for our measurements, made the preliminary SAXS and WAXS conversion and helped with the SAXS interpretation,

- M.J. Capitán and M.H. Lameiro made measurements at the beamline A2 of Hasylab at DESY.

It was published as:

Souza, S.L., Capitán, M.J., Álvarez, J., Funari, S., Lameiro, M.H., Melo, E. (2009). Phase behavior of aqueous dispersions of mixtures of N-Palmitoyl ceramide and cholesterol: a lipid system with ceramide-cholesterol crystalline lamellar phases. *J. Phys. Chem. B*, 113, 1367-1375.

2.1. Abstract

Ceramides are particularly abundant in the *stratum corneum* lipid matrix, where they determine its unusual mesostructure, are involved in the lateral segregation of lipid domains in biological cell membranes, and are also known to act as signaling agents in cells. The importance attributed to ceramides in several biological processes has heightened in recent years, demanding a better understanding of their interaction with other membrane components, namely cholesterol. Structural data concerning pure ceramides in water are relatively scarce and this is even more the case for mixtures of ceramides with other lipids commonly associated with them in biological systems. We have derived the thermotropic binary phase diagram of mixtures of N-palmitoyl-D-*erythro*-sphingosine, C16:0-ceramide, and cholesterol in excess water, using differential scanning calorimetry and small and wide angle X-ray diffraction. These mixtures are self-organized in lamellar mesostructures that, between other particularities, show two ceramide: cholesterol crystalline phases with molar proportions that approach 2:3 and 1:3. The 2:3 phase crystallizes in a tetragonal arrangement with a lamellar repeat distance of 3.50 nm, which indicates an unusual lipid stacking, probably unilamellar. The uncommon mesostructures formed by ceramides with cholesterol should be considered in the rationalization of their singular structural role in biological systems.

2.2. Introduction

Biological membranes are self-associations of amphipathic bilayer-forming lipids, and their physical-chemical properties reflect the characteristics of these lipids in interaction with other components, such as cholesterol and proteins. Ceramides, present in many membranes, are well documented as having a

biochemical role as signal transducers in cell differentiation and apoptosis[1,2]. They have not been considered “structuring lipids” of the cell membranes, a role that is commonly associated with lipids such as cholines, ethanolamines, sphingomyelin, etc. Recently, ceramides have been found to assist the formation of intermediate non-lamellar phases[3,4], to interact with cholesterol and sphingomyelin and modify the stability and composition of liquid ordered domains[5-8], and to induce protein aggregation[9]. Some authors also claim to have found ceramide-rich rigid domains not only in model membranes of cholines containing ceramides but also in cells[10,11]. If confirmed, this is an unforeseen discovery, because rigid domains were believed to be absent from cell membranes. Such domains can only arise because of the particularities of the interactions of ceramides between them and with other lipids. It stands to reason that the unusual biophysical properties of ceramides, alone and in interaction with other membrane components, are currently attracting much attention.

Over the last few decades, ceramides were mainly studied in the context of the only biological tissue where they were well known to be structural ingredients: the lipid matrix of the *stratum corneum* (SC), the uppermost layer of the skin of mammals. Its main components are ceramides (ca. 47 weight %), cholesterol (ca. 24 weight %) and saturated fatty acids (ca. 11 weight %)[12]. The SC lipids self-organize in lamellar structures with the remarkable thickness of ca. 13 nm, but the details of the molecular organization of the above-mentioned lipids in these *lamellae* is still unknown. There are many works dealing with these, or related, lipid mixtures, but most of them use complex lipid blends, and focus, not on the lipids themselves, but in replicating/explaining the properties of the SC[13].

Despite the recent increased interest in ceramides, the physical-chemical properties of mixtures involving ceramides have not been the object of systematic studies similar to those existing for ubiquitous lipids, such as cholines. However, ceramide-containing mixtures form lipid aggregates with unique structural properties[14,15] that deserve a more systematic approach.

In this work, we study the thermotropism of mixtures of *N*-palmitoyl-D-*erythro*-sphingosine (C16-Cer) with cholesterol (Ch) in excess water at low ionic strength (100 mM). From differential scanning calorimetry (DSC) we obtain the enthalpically active transitions and the plausible phase boundaries; these boundaries are subsequently checked, and the phases structurally characterized, by simultaneous small and wide angle X-ray scatter (SAXS and WAXS) as a function of temperature. Our work aims a better understanding of the interaction between ceramides and cholesterol, a key interaction for the properties of the lipid matrix of SC and for the perturbation/induction of the formation of liquid ordered or rigid domains.

A highly relevant and exhaustive study of synthetic C16-Cer was presented by Shah *et al.*[16], who examined its thermotropism and structure by DSC, SAXS and WAXS in the presence and absence of water. Fourier transform infrared (FTIR) has been used for accessing the short-range structure and the dynamics of C16-Cer in aggregates[17-19]. Comparison of the dependence of the chain dynamics and thermotropic properties of C14-Cer, C16-Cer, C18-Cer and C20-Cer using FTIR show little dependence on chain length, at least much weaker than that in equivalent cholines[18]; however, our preliminary results with C24:0-ceramide:Ch reveal a phase behavior very different from that of C16:0. Most other works with synthetic ceramides use ω-hydroxylated derivatives, phytosphingosine derivatives, and since the H-bond network will be different, the results are not directly comparable with ours. Another approach to the self-organization of ceramides, pure or in mixtures with other lipids, is the study of the characteristics of the monolayers formed at the air/water interface[20-22]. Of particular relevance for our work are the results of Scheffer *et al.*[22] concerning Langmuir monolayers of mixtures of ceramide C16 with cholesterol, in concentrations that range from pure cholesterol to pure ceramide.

2.3. Materials and methods

Reagents

Synthetic (2S, 3R, 4E)-2-hexadecanoylaminooctadec-4-ene-1,3-diol and egg ceramide, 84% C16, were obtained from Avanti Polar Lipids, stearic acid from BDH, and cholesterol from Sigma; benzene is from Panreac and methanol from Merck, both HPLC grade; boric acid, potassium chloride, etylenediaminetetracetic acid, EDTA, and sodium hydroxide were from Riedel-de Haën. All chemicals were used without further purification with the exception of Ch, which was recrystallized from methanol. Water used for buffer preparation was double distilled and further purified with an Elgastat UHQ-PS system. Borate buffer was prepared by adding NaOH 1 M to a solution 30 mM in boric acid, 70 mM in NaCl and 0.2 mM in EDTA until pH = 9.0 was reached.

Preparation of lipid dispersions

It is known that lipid mixtures containing high relative percentage of cholesterol are prone to lipid demixing during organic solvent removal[23]. To avoid lipid separation, the organic solvent in which the lipids are dissolved was removed by freeze-drying. The subsequent hydration was done at a temperature above the main transition temperature of C16-Cer (93 ºC). In the course of the work with ceramide containing systems, we have found that if there is lipid demixing in the preparation step it is impossible to induce homogenization by posterior annealing. The protocol used proved to give reliable and reproducible samples.

Procedure: Adequate amounts of lipid stock solutions of each lipid in benzene:methanol, 7:3 (v:v), were mixed in the intended proportions and allowed to stand for 30 minutes at room temperature with occasional vortexing. The system was subsequently frozen to –20 ºC and left at this temperature for at least 2 hours, after which it was freeze-dried. To the resulting powder,

borate buffer (pH = 9) at 98 º C was rapidly added under vortexing such that a dispersion 10 mM in total lipid was obtained. The suspension was maintained for 30 min at 98 ºC to allow for complete hydration. The same protocol was used for all the preparations.

Due to the high temperatures and pH used in the experiments, the possibility of decomposition or hydrolysis of the ceramide was a matter of concern. Thin layer chromatography (TLC) performed after DSC did not reveal additional spots. It must be added that there is no justification for the use of pH 9.0 in this study. We opted for this high pH because a related work required the use of high pH; however, as expected, no differences in the X-ray diffractograms were observed between samples of C16-Cer:Ch measured at pH 4, 7 or 9. In fact, the interfaces lipid water are not charged and the amide group is not susceptible to change the protonation state in this pH range.

Differential scanning calorimetry

As recognized by several authors[16,17,24-26] systems containing ceramides are prone to be trapped into metastable states upon cooling. This is evidenced by the observation of exothermic events prior to the main transition in subsequent heating runs. The method we found to be safe to avoid non-equilibrated systems, consisted in rejecting the first scan done at 1 ºC/min until 98 ºC, where C16-Cer is fluid, cool the sample at the rate of 1 ºC/min or slower, and only consider the second and/or subsequent heating scans. Alternatively, the samples were heated and cooled in a computer-controlled cryostat following exactly the protocol described for the first heating and cooling runs in the microcalorimeter chamber, and then transferred to the calorimeter chamber. The heating thermograms obtained after this annealing protocol do not show the exotherm observed for out-of-equilibrium systems. The thermograms were obtained at a lipid concentration of 10 mM, and with a heating rate of 1 ºC/min, unless otherwise stated in the text, and subsequently cooled back to 15 ºC at the same speed in a calorimeter VP-DSC from MicroCal, Northampton, MA.

X-Ray diffraction

SAXS and WAXS data were collected simultaneously at the synchrotron radiation X-ray scattering facility on the Soft Condensed Matter beamline A2 of HASYLAB at the storage ring DORIS III of the Deutsches Elektronen Synchrotron (DESY), using a setup previously described[27]. The samples were prepared as for DSC, except that the 4.0 micromole of lipid were hydrated with only 0.3 ml of buffer. After the hydration step, the lipid and part of the buffer in suspension were transferred to glass capillary tubes with 1.0 mm diameter and 0.01 mm wall, Markröhrchen, Germany, subsequently closed and the samples annealed in a cryostat as previously explained. The more convenient alternative of inserting the lyophilized lipids in the capillary and adding buffer above the T_m of C16-Cer was tried, but the resulting samples were not macroscopically uniform. For each composition, three samples were prepared independently, two sets of data were collected for each sample, and the sample was submitted to a new complete annealing cycle between measurements. The C16-Cer:Ch suspensions consist of relatively rigid granules differing in physical appearance, raising the possibility of differences in composition. When in doubt about the uniformity of the sample in the capillary, different regions of the sample were examined, but identical diffractograms were obtained in all cases.

The temperature of the samples in the sample holder was continuously raised from 20 to 98 ºC at 1.0 ºC/min, maintained at the maximum for 4 min and some samples were then cooled to the lowest temperature at the same scan rate. Every 120 s (equivalent to 2 ºC), a local shutter, normally closed to protect the sample, was opened for 20 s, the interval during which SAXS and WAXS data were continuously acquired. The actual temperature of the sample holder at the beginning of each data collection was registered together with the data.

Positions of the observed peaks were converted into distances, *d*, or $s = 1/d$, after calibration using standards with well-defined scattering patterns. Rat tail tendon and tripalmitin were used to calibrate the SAXS and WAXS regions, respectively. The background scatter of identical capillary tubes with buffer was subtracted from all diffractograms. The evaluated error in *s* is relatively constant for each of the regions considered. In the range from 0.10 until 0.39 nm^{-1}, SAXS, it is of ± 0.001 nm^{-1} and for the region of 1.78 $nm^{-1} < s < 3.05$ nm^{-1} where the WAXS was measured it is of ± 0.005 nm^{-1}.

2.4. Results

Thermal studies

The heating thermograms obtained by DSC of aqueous dispersions of C16-Cer:Ch with concentrations ranging from 0:1, pure Ch, to 1:0, pure C16-Cer, are presented in Figure 2.1. a.

The cooling scans at 1 ºC/min present also a single exothermic event but with a large hysteresis, denoting the slow kinetics of the structural arrangement of the system (data not shown). No significant differences were observed for heating or cooling scans as slow as 0.1 ºC/min, leading us to conclude that at 1 ºC/min the system evolves in equilibrium. However, along the heating subsequent to a cooling scan at a rate of about 6.5 ºC/min a strong and broad exotherm beginning at around 60 ºC is observed (data not shown). We verified that this behavior, previously reported in the mentioned work of Shah *et al.*, is due to the system being retained in a metastable structure, and is common to many pure ceramides and lipid mixtures involving ceramides.

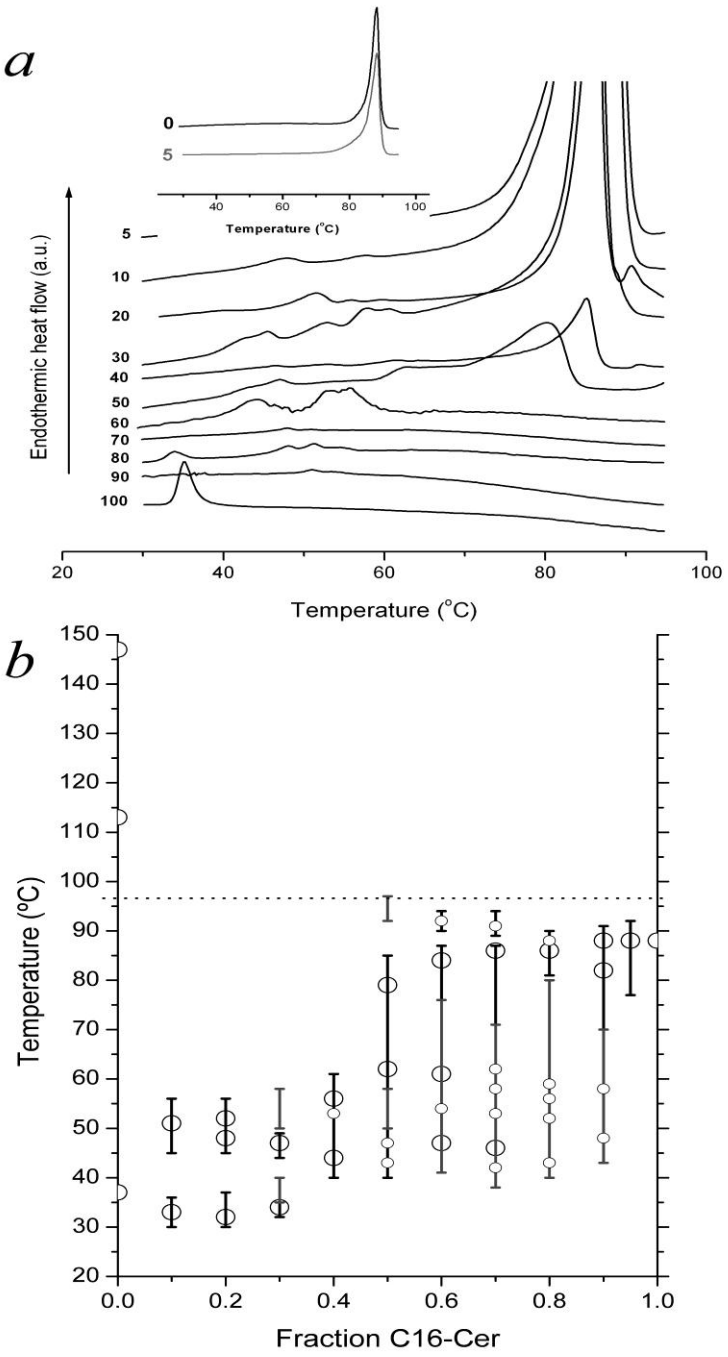

Fig. 2.1. – *a*: DSC traces of mixtures C16-Cer:Ch ranging from 5 to 100 mol % Ch. Only the lower portion of the plot is presented to better evaluate the transitions detected, and the traces have been vertically shifted for clarity. In the insert, a complete DSC trace for pure C16-Cer compared with that of 5 mol % Ch. *b*: Plot of the transitions obtained by DSC for the several

mixtures analyzed. In the diagram, the larger circles represent well-defined peaks while the smaller ones are placed at the temperatures where small peaks or shoulders appear. The vertical lines represent regions where endothermic events are observed, black lines for the stronger endotherms. The two upper transitions of Ch are from the literature, since our thermograms finish at the temperature indicated by the dotted line.

In the mixtures of C16-Cer and Ch several peaks and shoulders are observed in the thermograms, Figure 2.1. a. In the absence of further information about the meaning of these thermotropic events we present a first tentative phase diagram in Figure 2.1. b where the lines are derived from the beginning and end of the observed endotherms. In the same figure, the various apexes and shoulders are indicated, their meaning to be clarified after the X-ray experiments. From the DSC data it seems evident that for more than 70 mol% Ch a transition is present at about 32 ºC, and it may extend until ca. 57 ºC. The transition, or transitions, of the mixtures containing less than 50% Ch extend from about 45 to 85 ºC. For the mixtures with low Ch content we also observe a small peak at high temperature, appearing as a shoulder of the main endotherm or as a well-defined peak with T_m = 93 ºC for the sample with 20 mol % Ch. This may result from the interaction of fluid C16-Cer with Ch in states not present in the temperature range of our study.
In the pure cholesterol thermogram, the endotherm at 37 ºC in the heating run, Figure 2.1. a, corresponds to the transition between the two polymorphic forms of anhydrous cholesterol[28,29].

X-ray diffraction studies

To characterize the structure of the several thermotropic transitions of the phases observed by DSC, C16-Cer:Ch mixtures with relative molar compositions of 100:0, 95:5, 80:20, 54:46, 45:55, 35:65, 30:70, 20:80, 10:90 and 0:100, were investigated by SAXS and WAXS. In these studies, only the synthetic ceramide was used. The plots of the SAXS and WAXS regions for three key mixtures as a function of temperature are presented in Figure 2.2. and a synopsis of the data presented in Table 2.1

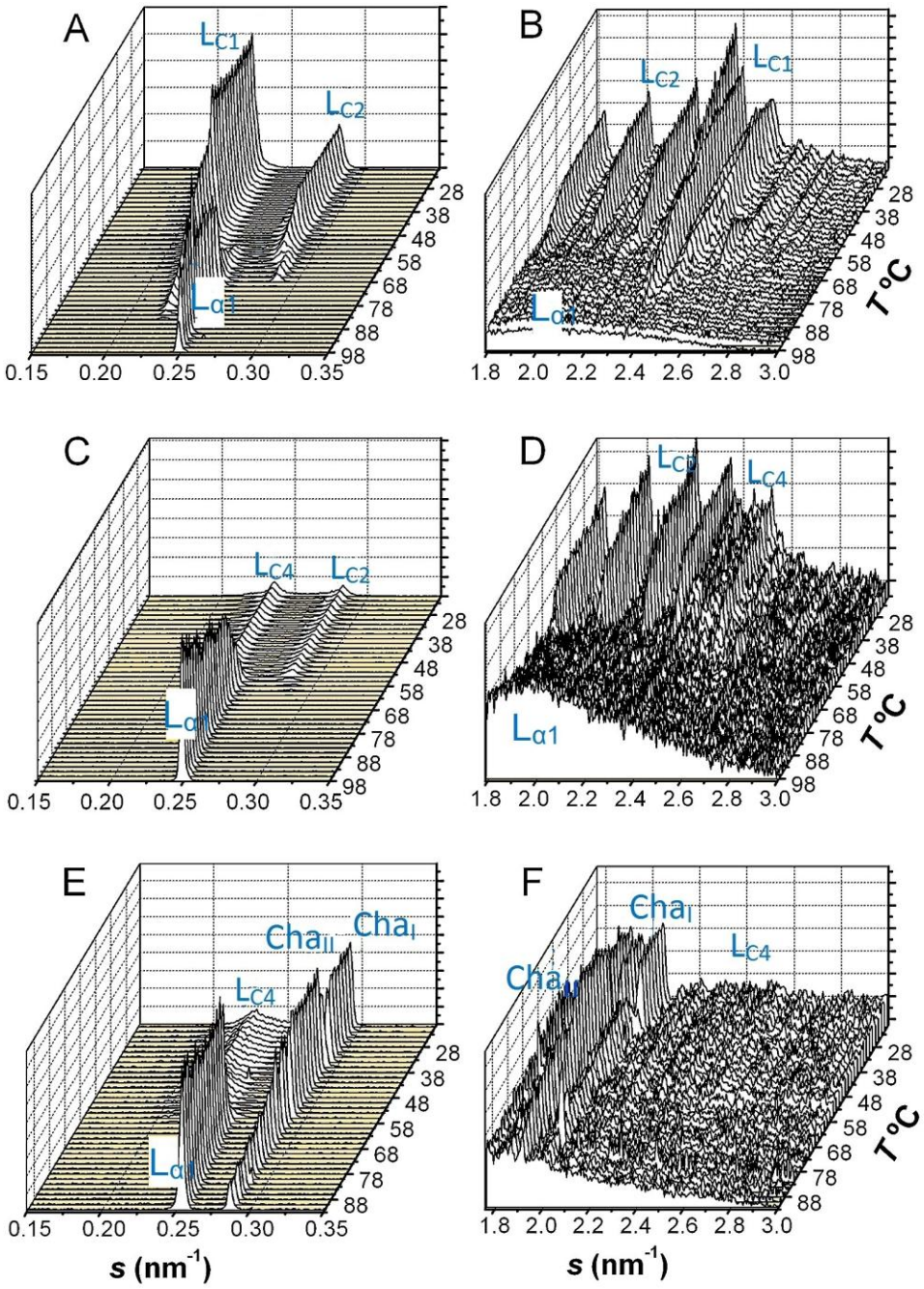

Figure 2.2. - WAXS and SAXS measured simultaneously as a function of temperature in steps of 2 ºC for the mixtures: 55 mol % Ch A and B, 65 mol % Ch C and D, 80 mol % Ch E and F. All diffractograms are from heating scans obtained at a rate of 1 ºC/min.

Table 2.1. - Characteristic X-ray diffraction peaks in values of *s* (nm^{-1}), for the several phases identified in the text for the relevant temperatures within the range of existence.

	C16-Cer	**C16-Cer:Ch (ca. 2:3)**	**C16-Cer:Ch (ca. 1:3)**	**Ch**	
Crystalline phases	**L_{C1}**	**L_{C2}**	**L_{C4}**	**Ch_m**	**$Ch_{al\ \&\ II}$**
22 ºC	0.224	0.283	0.236	0.288	0.289
	2.38, 2.41, 2.46, 2.55	1.83, 2.02, 2.21	2.3-2.6	1.84, 2.56, 2.61	1.82, 1.91, 1.96, 2.04
40 ºC					0.287
					1.82, 1.85, 1.90,1.95, 1.99
Fluid phases		**$L_{\alpha 1}$**			
82 ºC	0.292				
88 ºC		0.247 – 0.251			

Mixtures from pure C16-Cer to pure Ch below 30 ºC

In Figure 2.3. the small and wide-angle diffractograms of several mixtures at 22 ºC are presented side by side.

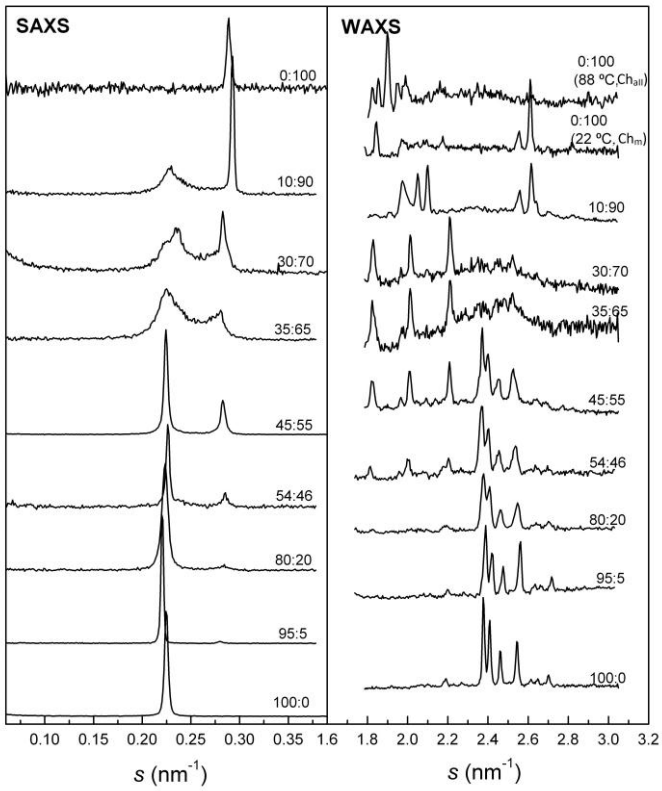

Figure 2.3. - SAXS (left) and WAXS (right) at 22 ºC for several measured C16-Cer:Ch mixtures ranging from pure C16-Cer to pure Ch. Also shown the WAXS of the Ch_{all} polymorph of Ch at 88 ºC.

The small angle region of the diffractogram of pure C16-Cer in excess water displays a single strong diffraction at s = 0.224 nm^{-1}. At this temperature, the wide-angle region is dominated by several intense diffractions, at 2.38, 2.41, 2.46 and 2.55 nm^{-1}, and other much less intense peaks at 2.19, 2.62, 2.65 and 2.70 nm^{-1}. Upon addition of 5 to 55 mol % Ch, a new peak appears in the small angle region, with reflection at 3.50 nm (s = 0.283 nm^{-1}) which is accompanied by three very intense and sharp diffractions at 1.83, 2.02, 2.21 nm^{-1} that appear and disappear always in consonance with the small-angle signal. In this range, the only apparent change in the SAXS with the variation of Ch

concentration is an increase, concomitant with the rise of the Ch content, in the intensity of the 0.283 nm^{-1} peak relative to that at s = 0.224 nm^{-1}. This diffraction is not far from that characteristic of free Ch but in no way can it be attributed to unmixed Ch due to the absence of the Ch peaks in the wide-angle region. In fact, in one of the 45:55 samples non-mixed Ch was present; here a typical SAXS band of Ch monohydrate together with the Ch WAXS pattern coexists with the new phase, confirming that it is distinct from Ch. The phase that gives origin to this SAXS/WAXS pattern will hereafter be designed as the L_{C2} phase. Not noticeable in the drawings, due to the difference of intensities, a broad diffraction centered at 0.230 nm^{-1} smears the base of the very sharp and intense SAXS peak of C16-Cer in this range of compositions. This wide band is present in only some samples, and in those where it appears a corresponding WAXS signal is not discernible; as we will see later, it seems to arise from a contamination of phases found at higher Ch concentrations.

Small gradual changes in the ceramide lamellar repeat spacing are observed with the addition of Ch, eg. 0.220 nm^{-1} for the mixtures with 20 mol% Ch content and a return to the original 0.224 nm^{-1} for the 45:55 C16-Cer: Ch composition (compare in Figure 3 the traces for 100, 95, 80 and 54 mol% C16-Cer). This points towards the existence of a residual solubility of Ch in the ceramide main phase. The phase giving rise to these diffractions is pure, or almost pure, C16-Cer, and will hereafter be called the L_{C1} phase.

For the samples with 45 and 55 mol % Ch, the 1.83, 2.02, 2.21 nm^{-1} diffractions are prevalent in WAXS, but the original s = 0.224 nm^{-1} C16-Cer phase diffraction is still present, and the position and relative intensity of the peaks is maintained along the entire range of concentrations. The only change observed is a decrease in the WAXS diffraction intensity concomitant with that of the 0.224 nm^{-1} L_{C1} peak in the SAXS.

For 65 and 70 mol % Ch the L_{C2} phase diffractions remain strong in WAXS as well as in SAXS (peak at s = 0.283 nm^{-1}). However, a new set of wide-angle peaks appear in the same region as that of C16-Cer, but with a clearly different pattern from that of C16-Cer. This new set replaces the diffractions of the L_{C1}

phase observed for lower concentrations. The WAXS signal also contains a new group of lines at 1.99, 2.06 and 2.11 nm^{-1} difficult to discriminate from those of phase L_{C2} and Ch. In the SAXS region the signal of the L_{C1} phase is no longer visible, and besides the already mentioned L_{C2} sharp diffraction at 0.283 nm^{-1}, a broad peak at 0.230 nm^{-1} and/or a sharp one at 0.236 nm^{-1} appears. Both are thermally connected to the new C16-Cer-like diffraction appearing in the WAXS, and define another phase, apparently lamellar, here named L_{C4}. In one sample where the broad 0.230 nm^{-1} band exists at 22 ºC, unaccompanied by the 0.236 nm^{-1} peak, the wide-angle signal due to the L_{C4} phase is strong and well defined. In this sample, above 44 ºC the broad band converts into the typical 0.236 nm^{-1} peak without change in the WAXS. We conclude that the broad band is the L_{C4} phase. This band seems to coincide with the already mentioned weak signal, masked by the L_{C1} phase peak, sometimes appearing at low Ch content.

For the C16-Cer:Ch composition 10:90 mol ratio, the WAXS signal is essentially that of Ch monohydrate (see below). Besides Ch monohydrate, here named phase Ch_m, phase L_{C4} is also detectable in both SAXS and WAXS, as evidenced by a weak 0.230 nm^{-1}, band that at higher temperature transforms into a small peak at 0.236 nm^{-1} and peaks at 1.99, 2.06 and 2.11 nm^{-1}. The results from the sample with 80 mol % Ch are identical, but the relative intensity of the SAXS diffraction of pure Ch is much smaller (trace not shown in Figure 3).

For 100% Ch at 22 ºC we have obtained the SAXS and WAXS signals characteristic of monohydrate cholesterol, Ch_m, at 1.84, 2.56 and 2.61 nm^{-1}, as expected for samples that were left for more than 24h at room temperature in excess water[28].

Thermotropic behavior of pure C16-Cer

The variation of the diffractograms of pure C16-Cer between 20 and 98 ºC is presented in Figure 2.4.: heating in panels A and B, and cooling in C and D.

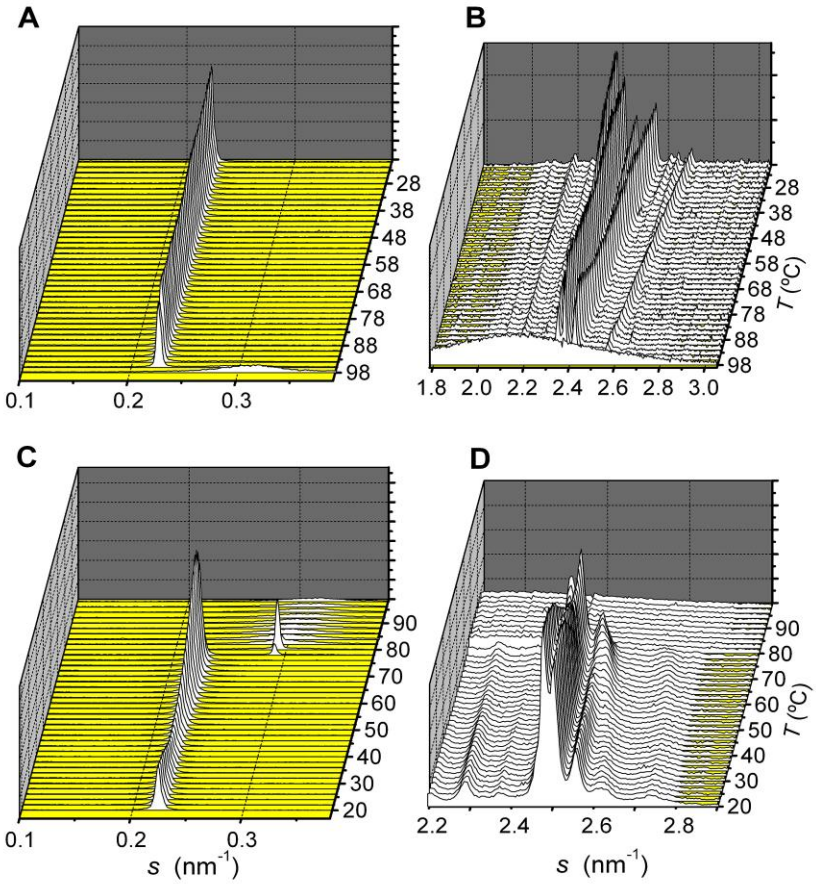

Figure 2.4. - Plots of the SAXS and WAXS of the sample of pure C16-Cer as a function of temperature (only the region of interest of the WAXS is shown), where consecutive diffractograms are spaced by 2 ºC. Panels A and B refer to the heating and C and D to the cooling scans.

In the small angle region, panel A, the single diffraction peak at s = 0.224 nm^{-1} (4.46 nm) remains constant with the increase of temperature. At 92 ºC the intensity of this signal begins to decrease approaching zero at 98 ºC. Simultaneously a new very broad band develops centered at 0.317 nm^{-1} (3.15 nm). On the WAXS side, panel B, the evolution of the signal with temperature is complex, and somewhat similar to what has been previously described as a Y shape pattern[30]. After complete melting, 98 ºC, only a broad diffraction

remains, centered at 2.2 nm^{-1} (0.45 nm) typical of stacked melted aliphatic hydrocarbon chains.

The diffractograms obtained during the cooling of C16-Cer at 1 ºC/min show the large hysteresis already observed and commented upon in the DSC section. Crystal formation only begins with a temperature lag of ca. 14 ºC, never attaining the well-resolved WAXS of the samples kept for several days at room temperature or below. What is very particular is that in the small angle the broad band of the melted sample centered at 0.317 nm^{-1} (3.15 nm) slowly shifts towards smaller *s* values until it converts into a sharp signal at 0.292 nm^{-1} (3.42 nm) at 82 ºC. This diffraction was not observed in the heating run, where the 0.224 nm^{-1} (4.46 nm) peak directly converts in the broad at 0.317 nm^{-1} band. This diffraction is not accompanied by an observable change of the WAXS diffraction, which maintains the appearance characteristic of melted chains, nor by a thermal event observable in DSC.

Thermotropic behavior of pure cholesterol

For pure Ch we obtained the well known dependence of the crystalline forms on the recent thermal history of the sample[28,31]. In the samples left at low temperature for more than 24 h, Ch starts as monohydrate, phase Ch_m, with diffractions in the wide-angle region at 1.84, 2.56 and 2.61 nm^{-1}. Above 86 ºC these diffractions disappear and are replaced by Bragg reflections at 1.85, 1.86, 1.90 and 2.00 nm^{-1}, characteristic of anhydrous Ch in the polymorph II. In samples measured immediately after annealing above the temperature required for monohydrate to anhydrous transition, the 0.54 nm Bragg reflection (1.85 nm^{-1}) appears only at 36 ºC, the temperature at which the polymorph I converts into polymorph II[28,31]. The two polymorphs of anhydrous Ch are named hereafter Ch_{aI} and Ch_{aII}. There is no large difference in the (001) spacing between the several forms of Ch, always appearing at *ca.* 0.288 nm^{-1}, but a small variation of peak shape and relative intensity is observed for the transition from Ch_{aI} to Ch_{aII} at 36-38 ºC simultaneous with the appearance of the 1.85 nm^{-1} peak.

Thermotropic behavior of samples with 5, 20, 46 and 55 mol % cholesterol

The qualitative behavior of all these samples is identical in both SAXS and WAXS. From 20 ºC upwards the diffraction pattern described for low temperature is maintained until 62 ºC. Beyond this temperature the L_{C2} phase disappears within 2-4 degrees, and at still higher temperatures the L_{C1} phase coexists with a new sharp diffraction at 0.247 nm^{-1}, together with a broad band with maximum at 2.1 nm^{-1}. The growth of this diffraction is accompanied by the disappearance of the 0.224 nm^{-1} peak and the corresponding WAXS signal with the formation of the characteristic broad band of melted lipid chains, features indicating a fluid lipid bilayer, phase $L_{\alpha 1}$. In the low temperature range both L_{C1} and L_{C2} phases maintain their diffraction characteristics, indicative of a constant composition. Above 62 ºC the diffraction signal of the $L_{\alpha 1}$ phase drifts towards larger spacing because of the change in composition, and once the L_{C1} phase completely disappears, the $L_{\alpha 1}$ phase contracts, as usually observed with regular bilayers. The only oddity that conflicts with this simple scenario is the appearance, a few degrees below and above 62 ºC, of free Ch in most but not in all the samples.

Above a given temperature—90 ºC for the 46 mol % Ch and 86 ºC for the 55 mol % Ch—the only phase present is $L_{\alpha 1}$. At 94 ºC a new Bragg reflection appears at 0.275 nm^{-1} in the sample with 46 mol% Ch. Above this temperature and until the maximum observed, 98 ºC, the $L_{\alpha 1}$ phase coexists with this new fluid lamellar phase, data not shown. This transformation must correspond to the small endotherm observed in DSC above the main transition.

Thermotropic behavior of samples with 65 and 70 mol % cholesterol

These two samples have essentially the same diffraction patterns and no residue of the ceramide L_{C1} phase is left at these concentrations. In Figure 2.2 C and D the typical temperature evolution of the SAXS and WAXS of these mixtures is presented. Below 50 ºC the pattern is constant, with the presence

of only L_{C2} and L_{C4} phases. In many samples the diffraction of the L_{C4} phase in SAXS is broad, centered at 0.230 nm^{-1}. At 52 ºC the original L_{C2} phase disappears and only L_{C4} and $L_{\alpha 1}$ phases remain. Upon heating, this last phase increase in importance at the cost of L_{C4}. For the mixture with 65 mol % Ch the two phases are visible until 70 ºC, temperature above which only the $L_{\alpha 1}$ phase is present. For the composition with 70 mol % Ch the L_{C4} phase disappears at 64 ºC.

The above is a rough description of what happens in this concentration and temperature range. In fact, some other broad diffractions appear in the small angle region with no counterparts in the wide angle. Their presence is sample dependent and we have no reason to identify other phases, but we suspect that the scenario may be much more complicated than the one described.

Thermotropic behavior of samples with 80 and 90 mol % cholesterol

It has already been said that for these high Ch concentrations, at low temperatures the WAXS diffractogram has no residue of either the C16-Cer pattern or the L_{C2} phase, Figure 2.2 E and F. The signal of L_{C4} phase, small but visible in both the SAXS and WAXS, disappears between 58 and 60 ºC with the formation of the fluid $L_{\alpha 1}$ phase for both concentrations. As with the samples in the region with 65-70 mol % Ch, we observe a variable contribution of the broad 0.23 nm^{-1} band that converts into the L_{C4} phase characteristic repeat distance with increasing temperature. The maximum of the diffraction of the $L_{\alpha 1}$ phase shifts from 0.247 nm^{-1} (4.05 nm) for the ceramide rich compositions to larger values with the increase of Ch, attaining, for these C16-Cer:Ch mol ratios (saturated in Ch?) 0.248 nm^{-1} (4.39 nm). Ch is present at all temperatures but the conversion from monohydrate to anhydrous takes place at ca. 74 ºC for the 80:20 mixture and at ca. 78 ºC for the 90:10 composition. For the sample richer in Ch the WAXS structure is maintained until 98 ºC, the upper temperature reached in these experiments.

2.5. Discussion

Pure ceramide and L_{C1} phase

The single strong diffraction at s = 0.224 nm^{-1} (repeat spacing d = 4.46 nm) observed below T_m for pure ceramide indicates a lamellar phase, a bilayer structure, as previously suggested for this[16] and other ceramides in excess water[32-34]. At 88 ºC for the egg ceramide, and 93 ºC for C16-Cer, the melting of ceramide occurs (for the X-ray studies only the synthetic ceramide was used) with the formation of the typical 0.46 nm broad signal in the WAXS region, and the formation of a new 2.99 nm very broad reflection, Figure 2.4. The melting of the ceramide signal to a very broad SAXS band leaves no doubt that the melted ceramide does not maintain the regular lamellar structure even if some meso-order still exists. However, upon cooling, this large band gives rise to a sharp signal at 0.292 nm^{-1} with a lamellar repeat distance of 3.42 nm, Figure 2.4 C. This seems more a fluid structure where ceramides are laterally packed with headgroups facing both sides than a juxtaposition of two extended chain leaflets. It is not clear, with the available data, if this phase is thermodynamically stable or just a more organized form of the fluid above T_m, because the nonappearance of the sharp 3.42 nm signal during heating may be due to the difficulty in the rearrangement of C16-Cer molecules and stacking of layers upon melting.

Shah *et al.*[16], using also synthetic non-hydroxyl ceramide C16, observe below T_m a lamellar phase, with an X-ray repeat distance of d = 4.69 nm and a strong broad wide-angle signal at 0.41 nm, interpreted as a metastable state. Upon heating the sample, an exothermic event was detected between 50 to 70 ºC, after which, a new ceramide lamellar phase considered by those authors as the thermodynamically stable phase, with a X-ray repeat distance d = 4.18 nm, and several wide angle reflections very similar to the wide angle diffraction

pattern of our ceramide phase. Apart from the difference in *d*, this phase coincides with our low temperature ceramide and L_{C1} phase. However, some of our samples show at low temperature a signal at 0.234 nm^{-1} (4.28 nm) that disappears at 62 ºC with a simultaneous increase of the 4.46 nm signal. The 4.28 nm phase seems to be a metastable phase but with quite different characteristics from that referred by previous authors[16].

The enthalpy of the transition determined by us, ΔH^o = 71.9 kJ/mol, is much higher than their value, 56.4 kJ/mol, but identical, within the experimental uncertainty, to that of Chen *et al.*[18] (74.9 kJ/mol). The ΔS of the transition, calculated from the ratio $\Delta H^o/T_m$ is 196 J mol^{-1} K^{-1} (155 J mol^{-1} K^{-1} Shah *et al.*) is comparable with that published for a $L_c \rightarrow L_\alpha$ transition of phospholipids of similar chain length, rather than with the ΔS typical of a $L_\beta \rightarrow L_\alpha$ transition 111 J mol^{-1} K^{-1} [35]. In fact, our WAXS results indicate that our low temperature ceramide phase is a crystalline phase and not a L_β type phase. Also the FTIR data for several ceramides is in all cases coherent with a crystalline arrangement in the low temperature range[17-19]. The value of ΔH^o of transition is about twice that of the main transition of C16 saturated phospholipids or sphingomyelins, both in the range of 35-40 kJ mol^{-1} [35]. This is consistent with previous findings that, relative to phosphocholines and sphingomyelins, ceramides have smaller and more strongly hydrogen-bonded headgroups; the hydrogen bonds are established between the hydroxyl of the sphingosine and the amide group of a neighbor[25]. It may also happen that the main transition is from a lamellar to a hexagonal H_{II} phase, as tentatively proposed by Shah *et al.*[16]; though the proposal is consistent with the large ΔS and ΔH^o, it cannot be reconciled with our X-ray data.

The WAXS of pure ceramide, is compatible with a hexagonal chain packing with parameters *a* = *b* = 4.87 Å and *c* = 45.5 Å, and angles $\alpha = \beta = 90^o$ and $\gamma = 120^o$. Data from grazing incidence X-ray diffraction (GIXD) of Langmuir monolayers of pure C16-Cer at low surface pressure were published by Scheffer *et al.*[22]. They suggest that an orthorhombic and a hexagonal phase coexist in the monolayers of pure C16-Cer. The prevailing phase gives origin

to three very broad strong diffractions from which they deduce a 2D orthorhombic crystalline structure with a = 5.02 Å, b = 8.17 Å and γ = 91.9º, almost coincident with that proposed by Vaknin and Kelly[20] for monolayers of ceramide C18 at low lateral pressure. The two phases may be the equivalent of those found by Shah *et al.*[16] for equilibrated and non-equilibrated samples, which were never observed in coexistence by us. Using FTIR spectroscopy for the analysis of the molecular organization of bovine brain CerIII, Moore *et al.*[17] propose an orthorhombic perpendicular two-dimensional chain arrangement below 60 ºC. With the small number of peaks in our WAXS (only from two families (00l) and (10l)) it is difficult to be sure about the structure, and, while the hexagonal structure fits our diffraction data, an acceptable fit is also possible to an orthorhombic lattice with a = 4.22 Å, b = 3.93 Å and c = 45.5 Å, and angles $\alpha = \beta = \gamma = 90º$. Based on these structures, the C16-Cer phase is in a perpendicular chain arrangement.

Mixtures rich in cholesterol. The L_{C2} and L_{C4} phases

From the range of appearance of the L_{C2} phase, along the ceramide-cholesterol mixture composition axis, we can conclude that the L_{C2} phase has a defined stoichiometry that lies somewhere between 45:55 and 35:65 mol C16-Cer:Ch. Attention should be called to the thickness of the L_{C2} phase (s = 0.283 nm^{-1}). Since the lamellar repeating distance (3.50 nm) is too short for a bilayer arrangement, it can be attributed to a single layer formed by C16-Cer and Ch molecules much in the same way Ch arranges itself. However, a thin lamellar structure that was observed in the slow cooling of pure C16-Cer, which indicates that C16-Cer is prone to assembling in thin structures with low hydration layers not usually found in other bilayer-forming lipids. Supposing that the bilayer structure is maintained, the smaller width of the *lamellae* may be a result of chain interdigitation or of some other molecular arrangement such that the two leaflets collapse into one single layer.

As with the deduction of the C16-Cer structure, the wide-angle information is insufficient to permit an unequivocal deduction of the L_{C2} phase crystallography. A good fit is obtained with a tetragonal lattice with $a = b = 6.96$ Å and $c = 35.6$ Å, and angles $\alpha = \beta = \gamma = 90^{o}$ but the available data do not warrant a proposal for the Ch:C16-Cer arrangement.

It is pertinent to compare our results with the corresponding monolayer data obtained by Scheffer *et al.* using GIXD[22]; they found for a C16-Cer:Ch molar ratio of 60:40 three well-defined diffractions at $s = 2.28$, 2.36 and 2.57 nm^{-1}, and interpreted this in terms of a near-rectangular unit cell with $a = 5.18$ Å, $b = 7.74$ Å and $\gamma = 92.2^{o}$. While the qualitative similarity between the diffraction pattern of our phase L_{C2} and the one presented by those authors is striking, the simulated powder pattern with the given crystal structure turned out to be incompatible with our diffraction peaks. The same authors also suggest a unique arrangement of Ch and C16-Cer for a composition of 33:67 mol ratio of C16-Cer:Ch giving rise to a single very broad diffraction in GIXD that gradually converts, with increasing Ch percentage, into a sharp signal at $s = 1.75$ nm^{-1} characteristic of pure Ch monolayers[36]. There is a remarkable similarity between the molar ratio of the two C16-Cer:Ch "crystalline arrangements" observed by Scheffer *et al.* and the compositions of our L_{C2} and L_{C4} phases, and it is also interesting that those authors found continuous miscibility between Ch and C16-Cer at high Ch concentrations. These same authors, using atomic force microscopy, do not find clear phase separation for 40 mol % Ch what is also supported by the observations of other authors[37]. However, the thickness of phase L_{C2} obtained by us indicates a structure difficult to accomplish in a Langmuir film justifying the absence of this phase in monolayers.

From the comparison of the diffractograms (Figure 2.3.), it seems that somewhere between 70 and 80 mol % Ch the L_{C2} phase disappears and the pure Ch phase coexists with phase L_{C4}. This L_{C4} phase is another distinct C16-Cer:Ch crystalline phase with a stoichiometry that must approach 1:3 (see its location in the phase diagram of Figure 2.5.). The diffraction of this phase is

quite broad, which probably derives from uneven packing of the layers resulting from lateral phase separation, or other reason affecting the regularity of thickness. The repeat distance obtained, 4.24 nm, is usual for a bilayer with a thin hydration layer. However, it is smaller than that of the L_{C1} phase what may result from a disordered inner region of the membrane or a thinner hydration layer, both caused by the large fraction of Ch. The WAXS peaks of the L_{C4} phase are not sufficiently resolved to allow the deduction of a crystal structure.

C16-Cer:Ch phase diagram

For the low temperature region, <30 ºC, this system shows four phases with definite compositions. Two of them are Ch, as monohydrate, phase Ch_m, and C16-Cer, phase L_{C1}, existing in nearly pure form at the extremes of the phase diagram. Besides the pure components there are two ordered rigid phases, both stoichiometric compounds of C16-Cer and Ch: one, for which the molar proportion ceramide:cholesterol is ca. 2:3, phase L_{C2}, and another, with a molar ratio that has been bracketed in the region around 1:3 ceramide:cholesterol, phase L_{C4}.

Above ca. 40 mol % C16-Cer the characteristics of the diagram are well defined and quite straightforward, typical of a eutectic system. In several, but not in all, samples with 5, 20, 46 and 55 mol % Ch, we observed the appearance of free cholesterol, a few degrees below and above 62 ºC. It seems that in this narrow temperature range, the L_{C2} phase undergoes decomposition, probably in $L_{\alpha 1}$ and/or L_{C1}, with production of a small amount of a phase with SAXS and WAXS identical to those of free Ch. Not to collide with the Gibbs rule, one may speculate that this is a kinetic effect due to the time taken for Ch to redistribute between phases; cholesterol that, at higher temperatures, is incorporated again in the fluid phase. These changes observed in the diffraction patterns explain the several endotherms detected in the DSC of these mixtures at and above ca. 50 ºC.

What happens in the region of coexistence of L_{C2} and L_{C4} for temperatures above 50 ºC is more difficult to define. There is a narrow range of temperatures, 52-58 ºC where L_{C2}, L_{C4} and $L_{\alpha 1}$ coexist, indicating the existence of an isothermal melting line, above which L_{C4} coexists with $L_{\alpha 1}$.

It is dubious if the Ch is still miscible with the system for concentrations ≥80 mol %. However, neither in our results nor in those of Scheffer *et al.*[22], is there any evidence of Ch separation. In some of our samples, as the one shown in Figure 2.3 for the mixture with 90 mol% Ch, what seems to appear in the WAXS is a structure qualitatively much similar to what was described by Scheffer *et al.* as distorted cholesterol. Below ca. 27 mol% C16-Cer either the Ch is not miscible, and what we observe is free Ch that at high temperature dissolves in phase $L_{\alpha 1}$, or it is included, and the transitions observed are for the complete system. The conversion of cholesterol monohydrate to anhydrous was observed to take place at ca. 74 ºC for the 80:20 mixture and at ca. 78 ºC for the 90:10 what is a clear indication that the detected cholesterol is in equilibrium with the system. The mixture with 20 mol % Ch becomes totally fluid at 94 ºC, suggesting again that Ch is in equilibrium with the system. Whatever the case, it should be stressed that the miscibility of Ch in C16-Cer is unusually high when compared with other amphiphilic lipids[23,35,38].

Joining the data from DSC and X-ray diffraction, with thermodynamic notions for binary systems, we have constructed the diagram in Figure 2.5.

In the diagram, dashed lines are simple separations between regions where different phases were detected and are not claimed to be phase boundaries. A complete overlap between X-ray and DSC data is not possible because, the DSC starts with the anhydrous form of Ch, hence the endotherms around 36 ºC, while the X-ray uses the monohydrate. The diagram presented in Figure 2.5. takes into account all the data obtained and leaves undefined the boundaries for which the available data do not allow an unequivocal solution.

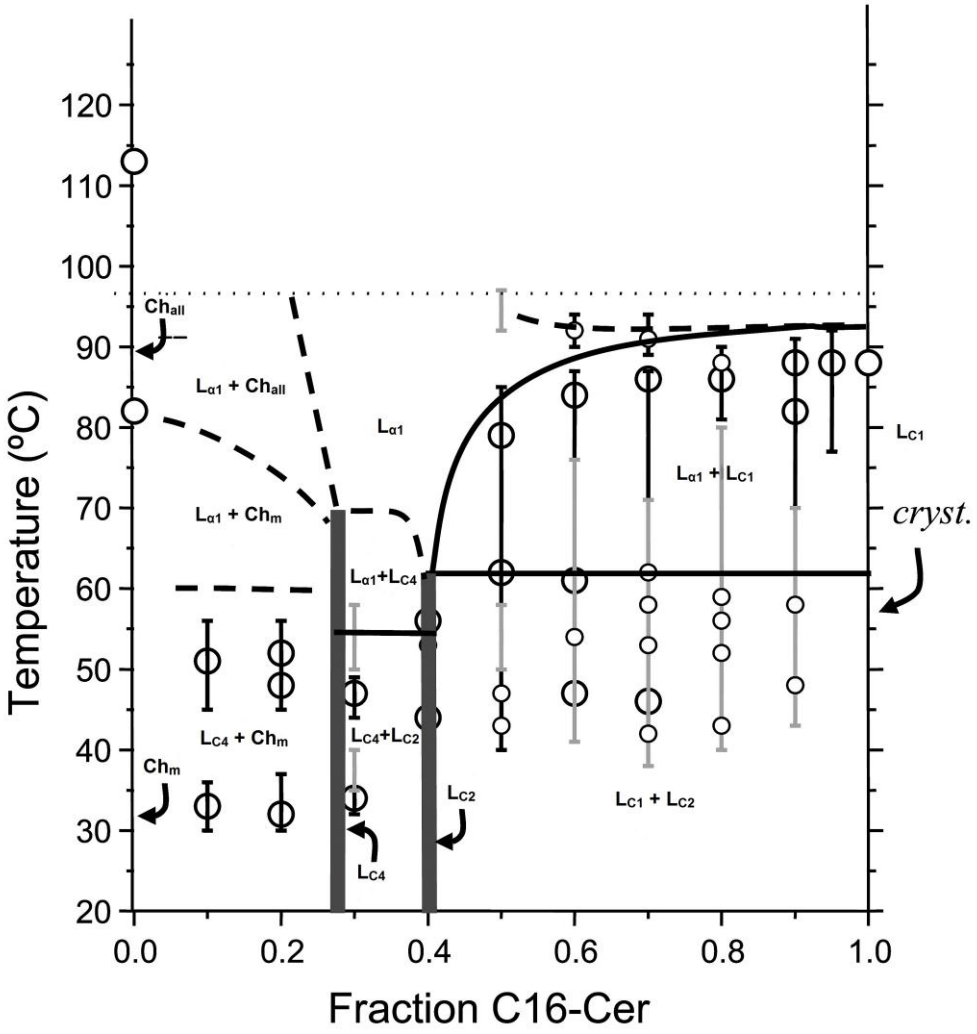

Figure 2.5. - Thermotropic phase diagram for the C16-Cer:Ch system as derived from DSC and X-ray diffraction. Data from DSC, as presented in Figure 2.1. b, is overlaid on the diagram obtained from the analysis of SAXS and WAXS. The solid lines result from the straightforward analysis of the experimental data and the dashed lines separate regions where different phases were observed, not intending to define exact positions of phase boundaries.

2.6. Conclusions

As found by us and earlier investigators, the difficulties in studying the C16-Cer:Ch system are essentially due to the slow molecular rearrangement of structures involving ceramides. Consequently, several metastable states may intervene, preventing the attainment of equilibrium, without which a phase diagram cannot be constructed. The phase diagram in Figure 2.5. is quite detailed while avoiding speculation, what was attained at the cost of oversimplifying the interpretation of the data, particularly those collected in the region of high Ch molar percentage.

We observe by diffraction techniques laterally organized crystalline structures formed between an amphiphilic lipid, ceramide, and cholesterol, in bilayers in excess water. To our knowledge, this is the first direct structural evidence of the existence in lipid bilayers of crystalline phases formed by cholesterol and a membrane-forming lipid. It should be stressed that when melted, the fluid obtained is still a lamellar phase that maintains the specific short distance molecular arrangement inherited from the crystal. While there is no reason to extrapolate our data to the case of membranes constituted by other lipids and cholesterol, this reopens the controversy concerning the existence of organized clusters induced by cholesterol, branded as “cholesterol-lipid condensed complexes”, in the fluid lamellar phase of biological membranes[39,40]. Although some authors[41,42] question a specific interaction, between lipids and cholesterol, evidence of organized structures have been derived in monolayers[43-46], in particular in mixtures of C16-Cer and Ch[22]. We have detected two ceramide-cholesterol stoichiometric phases with well-defined short-range structures: one with a molar ratio C16-Cer:Ch of 1:3, forming lamellar structures with 4.24 nm repeat distance, and another, deserving further consideration, with a molar ratio of 2:3 with a repeat distance

of 3.50 nm. These very stable structures are certainly involved in the phase-separation observed in biological membranes containing cholesterol and ceramides.

A thin fluid phase with a repeat distance of 3.15 nm is also observed in the diffractograms of pure C16-Cer when cooling from 98 ºC; probably this is the stable form of fluid C16-Cer above the main phase transition. Therefore, it seems that this ceramide, alone or in the presence of Ch, is prone to forming nearly single molecule thick lamellar phases, possibly by distributing the headgroups on both sides of the *lamellae*. This unusual lipid arrangement may have some relevance in the formation of the inner layers of the puzzling 13 nm thick *stratum corneum lamellae*.

2.7 Acknowledgments

This work was supported by FCT - Fundação para a Ciência e Tecnologia (Portugal), under Contract POCTI/QUI/45090/2002 and Projects I-05-031 EC and II-20060163 EC from HASYLAB of DESY (Germany). S.L.S. and M.H.L. are indebted to FCT, Portugal for Grants BD/6482/2001 and BD/13765/2003.

2.8. References

(1) Levade, T., Malagarie-Cazenave, S., Gouaze, V., Segui, B., Tardy, C., Betito, S., Andrieu-Abadie, N., Cuvillier, O. (2002). Ceramide in apoptosis: a revisited role. *Neurochem Res*., 27, 601-7.

(2) van Blitterswijk, W.J., van der Luit, A.H., Veldman, R.J., Verheij, M., Borst, J. (2003). Ceramide: second messenger or modulator of membrane structure and dynamics? *Biochem. J.*, 369, 199-211.

(3) Veiga, M.P., Arrondo, J.L.R., Goni, F.M., Alonso, A. (1999). Ceramides in phospholipid membranes: effects on bilayer stability and transition to nonlamellar phases. *Biophys. J.*, 76, 342-350.

(4) Sot, J., Aranda, F.J., Collado, M.I., Goni, F.M., Alonso, A. (2005). Different effects of long- and short-chain ceramides on the gel-fluid and lamellar-hexagonal transitions of phospholipids: a calorimetric, NMR, and X-ray diffraction study. *Biophys. J.,* 88, 3368-3380.

(5) Chiantia, S., Kahya, N., Schwille, P. (2007). Raft domain reorganization driven by short- and long-chain ceramide: a combined AFM and FCS study. *Langmuir*, 23, 7659-7665.

(6) Silva, L.C., de Almeida, R.F.M., Castro, B.M., Fedorov, A., Prieto, M. (2007). Ceramide-domain formation and collapse in lipid rafts: membrane reorganization by an apoptotic lipid. *Biophys. J.*, 92, 502-516.

(7) Xu, X.L., Bittman, R., Duportail, G., Heissler, D., Vilcheze, C., London, E. (2001). Effect of the structure of natural sterols and sphingolipids on the formation of ordered sphingolipid/sterol domains (rafts). Comparison of cholesterol to plant, fungal, and disease-associated sterols and comparison of sphingomyelin, cerebrosides, and ceramide. *J. Biol. Chem.*, 276, 33540-33546.

(8) London, M., London, E. (2004). Ceramide selectively displaces cholesterol from ordered lipid domains (rafts). Implications for lipid raft structure and function, *J. Biol. Chem.*, 279, 9997-10004.

(9) Chiantia, S., Ries, J., Chwastek, G., Carrer, D., Li, Z., Bittman, R., Schwille, P. (2008). Role of ceramide in membrane protein organization investigated by combined AFM and FCS. *Biochim. Biophys. Acta*, 1778, 1356-1364.

(10) Fanzo, J.C., Lynch, M.P., Phee, H., Hyer, M., Cremesti, A., Grassme, H., Norris, J.S., Coggeshall, K.M., Rueda, B.R., Pernis, A.B., Kolesnick, R.,

Gulbins, E. (2003). CD95 rapidly clusters in cells of diverse origins. *Cancer Biol. Ther.*, 2, 392-395.

(11) Silva, L., de Almeida, R.F.M., Fedorov, A., Matos, A.P.A., Prieto, M. (2006). Ceramide platform formation and induced biophysical changes in a fluid phospholipid membrane. *Mol. Membr. Biol.*, 23, 137-148.

(12) Wertz, P.W., Norlén, L.P.O. (2004). "Confidence intervals" for the "true" lipid composition of the human skin barrier? In Skin, Hair, and Nails. Forslind, B., Lindberg, M., Eds., Marcel Dekker, New York, pp. 85-106.

(13) de Jager, M.W., Gooris, G.S., Ponec, M., Bouwstra, J.A. (2005). Lipid mixtures prepared with well-defined synthetic ceramides closely mimic the unique *stratum corneum* lipid phase behavior. *J. Lipid Res.*, 46, 2649-2656.

(14) Ohta, N., Hatta, I. (2002). Interaction among molecules in mixtures of ceramide/stearic acid, ceramide/cholesterol and ceramide/stearic acid/cholesterol. *Chem. Phys. Lipids*, 115, 93-105.

(15) de Jager, M.W., Gooris, G.S., Dolbnya, I.P., Bras, W., Ponec, M., Bouwstra, J.A. (2004). Novel lipid mixtures based on synthetic ceramides reproduce the unique *stratum corneum* lipid organization. *J. Lipid Res.,* 45, 923-932.

(16) Shah, J., Atienza, J.M., Duclos, R.I., Rawlings, A.V., Dong, Z.X., Shipley, G.G. (1995). Structural and thermotropic properties of synthetic C16:0 (palmitoyl) ceramide: effect of hydration. *J. Lipid Res.*, 36, 1936-1944.

(17) Moore, D.J., Rerek, M.E., Mendelsohn, R. (1997). FTIR studies of the conformational order and phase behavior of ceramides. *J. Phys. Chem. B*, 101, 8933-8940.

(18) Chen, H.C., Mendelsohn, R., Rerek, M.E., Moore, D.J. (2000). Fourier transform infrared spectroscopy and differential scanning calorimetry studies of fatty acid homogeneous ceramide 2. *Biochim. Biophys. Acta,* 1468, 293-303.

(19) Velkova, V., Lafleur, M. (2002). Influence of the lipid composition on the organization of skin lipid model mixtures: an infrared spectroscopy investigation. *Chem. Phys. Lipids*, 117, 63-74.

(20) Vaknin, D., Kelley, M.S. (2000). The structure of D-*erythro*-C18 ceramide at the air-water interface. *Biophys. J.*, 79, 2616-2623.

(21) Vaknin, D., Kelley, M.S., Ocko, B.M. (2001). Sphingomyelin at the air-water interface. *J. Chem. Phys.*, 115, 7697-7704.

(22) Scheffer, L., Solomonov, I., Weygand, M.J., Kjaer, K., Leiserowitz, L., Addadi, L. (2005). Structure of cholesterol/ceramide monolayer mixtures: implications to the molecular organization of lipid rafts. *Biophys. J.*, 88, 3381-3391.

(23) Huang, J.Y., Buboltz, J.T., Feigenson, G.W. (1999). Maximum solubility of cholesterol in phosphatidylcholine and phosphatidylethanolamine bilayers. *Biochim. Biophys. Acta*, 1417, 89-100.

(24) Lafleur, M. (1998). Phase behaviour of model *stratum corneum* lipid mixtures: an infrared spectroscopy investigation. *Can. J. Chem.*, 76, 1501-1511.

(25) Rerek, M.E., Chen, H.C., Markovic, B., van Wyck, D., Garidel, P., Mendelsohn, R., Moore, D.J. (2001). Phytosphingosine and sphingosine ceramide headgroup hydrogen bonding: structural insights through thermotropic hydrogen/deuterium exchange. *J. Phys. Chem. B,* 105, 9355-9362.

(26) Hsueh, Y.W., Giles, R., Kitson, N., Thewalt, J. (2002). The effect of ceramide on phosphatidylcholine membranes: a deuterium NMR study. *Biophys. J.*, 82, 3089-3095.

(27) Funari, S.S., Barcelo, F., Escriba, P.V. (2003). Effects of oleic acid and its congeners, elaidic and stearic acids, on the structural properties of phosphatidylethanolamine membranes. *J. Lipid Res.*, 44, 567-575.

(28) Loomis, C.R., Shipley, G.G., Small, D.M. (1979). The phase behavior of hydrated cholesterol. *J. Lipid Res.*, 20, 525-535.

(29) Epand, R.M., Bach, D., Borochov, N., Wachtel, E. (2000). Cholesterol crystalline polymorphism and the solubility of cholesterol in phosphatidylserine. *Biophys. J.*, 78, 866-873.

(30) Tenchov, B., Koynova, R., Rappolt, M., Rapp, G. (1999). An ordered metastable phase in hydrated phosphatidylethanolamine: the Y-transition. *Biochim. Biophys. Acta*, 1417, 183-190.

(31) Shieh, H.S., Hoard, L.G., Nordman, C.E. (1977). Crystal structure of anhydrous cholesterol. *Nature*, 267, 287-289.

(32) de Jager, M.W., Gooris, G.S., Dolbnya, I.P., Bras, W., Ponec, M., Bouwstra, J.A. (2003). The phase behaviour of skin lipid mixtures based on synthetic ceramides. *Chem. Phys. Lipids,* 124, 123-134.

(33) Neubert, R., Rettig, W., Wartewig, S., Wegener, M., Wienhold, A. (1997). Structure of *stratum corneum* lipids characterized by FT-Raman spectroscopy and DSC. II. Mixtures of ceramides and saturated fatty acids. *Chem. Phys. Lipids*, 89, 3-14.

(34) Shah, J., Atienza, J.M., Rawlings, A.V., Shipley, G.G. (1995). Physical properties of ceramides: effect of fatty acid hydroxylation. *J. Lipid Res.*, 36, 1945-1955.

(35) Marsh, D. (1990). Handbook of Lipid Bilayers. CRC Press, Boca Raton.

(36) Lafont, S., Rapaport, H., Somjen, G.J., Renault, A., Howes, P.B., Kjaer, K., Als-Nielsen, J., Leiserowitz, L., Lahav, M. (1998). Monitoring the nucleation

of crystalline films of cholesterol on water and in the presence of phospholipid. *J. Phys. Chem. B*, 102, 761-765.

(37) tenGrotenhuis, E., Demel, R.A., Ponec, M., Boer, D.R., van Miltenburg, J.C., Bouwstra, J.A. (1996). Phase behavior of *stratum corneum* lipids in mixed Langmuir-Blodgett monolayers. *Biophys. J.*, 71, 1389-1399.

(38) Huang, J.Y., Feigenson, G.W. (1999). A microscopic interaction model of maximum solubility of cholesterol in lipid bilayers. *Biophys. J.,* 76, 2142-2157.

(39) McConnell, H.M., Radhakrishnan, A. (2003). Condensed complexes of cholesterol and phospholipids. *Biochim. Biophys. Acta,* 1610, 159-173.

(40) McConnell, H.M., Vrljic, M. (2003). Liquid-liquid immiscibility in membranes. *Annu. Rev. Biophys. Biomol. Struct.,* 32, 469-492.

(41) Guo, W., Kurze, V., Huber, T., Afdhal, N.H., Beyer, K., Hamilton, J.A. (2002). A solid-state NMR study of phospholipid-cholesterol interactions: sphingomyelin-cholesterol binary systems. *Biophys. J.,* 83, 1465-1478.

(42) Holopainen, J.M., Metso, A.J., Mattila, J.P., Jutila, A., Kinnunen, P.K.J. (2004). Evidence for the lack of a specific interaction between cholesterol and sphingomyelin. *Biophys. J.,* 86, 1510-1520.

(43) Gershfeld, N.L. (1978). Equilibrium studies of lecithin-cholesterol interactions I. Stoichiometry of lecithin-cholesterol complexes in bulk systems. *Biophys. J.,* 22, 469-488.

(44) Radhakrishnan, A., McConnell, H.M. (1999). Condensed complexes of cholesterol and phospholipids. *Biophys. J.,* 77, 1507-1517.

(45) Chong, P.L.G. (1994). Evidence for regular distribution of sterols in liquid crystalline phosphatidylcholine bilayers. *Proc. Natl. Acad. Sci. USA*, 91, 10069-10073.

(46) Ege, C., Ratajczak, M.K., Majewski, J., Kjaer, K., Lee, K.Y.C. (2006). Evidence for lipid/cholesterol ordering in model lipid membranes. *Biophys. J.,* 91, L1-3.

3. The thermotropism and prototropism of ternary mixtures of ceramide C16, cholesterol and palmitic acid. An exploratory study

The co-authors of the work presented in this Chapter had the following contributions:

- J. Valério made measurements at the beamline A2 of Hasylab at DESY,
- S.S. Funari is the beamline scientist of A2 of Hasylab at DESY, optimized the experimental setup for our measurements, made the preliminary SAXS and WAXS conversion and helped with the SAXS interpretation.

It was published as:

Souza, S.L., Valério, J., Funari, S.S., Melo, E. (2011). The thermotropism and prototropism of ternary mixtures of ceramide C16, cholesterol and palmitic acid. An exploratory study. *Chem. Phys. Lipids*, 164, 643-653.

3.1. Abstract

Mixtures of ceramides with other lipids in the presence of water are key components of the structure of the lipid matrix of the *stratum corneum* and are involved in lateral phase separation processes occurring in lipid membranes. Besides their structural role, ceramides are functional for cell signaling and trafficking. We elected, as our object of study, a mixture of N-hexadecanoylceroyl-D-*erythro*-sphyngosine (C16-Cer), with cholesterol (Ch), in a molar proportion 54:46 in excess water to which palmitic acid (PA), is added in varying amounts. The chosen C16-Cer:Ch proportion replicates the relative abundance of ceramides and cholesterol found in the *stratum corneum* lipid matrix. For each lipidic composition, we identify the phases in equilibrium and study the thermotropism of the system, using differential scanning calorimetry and temperature-dependent small and wide-angle X-ray powder diffraction. Since the molecular aggregation of the system and its mesoscopic properties are affected by the degree of protonation of the PA, we explore mixtures with several PA contents at two extreme pH values, 9.0 and 4.0. A specific C16-Cer:Ch:PA composition forms at pH 9.0 a lamellar crystalline aggregate, to which we attribute the stoichiometry C16-$Cer_5Ch_4PA_2$, that melts at 88–90 ºC to give a H_{II} phase. For pH values at which there is partial or total protonation of PA another L_C C16-Cer:Ch (2:3) stoichiometric aggregate is observed, identical to that previously reported for C16-Cer:Ch mixtures (Souza *et al.,* 2009, J. Phys. Chem.B, 113, 1367–1375), coexisting with a lamellar fluid phase. For pH 4.0 and 7.0, the existing lamellar liquid crystalline converts into a isotropic fluid phase at high temperatures. It is also found that the miscibility of PA in the C16-Cer:Ch mixture at pH 4.0 does not exceed ca. 18 mol %, but for pH 9.0 no free PA is detected at least until 60 mol %.

3.2. Introduction

Most membrane-forming lipids used by nature in the building of cellular membranes or other biological structures are fluid at the physiological temperature or, at least, the mixtures in which they are found in nature are fluid. The notable exception is the lipid matrix of the *stratum corneum* whose properties rely on the rigidity conferred by a particular mixture of ceramides and hydroxylated ceramides, together with cholesterol and saturated fatty acids. Ceramides by themselves form lamellar crystalline phases that melt to give lamellar liquid crystalline phases at quite high temperatures[1,2]. This happens even for relatively short-chain ceramides because of the strong hydrogen-bonds connecting the headgroups and the network formed between the headgroups and the adjacent water layer[3]. The lipidic mixture found in the *stratum corneum* is, at least in part, laterally organized in a crystalline structure[4] that has been referred as being important to the particular properties of this system[5,6]. The presence of a quite large molar percentage of fatty acid (ca. 18%) and the fact that the *stratum corneum* interfaces a region with pH 7.4 and pH ca. 5.5, raised the interest of several researchers on how the physical–chemical characteristics of the lipid matrix is modulated by pH[7-10].
Ceramides are also known to be involved in cell signaling[11] and are a potent inducer of apoptosis[12]. Although the mechanism is unknown, recent findings suggest that the biological functions of ceramides result from changes in local membrane structure, namely the formation of ceramide-rich lipid domains[11].
In this work, we explore the thermotropic and prototropic behavior of mixtures of N-hexadecanoylceroyl-D-*erythro*-sphyngosine (C16-Cer), with cholesterol (Ch), to which palmitic acid (PA), is added. The matching of the fatty acid and ceramide hydrocarbon chains reduces the possibility of demixing, interdigitation, and other effects peripheral to our objective. The experiments presented here are not an attempt to map the thermotropism and prototropism

of the ternary mixtures of C16-Cer:Ch:PA to the detail of a ternary phase diagram. Our approach was to maintain fixed the C16-Cer to Ch ratio and change the molar percentage of palmitic acid and the pH.

In all the ternary compositions studied in the present work the molar proportion between C16-Cer and cholesterol respects that published by Norlen *et al.*[13] for the ratio between the total ceramides and cholesterol in the lipid matrix of the *stratum corneum*, 54:46. In face of the large diversity of compositions available in the literature, namely in the more recent works[14-16], our option was to use this particular C16-Cer:Ch ratio that is supported by the review of Wertz and Norlen[17]. We start with the study of the thermotropism of ceramide C16:cholesterol to which palmitic acid is progressively added. The experiments were made at pH 9.0, theoretically allowing complete ionization of the acid. This isopleth was made to explore the main phases present along this section of the ceramide C16:cholesterol:palmitoate ternary diagram. At this pH the mixture of C16-Cer:Ch:PA in a molar proportion of 44:38:18 was found to form a stoichiometric molecular 2D crystal. Subsequently, this mixture was progressively neutralized to explore the prototropism of this particular composition. Additionally, we analyzed the phase changes induced by increasing the amount of palmitic acid up to 100% at pH 4.0 and 9.0. The study was made using differential scanning calorimetry (DSC), and simultaneous acquisition of small and wide-angle X-ray scattering, (SAXS) and (WAXS), respectively.

The thermotropism and lyotropism of pure synthetic C16-Cer has been analyzed by Shah *et al.*[1] and we have recently derived experimentally the binary phase diagram for the mixtures of C16-Cer with cholesterol in excess water. It was found that C16-Cer forms a lamellar crystalline phase, L_C, that melts at 93 ºC to give a lamellar liquid crystalline phase, L_α. Cholesterol is practically insoluble in crystalline C16-Cer but forms at least one stoichiometric lamellar crystalline phase with a 2:3 C16-Cer:Chol molar ratio. It is reasonable to expect that L_C ceramide layers have difficulty in accommodating solutes with quite different bulkiness (or cross-section), such as cholesterol. Fatty acids

may behave in a different way since they can substitute one of the ceramide chains without much distortion.

Some authors have already studied the effect of the pH in lipid mixtures containing natural ceramides, cholesterol and fatty acid. Using ^{2}H NMR Kitson *et al.* observed that the thermotropic phase-behavior of a mixture equimolar in bovine brain ceramide (SigmaType III), cholesterol and palmitic acid, is pH sensitive[8]. At pH 7.4 the mixture melts to give an inverted hexagonal phase, whereas at lower pH values, 6.2 and 5.2, the system gives origin to a isotropic fluid phase. With X-ray diffraction, Bouwstra *et al.* using skin-extracted ceramides observed that the pH had no effect on the in-plane lipid lateral packing of the ternary mixtures, but the signal due to the diffraction of the so-called long periodicity phase was stronger at pH 7.4 than at pH 5 [18,10]. In another X-ray study, a mixture of extracted ceramides, cholesterol and palmitic acid in a composition 2:1:1 was studied as a function of pH in the range 6–8.5 and the lamellar repeat distance of the thick phases increased due to electrostatic repulsion[19]. With Laurdan generalized polarization fluorescence microscopy, Plasencia *et al.*[20] analyzed structures formed with mixtures of skin-extracted ceramides with cholesterol and fatty acids in the relative molar proportions 1:0.9:0.4. According to their interpretation, at pH 5 two lipid phases coexist, both in the gel state, while at pH 7 one single gel phase is present. In an FTIR study[7] it was observed that a decrease from 7.4 to 5.2 in pH changed the thermotropic behavior of equimolar mixtures of bovine brain ceramide (Sigma Type III, a non-hydroxylated ceramides mixture), cholesterol and palmitic acid.

3.3. Materials and methods

Reagents

Egg ceramide (84% C16) and synthetic (2S,3R,4E)-2-hexadecanoylaminooctadec-4-ene-1,3-diol (N-palmitoyl-D-*erythro*-sphingosine or, according to Motta *et al.* classification of human SC ceramides[21], CER-NS-

C16), were obtained from Avanti Polar Lipids, stearic acid from BDH, and cholesterol from Sigma. Benzene is from Panreac and methanol from Merck, both HPLC grade. All chemicals were used without further purification. Water for buffer preparation was double distilled and further purified with an Elgastat UHQ-PS system (Marlow, U.K.). Buffers were as follows: pH 9.0 sodium borate, pH 7.0 phosphate sodium salts, pH 5.0 and 4.0 succinic acid and pH 3.0 chloroacetic acid. Ionic strength was corrected for 100 mM with NaCl and all buffers were 0.2 mM in EDTA. Reagents for buffer preparation were either Merck or Riedel de Haen pa. grade.

Preparation of lipid dispersions

To avoid lipid demixing in the step of organic solvent removal, usual in mixtures containing high relative percentage of cholesterol[22], the solvent in which the lipids are dissolved is removed by freeze-drying. The subsequent hydration is done at 98 ºC, above the transition temperature of the ceramide. As we have shown elsewhere, in these systems lipid demixing is irreversible[2] and the protocol here described proved to give reproducible and equilibrated samples. Equilibrated, or, at least, not presenting signs of metastability.

Preparation was as follows: adequate amounts of lipid stock solutions of each lipid in benzene/methanol, 7:3 (v:v), were mixed in the intended proportions and allowed to stand for 30 min with occasional vortexing. The system was subsequently frozen to −20 ºC and left at this temperature for at least 2 h after which it was freeze-dried. To the resulting powder, the appropriate buffer at 98 ºC was rapidly added under vortexing such that a dispersion is obtained. This dispersion is maintained for 30 min at 98 ºC to allow for complete hydration. The physical appearance of the samples containing fatty acid at pH 9.0, was turbid, with small white lumps that float after centrifugation. At and below pH 7.0 the buffer is transparent with apparently compact aggregates floating. This visual aspect resembles that of pure ceramide or C16-Cer:Ch dispersions.

The possibility of decomposition or hydrolysis of the ceramide was excluded by thin layer chromatography (TLC).

Differential scanning calorimetry

Many authors have, like us, observed that ceramides and lipid mixtures containing ceramides may easily be trapped in metastable states upon cooling[1,23,3,24,25]. The reason for this is the strength of the interaction between the hydroxyl of the sphingosine and the amide group of a neighbor molecule[24] that not only result in transition temperatures much higher than those of similar chain-length phosphocholines[26,27] but also impede molecular rearrangement. The method we found to be safe to avoid non-equilibrated systems, consisted in rejecting the first DSC scan done at 1 ºC/min until 95 ºC, cool the sample at the rate of 1 ºC/min and only consider the second and/or subsequent heating scans. Alternatively, the samples were previously heated and cooled in a computer-controlled thermo-cryostat bath (F25 Julabo Labortechnik GmbH, Germany) mimicking the first heating and cooling in the microcalorimeter chamber. The heating thermograms in this way obtained (VP-DSC from MicroCal, Northampton, MA) do not show the exothermic event typical from out of equilibrium systems.

Cholesterol quantification by ^{1}H NMR for ΔH^o determination

The lipids were extracted from the dried aqueous suspensions with chloroform and filtered through a 10.0 µm pore Teflon filter (SRi Scientific Resources, NJ, U.S.A.) to remove the solid particles with origin on the buffer salts. The chloroform was evaporated and substituted by a fixed amount of deuterated chloroform.

The proton NMR spectra were acquired with a Bruker AMX 300 NMR spectrometer (Wissenbourg, France) operating at 300 MHz, and the delay time used was of 5 s. For determining the cholesterol amount we compared the

area of the peak at δ = 3.5 ppm with a calibration curve. Since this technique only allows the determination of cholesterol, quantification of ceramide and palmitic acid was done supposing that there was no change of the original relative proportions. The precision of the method was found to be of 5%.

X-ray diffraction

Small and wide angle X-ray scattering were collected simultaneously at the synchrotron radiation facility at the Soft Condensed Matter beamline A2 of the storage ring DORIS III of the Deutsches Elektronen Synchrotron (DESY), using a setup previously described[28]. In the setup used at the A2 beamline measurements were done with a Mar165 CCD and a Gabriel-type gas detector, for SAXS and WAXS, respectively. The wavelength of the X-ray is 0.15 nm. The protocol of sample preparation was identical to what was used for DSC, except that the 4.0 µmol of lipid were hydrated with only 0.3 ml of buffer and the lipid and a small amount of buffer were transferred to capillary tubes (1.0 mm diameter with 0.01 mm wall glass, Markrohrchen, Germany). The tubes were saturated with argon overnight, closed and the samples annealed in a thermo-cryostat bath as previously explained for the DSC samples.

The measurement was done with the capillary in a temperature controlled holder heated from 20 to 98 ºC at 1.0 ºC/min, maintained at 98 ºC for 6 min to check for sample structural stability and subsequently returned to 20 ºC at the same T scan rate. Measurements lasted for 20 s every 120 s (ca. 2 ºC steps), for SAXS and WAXS acquisition. The real temperature of the sample holder at the beginning of each data collection was registered together with the data.

Channel positions of the observed peaks were converted into reciprocal spacing, $s = 1/d$, where d is the distance between the diffracting planes. The SAXS and WAXS regions were calibrated with rat tail collagen and poly(ethylene terephthalate), respectively, and the marCCD output for the

small angle region linearized with a in-house developed program (A2tool, A. Rothkirch, Hasylab, DESY). The background scatter of identical capillary tubes with buffer was subtracted from all diffractograms. The evaluated error in *s* is relatively constant for each of the regions considered. In the range from 0.10 until 0.39 nm^{-1}, SAXS, it is of 0.001 nm^{-1} and for the region of 1.78 $nm^{-1} < s <$ 3.05 nm^{-1}, where the WAXS was measured, it is of 0.005 nm^{-1}.

Calculations

Dipole moments of glycerophosphocholine and ceramide headgroups were calculated with the software package HyperChem, Release 8 (Hypercube, Inc., USA), with the molecular structure optimized using the force field MM+ method and the electronic density distribution calculated by the semi-empirical method AM1. The procedure was validated by comparison of the calculated dipoles with the experimental dipole moments published for molecules with similar size and kind of atoms. In all our tests, the calculated dipoles were within ±10% the experimental value.

The calculation of the Debye screening length, $1/\kappa$, and of the fraction of ionized PA, α, was done based on the theory of the diffuse electric double layer[29] closely following the implementation of Vaz *et al.*[30] with the necessary adaptation to our objective. For a known proton concentration, $[H+]$, the fraction of fatty acid ionized, with acidic constant K_a, is given by

$$\alpha = \frac{1}{1+[H^+]\,\phi_0 / K_a} \qquad (1)$$

where ϕ_0 is the surface enhancement factor, that is related to the potential at the interface, Ψ_0, by

$$\phi_0 = \exp\left(-\frac{e\,\Psi_0}{k_B T}\right) \qquad (2)$$

where e is taken as the positive elementary charge and the other constants have their usual meaning. The potential created by the ionized fatty acid, considered at the surface of the membrane, is calculated with the Gouy–Chapman formalism[29]

$$\Psi_0 = \frac{2k_B T}{e} \quad \sinh\left(-\frac{2\pi\, b\, \alpha}{\kappa A_L}\right) \qquad (3)$$

where b is the Bjerrum length, given by $b = e^2 / 4\pi\varepsilon_0\varepsilon\, k_B T$, and the reciprocal screening length, κ, by $\kappa = \sqrt{8\pi\, b\,[\mathrm{S}]}$. The value of A_L, the average area per charged lipid, was calculated for the mixture of C16-Cer:Ch:PA 44:38:18 based on the relative proportions and the area occupied by each molecular species. For C16-Cer an area per molecule of 41 Å^2 was calculated from the lattice parameters[2], for Ch 32 Å^2 were used[31], and 20.2 Å^2 for PA (taken from the discussion of Casilla *et al.*[32] on fatty acids cross section), resulting in an approximate area per PA molecule of 180 Å^2. The Debye screening length depends from the concentration of the 1:1 electrolyte, $[\mathrm{S}]$, and the value of the relative static permittivity, ε, was taken as that of water, ε = 80. All the other parameters have the usual meaning.

Of course Eqs. (1)–(3) are implicit in α because the interface potential depends on the fraction of ionized fatty acid which, in turn, depends on the product $[\mathrm{H+}]\phi_0$, the effective proton concentration at the interface. Therefore, an iterative calculation is carried out to obtain α and κ for a set of given conditions, A_L, $[\mathrm{H}^+]$ and $[\mathrm{S}]$.

.

3.4. Results

Effect of progressive addition of fatty acid to mixtures of ceramide:cholesterol (54:46) up to 60 mol % of palmitic acid

X-ray studies for 0 mol % PA

Mixtures of ceramide and cholesterol in a molar proportion 54:46 in excess water have already been characterized concerning its structure and thermotropic behavior[2]. Briefly, it was observed that at low temperature two lamellar crystalline phases coexist melting between 62 and 87 ºC to give a single lamellar liquid crystalline phase. One of the two crystalline phases that are present at 20 ºC is practically pure ceramide with a lamellar repeat distance of 4.46 nm (s = 0.224 nm^{-1}) and a characteristic X-ray wide angle pattern with strong peaks at 2.38, 2.41, 2.46 and 2.55 nm^{-1} and weaker peaks at 2.19, 2.62, 2.65 and 2.70 nm^{-1}, named L_{C1}. The other, L_{C2}, is a 2:3 stoichiometric aggregate C16-Cer:Ch with a lamellar repeat distance of 3.53 nm (s = 0.283 nm^{-1}) and a diffraction pattern in the WAXS region constituted by peaks at 1.83, 2.02 and 2.21 nm^{-1}. Both crystal structures were characterized: the L_{C1} phase was found to be compatible with a hexagonal chain packing with parameters $a = b$ = 4.87 Å and c = 45.5 Å , and angles $\alpha = \beta = 90^{o}$ and $\gamma = 120^{o}$, and the L_{C2} phase as being a tetragonal lattice with $a = b$ = 6.96 Å and c = 35.6 Å , and angles $\alpha = \beta = \gamma = 90^{o}$ [2]. Above 62 ºC a lamellar liquid phase, $L_{\alpha 1}$, is formed, which is characterized by a diffraction located at s = 0.247 nm^{-1} (4.05 nm). The L_{C2} phase vanishes at this temperature while the L_{C1} phase is present until 87 ºC.

X-ray studies for 5 mol % PA

At this PA concentration the SAXS and WAXS peaks are, within the experimental resolution, identical to those observed in the absence of PA. However, the temperature at which the L_{C2} disappears with formation of $L_{\alpha 1}$ is now 70 ºC, and at the same temperature the intensity of the diffraction attributed to the phase L_{C1} begins to decrease. Since both L_C phases previously described do not contain PA the question of where the acid is located should be raised. The amount being relatively small it may reside as a solute in the phases present, but, as we will see later, it can also form a separate L_C phase hard to distinguish from L_{C1}.

X-ray studies for 12 mol % PA

For the samples with 12 mol % PA the typical diffractions of phases L_{C1} and L_{C2} are present at 20 ºC. The L_{C2} diffraction disappears at 66 ºC and the fluid phase $L_{\alpha 1}$ begins to appear at 62 ºC coexisting with L_{C1} phase until 88 ºC. Between 88 and 90 ºC the L_{C1} phase melts and a new fluid phase with broad diffraction at ca. 0.208 nm^{-1} is formed, that, as we will see in the analysis of the mixture with 18 mol% PA, is an inverted hexagonal phase, H_{II}. Above 88 ºC the two liquid phases $L_{\alpha 1}$ and H_{II} coexist, the WAXS of this mixture being typical of the arrangement of the hydrocarbon chains in liquid crystalline lipid lamellae.

X-ray studies for 18 mol % PA

Contrarily to what happens for the samples with lower PA content, only one SAXS diffraction peak, located at s = 0.224 nm^{-1}, is observed at 20 ºC, Figure 3.1 panels B (heating) and C (cooling).

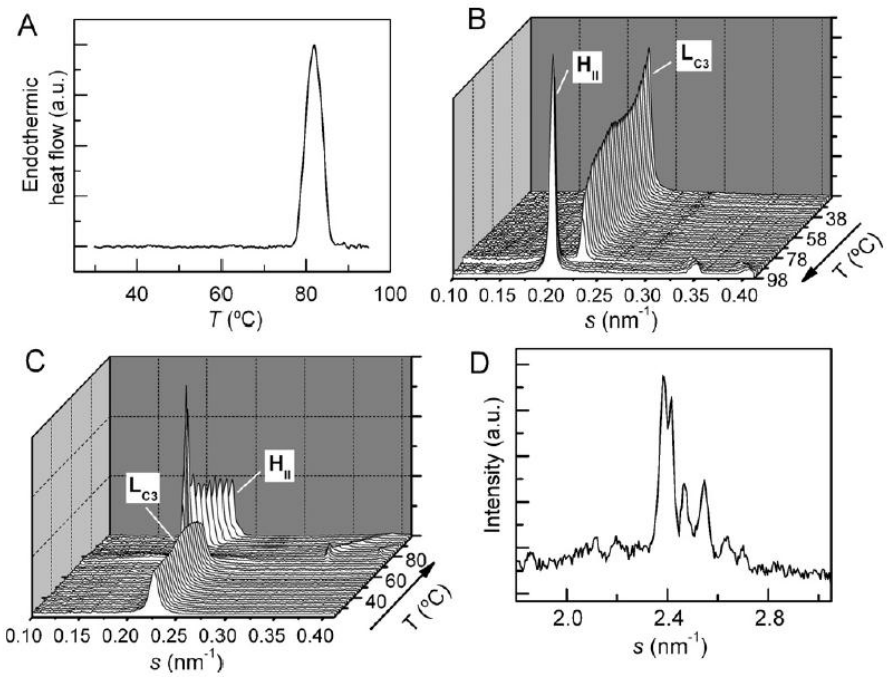

Figure 3.1. – Characteristic heating thermogram and X-ray diffraction pattern of the C16-Cer:Ch:PA 44:38:18 in excess water at pH 9.0. In the heating DSC trace acquired at 1 ^{o}C/min, shown in panel A, the ternary lipid mixture displays a single endothermic event. Panels B and C illustrate the SAXS data for heating from 20 until 98 ^{o}C, panel B, followed by cooling back to the start temperature, panel C, both at 1 ^{o}C/min and displayed at 2 ^{o}C intervals. The three lipids that compose the mixture form a single phase, a stoichiometric aggregate, diffracting at s = 0.224 nm^{-1} (d = 4.46) that melts congruently at 88-90 ^{o}C (see text), to give an inverted hexagonal phase, as can be deduced from the appearance of two new diffraction peaks in panels B and C. The wide angle diffraction pattern at 20 ^{o}C of the stoichiometric structure of ceramide, cholesterol and palmitic acid is presented in panel D.

To be exact, in the sample shown in Figure 3.1B there is a residual signal from L_{C2} barely visible in the heating diffractogram that is not present when cooling. The WAXS presents diffractions in the wide-angle region located at s = 2.38, 2.42, 2.47, 2.55, 2.64 and 2.70 nm^{-1}, Figure 3.1 panel D, that coincide with those of pure ceramide. As it will be later discussed, the crystal phase diffracting at 0.224 nm^{-1} cannot be the L_{C1} phase, and we name it phase L_{C3}.

When the temperature is increased, the phase responsible for the SAXS diffraction at 0.224 nm^{-1} melts between 88 and 90 ºC originating an hexagonal phase characterized by three new peaks at s_1 = 0.207, s_2 = 0.356 ≈ $s_1\sqrt{3}$ and s_3 = 0.407 nm^{-1}. Being in excess water it is most likely of type H_{II}[33], with a = 5.58 nm calculated from the relation $a = 2d_{10}/\sqrt{3}$. The progress of the peaks during the cooling subsequent to the heating run is reversed, with the transition placed between 80 and 72 ºC, Figure 3.1 panel C. A further confirmation that no other thermotropic events besides the L_{C3} to H_{II} conversion exist for this composition and pH, is given in the DSC trace presented in Figure. 3.1 panel A, later discussed.

X-ray studies for 60 mol % PA

For this high PA concentration, a completely different X-ray pattern is observed but no segregated palmitic acid exists, which would be easily identifiable by its characteristic lamellar diffraction located at s = 0.219 nm^{-1} and wide angle signals at s = 2.17, 2.22, 2.65 and 2.74 nm^{-1}, determined in an independent measurement of PA at pH 9.0. In our samples two diffractions at 0.200 nm^{-1} and 0.188 nm^{-1} are detected. The phase diffracting at 0.188 nm^{-1} at low temperature, has a single thermally coupled wide-angle sharp diffraction, located at 2.43 nm^{-1}, and melts from 51 to 63 ºC. The WAXS is compatible with a hexagonal acyl chain packing with a = b = 0.411 nm. The diffraction located at 0.200 nm^{-1}, independent from that at 0.188 nm^{-1}, is a lamellar fluid phase to which corresponds a broad band centered at 2.20 nm^{-1}. At 74 ºC this phase gives origin to another lamellar fluid phase, with diffraction located at 0.220 nm^{-1} associated with a similar wide angle broad band centered at 2.20 nm^{-1}. This phase is present until 90 ºC, the maximum temperature attained by this sample.

DSC studies for 0, 5, 10, and 20 mol % PA

In Figure 3.2 the heating thermograms of the samples at pH 9.0 are presented, for mixtures of egg-Cer:Ch in the relative molar proportion 54:46 with increasing amounts of palmitic acid up to 20 mol%.

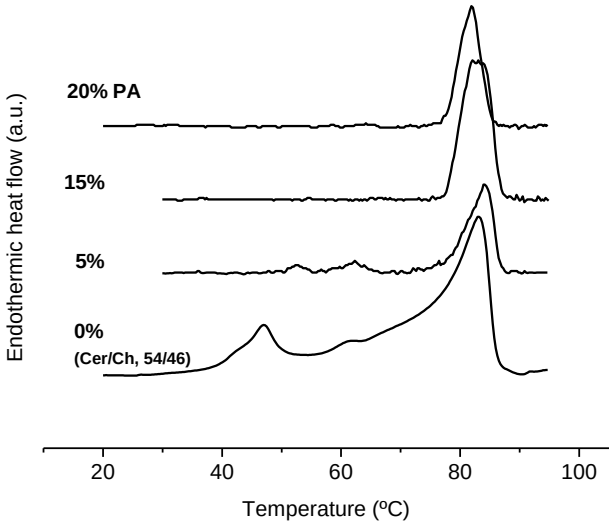

Figure 3.2. - Thermograms of mixtures of egg ceramide and cholesterol in the relative molar proportion 54:46 along increasing amounts of palmitic acid, up to 20 mol %. All samples at pH 9.

The sample without palmitic acid displays several endothermic transitions with maxima at 48, 62, and 84 ºC. When 5% palmitic acid is added, the transitions at 63 and 84 ºC are maintained and a new small endotherm at 53 ºC is now evident which may or not be already present at 0 mol% FA masked by the 48 ºC relatively large peak. The change in the thermogram from 0 to 5 mol % does not seem consistent with PA being a simple solute in the mixture, a question left open by the X-ray data. With the addition of higher amounts of palmitic acid, 10 (not shown), 15 and 20 mol%, only the endotherm at higher temperature is observed.

While at 0 mol % palmitic acid the T_m of the stronger endotherm is at 84 ºC and relatively broad, for 20 mol % palmitic acid the high temperature transition T_m = 82 ºC. For the intermediate concentrations, the peak is a composition of the 84 and 82 ºC transitions. It should be noted that the DSC data were acquired using egg ceramide, 84% C16 (egg-Cer), and it is to expect a small discrepancy of the temperatures and a broader transition in the DSC experiment compared to X-ray which were done with synthetic C16 ceramide. Considering this, we attribute the transition at 82 ºC for the 20 mol % PA composition to the melting of the L_{C3} phase to give H_{II}, and the transition with apex at 84 ºC to the transformation of L_{C1} in $L_{\alpha 1}$. Similarly to what was observed by X-ray for the 12 mol % sample, the 15 mol % mixture exhibits both transitions.

Effect of pH variation for the mixture of ceramide C16, cholesterol and palmitic acid with 44:38:18 molar ratio

As already shown, the mixture with this composition forms a single L_{C3} phase that undergoes a congruent transition to H_{II} at pH 9.0, but, due to the presence of the fatty acid, there is no reason to expect a similar behavior at lower pH. According to the Gouy–Chapman model[29], Eqs. (1)–(3), for the ionic strength used, 100 mM, the PA at the interface is predicted to be 99.8% ionized at pH 9.0 and 98.8% protonated at pH 3.0. To study the structural changes induced by interface neutralization, we measured this mixture at pH 7.0, 4.0 and 3.0. Not much difference is expected between the samples at pH 4.0 and 3.0 because at pH 4.0 already 92% of the PA should be neutralized but the effect of charge may be noticeable at pH 7.0 where 87% is ionized.

At pH 9.0 no protonated PA is present; in consequence, the system can be treated as ternary. Identical reasoning can be made for pH 4.0 and 3.0. At intermediate pH the equilibrium between acid and base forms adds a forth component but also a new freedom constraint. Therefore, we may consider that the same number of coexistent phases is allowed irrespective of pH.

X-ray studies for pH 7.0. At pH 7.0 and 20 ºC, two strong main diffractions, at s = 0.224 and 0.235 nm^{-1} are observed. Increasing the temperature their intensity change independently indicating that they have origin in two distinct lamellar phases.

Between 35 and 54 ºC the intensity of the diffraction at 0.235 nm^{-1} is progressively reduced, originating a new diffraction at s = 0.243 nm^{-1}, that we interpret as being the $L_{\alpha 1}$ phase, while the intensity of the 0.224 nm^{-1} peak only decreases above 68 ºC, being completely absent by 88 ºC, its fusion also contributing to the $L_{\alpha 1}$ phase. The wide-angle region displays the same peaks with the same thermal behavior of both, pure ceramide and L_{C3} phase[2] that disappear concomitantly with the diffraction at s = 0.224 nm^{-1} and do not seem correlated with the diffraction at s = 0.235 nm^{-1} previously commented. We conclude that at low temperature two phases coexist, one that is the already characterized $L_{C1,3}$, and a new lamellar fluid phase with diffraction at s = 0.235 nm^{-1} that we will name $L_{\alpha 2}$ phase. This phase has no detectable wide-angle correspondent, namely the broad band centered at 2.2 nm^{-1} typical of the hydrocarbon liquid-like chains, what may be due to the presence of a large molar fraction of cholesterol randomly distributed, that disorder the palisade region of the *lamellae*.

The intensity of the diffraction of the phase $L_{\alpha 1}$, declines from 86 until 96 ºC, the maximum temperature at which the samples were analyzed. In this temperature range the $L_{\alpha 1}$ phase originates a isotropic fluid, without small and wide angle X-ray signal. Therefore, between the onset of isotropic fluid formation, 92 ºC, and the higher temperature attained, 96 ºC, the only phases present are $L_{\alpha 1}$ and isotropic fluid.

X-ray studies for pH 4.0. As shown in Figure 3.3, the scenario is very similar to what was described for pH 7.0, except that now two additional small reflections at s = 0.289 and 0.278 nm^{-1} are observed.

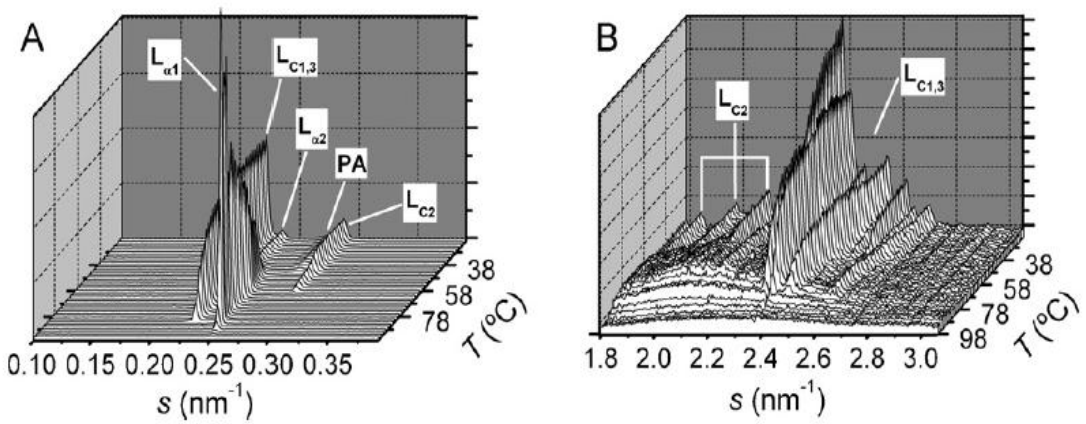

Figure 3.3 – Characteristic SAXS, panel A, and WAXS, panel B, of the C16-Cer:Ch:PA 44:38:18 matrix, in excess water at pH 4.0 as a function of temperature. The heating rate was of 1 ^{o}C/min and diffractograms are collected at 2 ^{o}C interval.

The reflection at s = 0.289 nm^{-1} has origin in the L_{C2} phase, since it is thermally associated with its characteristic wide-angle pattern. The reflection at s = 0.278 nm^{-1} is interpreted as a small amount of segregated neutral PA, not enough to be evident in the WAXS. This signal of PA is not observed in all 18 mol % samples. We interpret this variability as the result of this PA concentration being close to the maximum solubility of the acid in the mixture. The L_{C2} phase disappears between 48 and 52 ºC when $L_{\alpha 1}$ emerges and phase $L_{C1,3}$ starts melting. Above 86 ºC only $L_{\alpha 1}$ is present, but when temperature increases it transforms in a isotropic fluid with the concomitant disappearance of its SAXS and WAXS signals, Figure 3.3.

X-ray studies for pH 3.0. Except for small differences in the temperatures at which phenomena occurs the samples at pH 3.0 are identical to those at pH 4.0. At 42 ºC phase $L_{C1,3}$ begins to melt, and $L_{\alpha 1}$ appears. By 56 ºC L_{C2} is completely molten. Consequently, from 46 to 56 ºC phase $L_{C1,3}$ coexists with phase L_{C2}, $L_{\alpha 2}$ and $L_{\alpha 1}$. From 56 until a not very well defined region between 68 and 78 ºC phase $L_{C1,3}$ coexists with phase $L_{\alpha 2}$ and $L_{\alpha 1}$. In the range 68–78 ºC the phase $L_{\alpha 2}$ completely converts into $L_{\alpha 1}$, and above this temperature phase $L_{C1,3}$ coexists with $L_{\alpha 1}$ until 87 ºC, where the crystalline phase disappears.

Above 87 ºC only $L_{\alpha 1}$ is present. The isotropic fluid observed for pH 4.0 is not clearly seen because the heating of these samples stopped at 91 ºC.

DSC studies for pH 3.0, 4.0, 5.0 and 9.0. The heating thermograms obtained by DSC of mixtures of ceramide, cholesterol and fatty acid samples in excess water at several PA ionization states, are plotted in Figure 3.4.

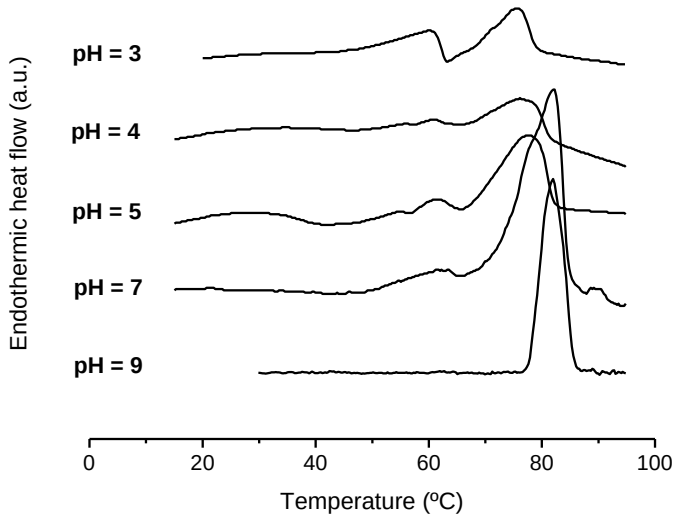

Figure 3.4 – Thermograms of mixtures of egg ceramide:cholesterol:palmitic acid (44:38:18 molar fractions) at pH 3.0, 4.0, 5.0, 7.0 and 9.0.

The sample at pH 9.0, has a sharp transition with T_m = 82 ºC that corresponds to the congruent melting of the ternary matrix with 54:46 egg-Cer:Ch plus 18 mol % PA, as already shown in Figure 3.1 panel A. At pH 7.0 the thermogram presents a shoulder at 77.6 ºC and this transitions is also observed at pH 4.0 and 3.0, with T_m at, respectively, 76.1 and 75.5 ºC. We interpret this transition to correspond to the transition of $L_{C1,3}$ to $L_{\alpha 1}$, which is observed by X-ray to occur in these pH samples in the same range. The

presence of free PA at pH 4.0, observed by X-ray, is not evident in the thermogram probably because its amount is too small to be detected. In the thermograms of Figure 3.4, as well as in the other DSC experiments, there are relatively small endotherms that do not correspond to noticeable changes in the X-ray data, not being possible to ascribe to them a known structural change.

Mixtures of ceramide, cholesterol, palmitic acid with increasing amounts of palmitic acid, at pH 4.0

In the following we analyze how the thermotropism of a C16-Cer, Ch 54:46 molar ratio mixture is affected by the addition of palmitic acid in molar percentages of 40%, 60% and 70% at pH 4.0.

Pure PA

Palmitic acid in excess water at pH 4.0 and 20 ºC gives a single diffraction in small angle at 0.273 nm^{-1} identified as a lamellar structure with a repeat distance of 3.66 nm. In the wide angle region there are two diffractions at 2.46 and 2.74 nm^{-1}, results that are in accordance with published data for palmitic acid[34]. Between 62 and 64 ºC the reflections in SAXS and WAXS vanish in a direct lamellar-crystalline to isotropic fluid phase transition, also coherent with what was observed by other authors[34]

X-ray studies for 40–70 mol % PA

Even if in some samples containing 18 mol % PA its diffraction is not visible, several others present a small diffraction peak characteristic of free PA,

namely in the SAXS shown in Figure 3.3A. This is an indication that 18 mol% is near the limiting concentration of PA that mixes with the other lipids at this pH. Indeed, all samples containing 40 or larger molar percentage of PA display at 22 ºC an intense and sharp diffraction located at 0.274 nm^{-1} accompanied by the characteristic wide angle reflections at 2.46 and 2.74 nm^{-1} that disappear between 56 and 58 ºC indicating the presence of free PA. Recalling that the system under study is prone to incomplete mixing we have to be sure that the observed free PA is not an artifact due to inadequate sample preparation, since the lower transition temperature may be due to contamination by the other components. If this was the case, addition of larger quantities of PA would only result in a stronger signal from the fatty acid and the pattern of the components in equilibrium would remain unchanged. However, we observe that the other structures coexisting with PA are not the same or do not have the same thermotropic behavior when the PA content increases from 18 to 70 mol %. It may be concluded that either PA is in equilibrium with the remaining lipids or, what is more plausible, part of it emulsifies the remaining lipids reducing the dimension of the aggregates.

In the samples with 40, 60 and 70 mol % PA a strong broad signal with apex located at ca. s = 0.22 nm^{-1} is observed at 20 ºC that seems to have origin in more than one diffraction. Despite the fact that the $L_{C1,3}$ phase has a diffraction at s = 0.224 nm^{-1} we are positive in that this phase/s is not present in these samples due to the absence of its characteristic wide-angle pattern.

In the 40, 60 and 70 mol % samples the broad signal with apex at ca. s = 0.22 nm^{-1} gives in part origin to the $L_{\alpha 2}$ phase at 38 ºC. Subsequently, a relatively broad peak at 0.216 nm^{-1} is revealed remaining visible until 78, 60 and 56 ºC, respectively, for 40, 60 and 70 mol % PA. The diffraction appearing in the wide-angle region at 2.31 nm^{-1} seems to be correlated with this peak because both disappear at the same temperature. Besides this signal and those already referred as pertaining to the PA, no other diffractions exist in the WAXS. Consequently, the broad band exhibiting a rather complex thermotropic

behavior is mainly due to fluid lipid phases observed in WAXS as the usual large band at 2.2 nm^{-1}. Refer to Figure 3.5 to examine the behavior of the 60 mol % sample.

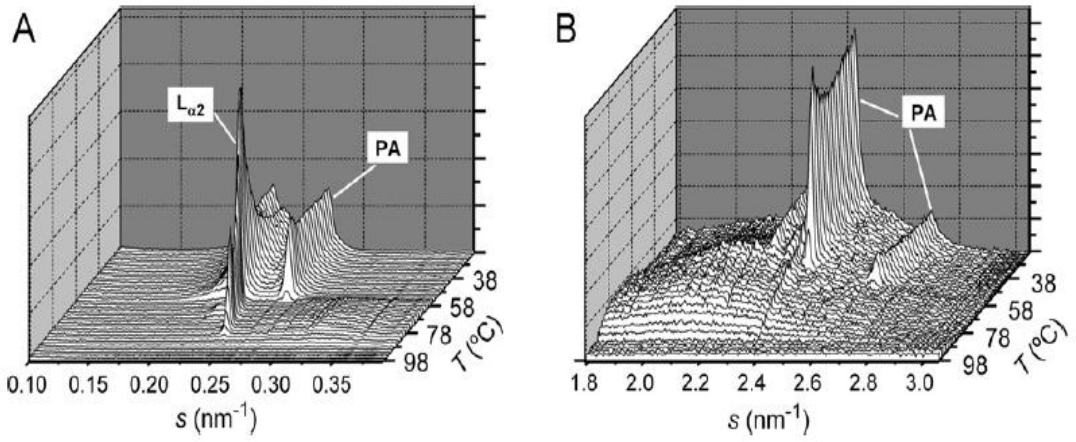

Figure 3.5 – Characteristic SAXS, panel A, and WAXS, panel B, of C16-Cer:Ch with 60 mol % PA in excess water at pH 4.0 as a function of temperature. The heating rate was 1 ^{o}C/min.

At temperatures above 60 ^{o}C a very broad signal centered at 0.3 nm^{-1} is detected only for 40 and 60 mol % PA, which seems to have origin in a poorly organized phase, eventually a micellar phase. The $L_{\alpha 2}$ phase gives a isotropic fluid at temperatures depending on the PA content: between 54 and 60 ºC for the 70 mol%, between 60 and 84 ºC for 60 mol % and between 58 and 82 ºC for 40 mol %.

DSC studies for 10, 30, 40 60 and 80 mol % PA. Figure 3.6 represents the heating thermograms of several ternary mixtures along increasing amounts of palmitic acid at pH 4.0.

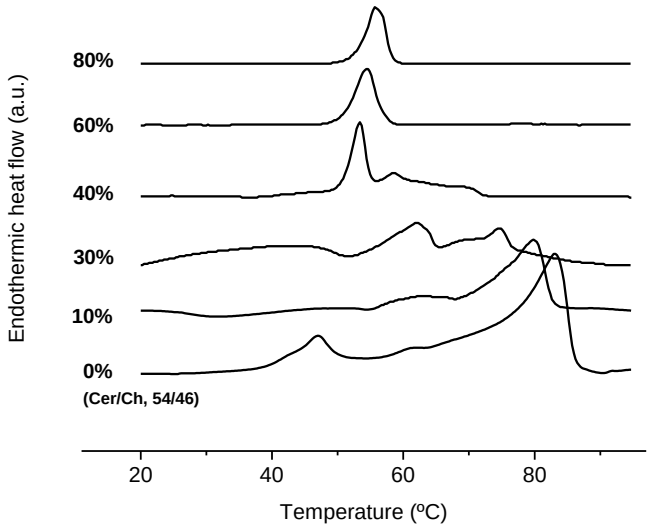

Figure 3.6. – Thermograms of several ternary mixtures with a constant C16-Cer:Ch 54:46 molar ratio, with 0, 10, 30, 40, 60 and 80 mol % of PA at pH 4.0.

As can be observed, the mixtures with 80–40 mol % PA have a clear endotherm between 55 and 58 ºC. This endotherm corresponds to the transition of both, the PA phase and the rigid phase, characterized by X-ray peaks at s = 0.216 and 2.31 nm^{-1}, that melts a few degrees before the PA. The free PA only appears in DSC above 30 mol % but residues of segregated PA are clearly detected by X-ray for many of the mixtures containing 18 mol % PA, at pH <7. The absence of the DSC signal of PA in all the samples used may result from its progressive dissolution in a liquid phase; either $L_{\alpha 1}$ which in the 18 mol % samples begins to form at 48–52 ºC, or in the fluid phase responsible for the broad band with s = 0.22 nm^{-1} observed in the 40 mol % sample.

3.5. Discussion

Between 20 and 88 ºC the sample of C16-Cer:Ch 54:46 with 18 mol % PA at pH 9.0 has, in our experimental conditions, an X-ray pattern that seems absolutely identical, in both the small and the wide angle regions, to that observed for the L_{C1} phase which is pure crystalline ceramide. The main transition temperature of the mixture occurs between 88 and 90 ºC, which is not very far from that of pure ceramide samples that melt at 93 ^{o}C[2]. Nevertheless, we sustain that C16-Cer:Ch 54:46 with 18 mol % PA form a new L_C phase, L_{C3}, distinct from L_{C1}, characterized by reflections at *s* = 2.38, 2.42, 2.47, 2.55, 2.64 and 2.70 nm^{-1}, Figure 3.1 panels B and D.

There are several experimental evidences that L_{C3} and L_{C1} are different phases despite the similarity of their X-ray diffraction. If this were not the case, PA and Ch, either mixed or separated, would show their presence by their own characteristic X-ray patterns. However, no sign of isolated Ch and/or PA is observed by either X-ray or DSC, and the same can be said in which concerns mixtures of Ch with PA because the behavior of Ch:PA suspended in water is known and the structures formed are easily detectable by X-ray. Mixtures of palmitic acid with cholesterol, both at relative molar proportions of 50:50 and 25:75 at pH 8.5, form fluid layers with a repeat distance of 4.9 nm between 25 ºC and 70 ºC [35] that we do not observe in our samples. Thus, the existence of cholesterol solubilized in palmitic acid coexisting with phase L_{C1} is excluded. We still may question if part of the C16-Cer may form, together with the Ch and PA, a phase which is invisible to X-ray and DSC. In support of this interpretation, the smaller transition enthalpy of the mixture compared with that of ceramide alone, 23.9 kJ/mol of C16-Cer and 36.8 kJ/mol, respectively, may arise from ca. 30% of the ceramide being mixed with ionized PA and Ch. To discard this possibility we have done a sample with C16-Cer:Ch:PA in the proportion 13:38:18 that, if this last interpretation is correct, should be clear without any kind of precipitate. What happens is the opposite; the usual

precipitate is formed, and the clear aqueous phase obtained by centrifugation, is free of lipid by TLC analysis. No doubt is left that the phase L_{C3} is distinct from L_{C1} and characterized by a different transition enthalpy.

There are other arguments that speak in favor of a compositional difference between L_{C3} and L_{C1}. If we do not consider the existence of a distinct L_{C3} phase, the only possible interpretation of the experimental observations would be that the PA emulsifies most of the cholesterol extracting it from the membrane at low temperature, but once the $L_{\alpha 1}$ phase appears (86 ºC) the excluded PA and Ch dissolve in it, giving origin to the H_{II} phase. However there are evidences that testimony against this interpretation: first, we are supposing that the hypothetic Ch:PA emulsion would readily dissolve in $L_{\alpha 1}$ converting it into H_{II}. This is not what happens with the sample containing 12 mol% PA. For this composition the $L_{\alpha 1}$ phase begins to appear at 62 ºC and H_{II} should begin to appear at this same temperature as the result of the incorporation of Ch and PA in $L_{\alpha 1}$, yet it is absent until 88 ºC; second, during cooling, the H_{II} phase gives the crystalline lamellar phase between 80 and 72 ºC that takes 8 min (at 1 ºC/min) a time that is too short if we take into consideration the known kinetics of the insertion and desorption of Ch and single-chain lipids in/from bilayers[36,37].

It should also be commented that the addition of ionized FA does not increase the interlamellar repeat distance of the L_{C3} as compared with the L_{C1} phase, what can be explained by a short Debye screening length compared with the interlamellar water phase. The calculated Debye screening length is about 1 nm for an electrical relative permittivity of the water at the interface identical to the bulk (80) and for an ionic strength of the aqueous phase of 100 mM. The typical thickness of the interlamellar water layer in phosphatidylcholine assemblies is 2–3 nm[38,39], value that seems quite large as compared with the Debye screening length for our conditions, what may lead to a non-significant interlamellar repulsion.

An alternative explanation, in some way opposed to this, would be the low hydration of the ceramide headgroup. If the hydration of the ceramide is such

that in the structures formed the PA is involved in the headgroup H-bond network, it may be “screened” from the effect of the external pH. Literature data is not clear about how thick the interlayer water in these systems is, but it is consensual that the hydration of ceramides is much lower than that of phosphorylcholines. Data from DSC and X-ray indicate that ceramides uptake 9.3 wt % water[1], to compare with the 15–18 wt % of phosphorylcholines, and from the comparative analysis of adsorption isotherms of cholines, ceramides and cholesterol the hydration of ceramides is much lower than that of cholines or even cholesterol[40]. Also McIntosh[19] concludes from X-ray electron density calculations for ceramide studies that “there are extremely narrow fluid spaces between adjacent bilayers at low pH”. In any case, the extent of hydration seems to be related to pH. As described in Section 3.3 the physical appearance of the suspensions is evidence for a better hydration at high pH, with structures that are similar to regular multilayered vesicles. At low pH, as well as with pure ceramide, the buffer is transparent with aggregates apparently compact that do not seem common vesicular structures. However, these visual differences are not clearly reflected in the structure obtained by X-ray.

If we depart from the C16-Cer:Ch 54:46, progressively increasing its PA content until 18 mol %, the amount of L_{C1} and L_{C2} phases decreases and, concomitantly, the new phase L_{C3} is formed. For 18 mol % PA the only phase that remains is the L_{C3} with a molar composition C16-Cer:Ch:PA 44:38:18. The melting of this phase occurs in a narrow temperature interval 88–90 ^{o}C, a congruent transition, that further confirms that we are in the presence of a crystalline molecular aggregate with approximate stoichiometry $C16\text{-}Cer_5:Ch_4:PA_2$. It happens that the relative proportions in which these lipid classes are, is that found in the *stratum corneum*[17] but, given the differences in the lipids involved and structure of the aggregates formed, it should be interpreted as a coincidence and not a meaningful fact with biological implications. We should recall that neither the chain length, nor the headgroup characteristics of C16-Cer are those prevalent in the *stratum corneum*. In

particular the headgroup of C16-Cer is non-hydroxylated while in SC ca. 70% of the ceramides are hydroxylated, and it is known that hydroxylation strongly influences the physical–chemical properties of the ceramides.

Compared with phosphocholines, ceramides have stronger headgroup interactions what may be equated to two independent causes: one is the strong H-bonds that are formed between headgroups as thoroughly described by several authors based on FTIR measurements[24,3], other is the much lower ceramide headgroup dipole repulsions. The calculated ceramide headgroup dipole moment is ca. 2.5 Debye; the same calculation made for glycero-3-phosphocholine group gives ca. 17 Debye, consequence of being zwitterionic. The enthalpic unfavorable alignment of the headgroups at the interface in a rigid conformation favors the fluid state in cholines[41]. Both effects, H-bonding and small dipole moment, are responsible for the relatively high melting temperatures of ceramides[26] and the preference for a crystalline phase below transition temperature. Being in the crystalline state it is not surprising that Ch does not dissolve randomly in the ceramide, preferring to form ordered 2D structures with a defined stoichiometry[2].

Since the L_{C3} phase is stoichiometric with a C16-Cer:Ch:PA ratio of ca. 44:38:18, L_{C2} has also a defined stoichiometry 2:3 ($C16\text{-}Cer_2Ch_3$), and L_{C1} is pure C16-Cer, it is possible to determine with a simple mass balance exercise the fractions of each of these crystalline aggregates for the 5 and 12 mol % PA at pH 9.0 in the low temperature region where only three phases coexist. For the case of 12 mol % PA, 6.5 mol % C16-Cer is in the L_{C1} phase, 11% and 16.5%, respectively, of ceramide and Ch in L_{C2}, and the total amount of PA, 12 mol %, is in the L_{C3} together with 30% C16-Cer and 24% Ch. Identical estimate for the 5 mol % sample conduce to values of 16.3 mol % free ceramide (L_{C1}), 22.4 mol % C16-Cer plus 33.7 mol % Ch in the L_{C2}, justifying the stronger SAXS signal observed, and 12.5 mol % of ceramide and 10 mol % Ch go with the remaining 5 mol % PA forming the L_{C3} phase.

In Figure 3.7 we condense our observations of the thermotropism of a mixture of C16-Cer:Ch 54:46 molar relation for several concentrations of PA at pH 9.0 based on the experimental data and the reasoning presented above.

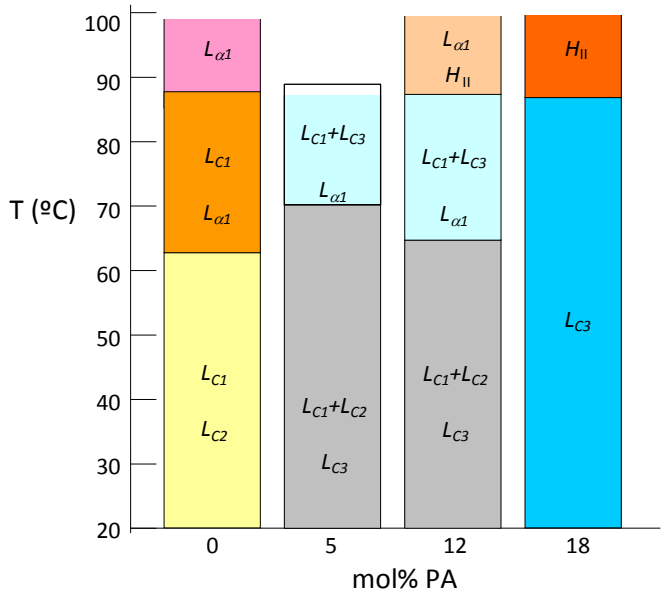

Figure 3.7. – Schematic diagram indicating the temperature range in which the several phases described in the text are stable for 0, 5, 12 and 18 mol% of PA added to the C16-Cer:Ch mixture in molar ratio 54:46 for pH 9.0 in excess water.

When this mixture is prepared at pH values ≤7.0, a phase with diffractions coherent with L_{C1}/L_{C3} is detected, together with $L_{\alpha 2}$, L_{C2} and for pH 4.0 and 3.0 pure neutral PA. There is evidence that at pH 7.0, and below, it is the L_{C1} phase that exists and not the L_{C3}. Since L_{C1} and L_{C2} do not contain PA, all the fatty acid, if not free, should be in the $L_{\alpha 2}$ and/or a neutralized L_{C3} phase. However, the L_{C3} phase retains the same SAXS and WAXS along progressive neutralization. Additionally, in some samples where the characteristic SAXS of

free PA is strong, the phase $L_{\alpha 2}$ is absent. These observations led us to conclude that the SAXS and WAXS signals have origin in L_{C1}.

In the totally or partially neutralized samples the fluid phase formed at high temperature is always lamellar, $L_{\alpha 1}$, and the transition to a hexagonal phase is only detected for pH 9.0. At this pH the solubility of the ionized palmitic acid attains at least 60 mol%, what makes the ionized form much more soluble in the ceramide:cholesterol mixture as compared to the neutral form. At pH 4.0, segregated co-existing pure palmitic acid is always detected above 18 mol %. However, this does not mean that the added PA is excluded from the remaining lipid system already saturated in fatty acid because the other phases present suffer a gradual change with further increase of the fraction of PA. Based on this observation we cannot discard PA as being one component of the equilibrated lipid system.

The addition of protonated fatty acids with 16 or more carbons to phosphocholines, is known to favor the formation of an inverted hexagonal phase above the main transition temperature[42]. The fatty acid induction of H_{II} phase in phosphocholine has been rationalized considering that the insertion of the fatty acid in the bilayer allows a closer interaction of the acyl chains. The larger choline head-group area compared to that of the acyl chains cross section becomes equilibrated. When the bilayer melts, the increase in the chain volume due to the larger number of *trans-gauche* conformations exceeds the head-group volume, favoring inverted structures[43]. In our case, the ceramide headgroups are relatively small, the cholesterol is already filling any possible interchain spaces and the structural effect of FA addition can hardly be imputed to the same cause. However, the formation of H_{II} phases is not unusual in mixtures of ceramide, cholesterol and fatty acid at high temperatures[8,10,44].

In the literature, there is a considerable number of studies, in which lipid mixtures intended to model the *stratum corneum* lipid matrix, usually containing ceramide, cholesterol, long chain fatty acids of several chain

lengths, and, in some cases, cholesterol sulfate, are characterized by several techniques such as small and wide angle X-ray scattering, FTIR and ^{2}H NMR. Depending on the work, the authors chose to use ceramides extracted from the *stratum corneum* employed as a full extract or separated in sub-classes, or commercially available, of synthetic or of natural origin (brain).

The characterizations of equimolar mixtures of ceramide commercially known as type III, cholesterol and palmitic acid have direct relevance for our study, because the type of ceramide is the same as ours, with non-hydroxy fatty acids and, despite the difference in the molar proportion used, a similar pattern in the phase thermotropism exists. This system was first characterized by ^{2}H NMR[8]. When the lipidic mixture was prepared at pH 7.4, at 20 ºC, the signal from a solid coexisting with a fluid phase was detected. Similarly, in our mixtures at pH 7.0 a crystalline phase, L_{C1}, coexists with a lamellar liquid crystalline phase, $L_{\alpha 2}$, at 20 ºC. Above 68 ºC, the authors observed a pattern compatible with an inverted hexagonal phase that we observe for our mixtures only at pH 9.0. For pH 5.2, besides the ^{2}H NMR study there are also works that use FTIR[23] and small and wide angle X-ray diffraction[45]. By FTIR a highly ordered/solid phase at 20 ºC was found, an observation in accordance with what was observed by NMR, which also detected a coexisting liquid phase. In the same conditions, the X-ray study reports two lamellar phases with repeat distance d = 5.38 nm and 4.10 nm, co-existing with pure PA and pure cholesterol monohydrate. In the same study several diffractions in the wide-angle region, denounced the presence of crystalline phases[45]. Comparing with our results at pH 4.0, we also detect, solid lamellar crystalline phases coexisting with a lamellar fluid phase and PA at 20 ºC. The small differences between the measured lamellar repeat distance compared with the literature X-ray data may be attributed to the difference in chain length of the ceramide used. It should, however, be noted that the wide-angle diffraction patterns of the mixture with the type III ceramide is completely distinct from what we obtain, indicating different acyl chain arrangements. Measurements by ^{2}H NMR[8] detect a isotropic fluid phase at 51–54 ºC that continuously growth in

intensity with increasing temperature being the only observed phase at 80 ºC. The correspondent X-ray characterization finds a transition of the L_{α} phase to a isotropic fluid between 80 and 90 ºC [45]. We also encounter a transition of the $L_{\alpha 1}$ phase to a region of isotropic fluid phase above 86 ºC. The absence of an inverted hexagonal phase at pH 5.4 is also in agreement with our pH 4.0 samples. However, contrarily to what we concluded for pH 7.0, some authors still find the H_{II} phase in mixtures prepared at pH 7.4 [8]. With an equimolar ternary mixture differing from the one above in that the type III ceramide was replaced by the synthetic ceramide C16 and pH 5.2 [46], measurements made with ^{2}H NMR, IR and Raman spectroscopies also show the coexistence of a solid and a fluid phase at 25 ºC and a isotropic phase at 75 ºC.

Table 3.1 summarizes the correspondence between the phases that we deduced from the experimental data and the diffraction pattern of each of them.

Table 3.1. – Small and wide angle characteristic X-ray diffractions of the main phases observed in the studied ceramide, cholesterol, and palmitic acid mixtures at 20 ^{o}C.

Phase	**SAXS region** s **(nm^{-1})**	**WAXS region** s **(nm^{-1})**
L_{C1} / L_{C3}	0.224	2.38, 2.41, 2.46, 2.55, 2.65 and 2.70
L_{C2}	0.289	1.83, 2.02, 2.21
$L_{\alpha 1}$	0.243	2.2 (broad)
$L_{\alpha 2}$	0.235	Fluid
H_{II}	0.207, 0.356	
PA	0.273	2.46, 2.74

The thermal range where these phases are stable for each pH is graphically schematized in Figure 3.8

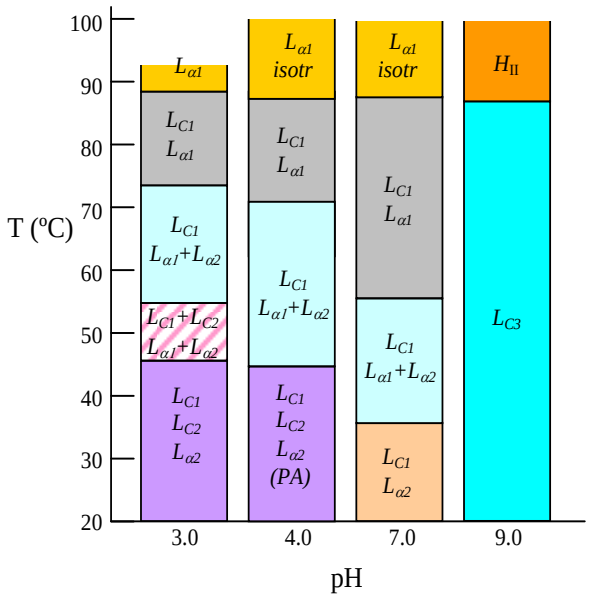

Figure 3.8. – Schematic diagram indicating the temperature range of stability of several phases described in the text for the mixture of ceramide with cholesterol in the relative molar proportion 44:38:18 of C16-Cer:Ch:PA for pH 3.0, 4.0, 7.0 and 9.0. In the dashed region for pH 3.0 there is not a clear transition from the domain of L_{C1} + L_{C3} + $L_{\alpha 2}$ and that of L_{C1} + $L_{\alpha 1}$ + $L_{\alpha 2}$.

3.6. Conclusion

The study of the thermotropism and prototropism of the mixtures of C16-Cer, cholesterol with several fractions of palmitic acid in excess water resulted in a general overview of the possible phases and phase transformations that may occur in this ternary system.

When adding PA to the mixture 54:46, of ceramide with cholesterol, at room temperature and pH 9.0, we start with two lamellar crystalline phases L_{C1} and L_{C2}, the last one being a stoichiometric aggregate of ceramide with cholesterol in the molar proportions 2:3. Adding PA, a third crystalline phase, L_{C3}, appears, and when attaining 18 mol % of PA it is the only phase present. This phase has a stoichiometry given by C16-Cer_5:Ch_4:PA_2 and forms a lamellar

crystalline structure characterized by X-ray diffractions undistinguishable from those of pure ceramide both in the small and wide-angle regions. We previously reported two lipidic stoichiometric aggregates forming L_C phases in binary mixtures of ceramide with cholesterol[2] and other authors have also found that ceramide:cholesterol monolayers organize in two-dimensional crystals composed of the two lipids[47]. The question may be raised why ceramides are so prolific in structures never observed with other membrane-forming lipids, namely glycero-phosphocholines. A possible explanation may reside in that ceramide, partially due to the strong H-bonds and in part also consequence of the lower headgroup dipole moment, adopts a stable lamellar crystalline structure at room temperature while most other lipids, even at temperatures at which the L_C is the thermodynamically more stable state, remain trapped in rigid non-crystalline structures such as the L_β or $L_{\beta'}$. Probably such structured molecular aggregates may also form with other common phospholipids, but they have never the opportunity to attain its final structure due to slow in-plane molecular rearrangement. When melted, this ternary mixture forms an inverted hexagonal, H_{II}, structure. The formation of H_{II} phases may be a general property of mixtures of ceramide, cholesterol and ionized fatty acid at high temperatures since other authors have found this phase for different compositions and ceramides[8,10,44].

For the composition 44:38:18, with pH ≤7.0, the fatty acid is partially or totally protonated. At low temperature, three main phases coexist: pure crystalline ceramide in L_{C1}, ceramide:cholesterol also forming a lamellar crystalline phase, L_{C2}, and a lamellar liquid phase, $L_{\alpha 2}$, that contains nearly all fatty acid, a small part of it being segregated as pure PA. In studies with the equimolar mixture of bovine brain ceramide, cholesterol and palmitic acid, other authors found a fluid at 20 ºC at both, pH 5.2 and 7.4 [8] coexisting with a crystalline phase. This fluid is probably similar to our $L_{\alpha 2}$.

For the system having the PA totally protonated, pH 4.0, when the amount of PA is progressively increased, coexisting segregated neutral PA is detected for concentrations equal or larger than 18 mol %. This contrasts with the behavior

at pH 9.0, for which PA is soluble in the ceramide:cholesterol system at least until 60 mol%. Also to be referred that in the presence of protonated PA (pH ≤7.0), the liquid lamellar phase/s convert, at high temperature, into a isotropic fluid.

Several characteristics of this system may be valuable to the interpretation of other similar mixtures, namely those found in the nature. In which concerns the particular case of the *stratum corneum*, we may speculate that there should always be a part of the system that remains in the fluid phase at the pH to which it is normally exposed. But a more general property of ceramides that has to be taken into account by those that propose the formation of ceramide-rich regions of cell membranes[48,11], is that, even when mixed with large amounts of cholesterol and fatty acids, they have an unusual tendency to form lamellar crystalline structures.

3.7. Acknowledgments

This work was financially supported by FCT – Fundação para a Ciência e Tecnologia, Portugal through contracts PTDC/QUI/68242/2006 and PTDC/SAU-FCT/69072/2006, and by HASYLAB of DESY, Germany with Project II-20060163 EC. S.L.S. is indebted to FCT, Portugal for Grant BD/6482/2001.

3.8. References

(1) Shah, J., Atienza, J.M., Duclos, R.I., Rawlings, A.V., Dong, Z.X., Shipley, G.G. (1995). Structural and thermotropic properties of synthetic C16-0 (palmitoyl) ceramide-effect of hydration. *J. Lipid Res.*, 36, 1936–1944.

(2) Souza, S.L., Capitan, M.J., Alvarez, J., Funari, S.S., Lameiro, M.H., Melo, E. (2009). Phase behavior of aqueous dispersions of mixtures of N-palmitoyl ceramide and cholesterol: a lipid system with ceramide-cholesterol crystalline lamellar phases. *J. Phys. Chem. B*, 113, 1367–1375.

(3) Moore, D.J., Rerek, M.E., Mendelsohn, R. (1997). FTIR spectroscopy studies of the conformational order and phase behavior of ceramides. *J. Phys. Chem. B*, 101, 8933–8940.

(4) White, S.H., Mirejovsky, D., King, G.I. (1988). Structure of lamellar lipid domains and corneocyte envelopes of murine *stratum-corneum* - an X-ray-diffraction study. *Biochemistry*, 27, 3725–3732.

(5) Elias, P.M. (2005). *Stratum corneum* defensive functions: an integrated view. *J. Invest. Dermatol.*, 125, 183–200.

(6) Madison, K.C. (2003). Barrier function of the skin: “La raison d’etre” of the epidermis. *J. Invest. Dermatol.*, 121, 231–241.

(7) Mimeault, M., Bonenfant, D. (2002). FTIR spectroscopic analyses of the temperature and pH influences on *stratum corneum* lipid phase behaviors and interactions. *Talanta*, 56, 395–405.

(8) Kitson, N., Thewalt, J., Lafleur, M., Bloom, M. (1994). A model membrane approach to the epidermal permeability barrier. *Biochemistry*, 33, 6707–6715.

(9) Kitagawa, S., Yokochi, N., Murooka, N. (1995). pH-dependence of phase transition of the lipid bilayer of liposomes of *stratum corneum* lipids. *Int. J. Pharm.*, 126, 49–56.

(10) Bouwstra, J.A., Gooris, G.S., Dubbelaar, F.E.R., Ponec, M. (2000). Phase behaviour of skin barrier model membranes at pH 7.4. *Cell. Mol. Biol.*, 46, 979–992.

(11) Stancevic, B., Kolesnick, R. (2010). Ceramide-rich platforms in transmembrane signaling. *FEBS Lett.*, 584, 1728–1740.

(12) Hannun, Y.A., Obeid, L.M. (1995). Ceramide - an intracellular signal for apoptosis.*Trends Biochem. Sci.*, 20, 73–77.

(13) Norlen, L., Nicander, I., Rozell, B.L., Ollmar, S., Forslind, B., (1999). Inter- and intraindividual differences in human *stratum corneum* lipid content related to physical parameters of skin barrier function in vivo. *J. Invest. Dermatol.*, 112, 72–77.

(14) de Paepe, K., Weerheim, A., Houben, E., Roseeuw, D., Ponec, M., Rogiers, V. (2004). Analysis of epidermal lipids of the healthy human skin: factors affecting the design of a control population. *Skin Pharmacol. Physiol.,* 17, 23–30.

(15) Pappinen, S., Hermansson, M., Kuntsche, J., Somerharju, P., Wertz, P., Urtti, A., Suhonen, M., (2008). Comparison of rat epidermal keratinocyte organotypic culture (ROC) with intact human skin: lipid composition and thermal phase behavior of the *stratum corneum*. *Biochim. Biophys. Acta,* 1778, 824–834.

(16) Merle, C., Laugel, C., Chaminade, P., Baillet-Guffroy, A., (2010). Quantitative study of the *stratum corneum* lipid classes by normal phase liquid chromatography: comparison between two universal detectors. *J. Liq. Chromatogr. Relat. Technol.,* 33, 629–644.

(17) Wertz, P.W., Norlén, L.P.O. (2004). “Confidence intervals” for the “true” lipid composition of the human skin barrier? In Skin, Hair, and Nails. Forslind, B., Lindberg, M., Eds., Marcel Dekker, New York, pp. 85–106.

(18) Bouwstra, J.A., Gooris, G.S., Dubbelaar, F.E.R., Ponec, M. (1999). Cholesterol sulfate and calcium affect *stratum corneum* lipid organization over a wide temperature range. *J. Lipid Res.*, 40, 2303–2312.

(19) McIntosh, T.J., (2003). Organization of skin *stratum corneum* extracellular *lamellae*: diffraction evidence for asymmetric distribution of cholesterol. *Biophys. J.,* 85, 1675–1681.

(20) Plasencia, I., Norlen, L., Bagatolli, L.A. (2007). Direct visualization of lipid domains in human skin *stratum corneum's* lipid membranes: effect of pH and temperature. *Biophys. J.*, 93, 3142–3155.

(21) Motta, S., Monti, M., Sesana, S., Mellesi, L., Ghidoni, R., Caputo, R., (1994). Abnormality of water barrier function in psoriasis - role of ceramide fractions. *Arch. Dermatol.,* 130, 452–456.

(22) Huang, J.Y., Buboltz, J.T., Feigenson, G.W. (1999). Maximum solubility of cholesterol in phosphatidylcholine and phosphatidylethanolamine bilayers. *Biochim. Biophys. Acta*, 1417, 89–100.

(23) Lafleur, M. (1998). Phase behavior of model *stratum corneum* lipid mixtures: an infrared spectroscopy investigation. *Can. J. Chem.*, 76, 1501–1511.

(24) Rerek, M.E., Chen, H.C., Markovic, B., van Wyck, D., Garidel, P., Mendelsohn, R., Moore, D.J. (2001). Phytosphingosine and sphingosine ceramide headgroup hydrogen bonding: structural insights through thermotropic hydrogen/deuterium exchange. *J. Phys. Chem. B*, 105, 9355–9362.

(25) Hsueh, Y.W., Giles, R., Kitson, N., Thewalt, J. (2002). The effect of ceramide on phosphatidylcholine membranes: a deuterium NMR study. *Biophys. J.*, 82, 3089–3095.

(26) Chen, H.C., Mendelsohn, R., Rerek, M.E., Moore, D.J. (2000). Fourier transform infrared spectroscopy and differential scanning calorimetry studies of fatty acid homogeneous ceramide 2. *Biochim. Biophys. Acta*, 1468, 293–303.

(27) Marsh, D. (1990). Handbook of Lipid Bilayers, CRC Press, Boca Raton.

(28) Funari, S.S., Barcelo, F., Escriba, P.V. (2003). Effects of oleic acid and its congeners, elaidic and stearic acids, on the structural properties of phosphatidylethanolamine membranes. *J. Lipid Res.*, 44, 567-575.

(29) Cevc, G. (1990). Membrane electrostatics. *Biochim. Biophys. Acta*, 1031, 311–382.

(30) Vaz, W.L.C., Nicksch, A., Jähnig, F. (1978). Electrostatic interactions at charge lipid membranes. Measurements of surface pH with fluorescent lipoid indicators. *Eur. J. Biochim.*, 83, 299–305.

(31) Engelman, D.M., Rothman, J.E., (1972). Planar organization of lecithin-cholesterol bilayers. *J. Biol. Chem.,* 247, 3694–3697.

(32) Casilla, R., Cooper, W.D., Eley, D.D. (1973). Temperature effect on stearic acid monolayers on water. *J. Chem. Soc. Faraday Trans. I,* 69, 257–262.

(33) Seddon, J.M. (1990). Structure of the inverted hexagonal (Hii) phase, and non-lamellar phase-transitions of lipids. *Biochim. Biophys. Acta*, 1031, 1–69.

(34) Koynova, R.D., Tenchov, B.G., Quinn, P.J., Laggner, P. (1988). Structure and phase-behavior of hydrated mixtures of L-dipalmitoylphosphatidylcholine and palmitic acid - correlations between structural rearrangements, specific volume changes and endothermic events. *Chem. Phys. Lipids*, 48, 205–214.

(35) Ouimet, J., Croft, S., Pare, C., Katsaras, J., Lafleur, M. (2003). Modulation of the polymorphism of the palmitic acid/cholesterol system by the pH. *Langmuir*, 19, 1089–1097.

(36) Abreu, M.S.C., Estronca, L.M.B.B., Moreno, M.J., Vaz, W.L.C. (2003). Binding of a fluorescent lipid amphiphile to albumin and its transfer to lipid bilayer membranes. *Biophys. J.*, 84, 386–399.

(37) Estronca, L.M.B.B., Moreno, M.J., Vaz, W.L.C. (2007). Kinetics and thermodynamics of the association of dehydroergosterol with lipid bilayer membranes. *Biophys. J.*, 93, 4244–4253.

(38) Maulik, P.R., Shipley, G.G. (1996). N-palmitoyl sphingomyelin bilayers: structure and interactions with cholesterol and dipalmitoylphosphatidylcholine. *Biochemistry*, 35, 8025–8034.

(39) Nagle, J.F., Tristram-Nagle, S. (2000). Structure of lipid bilayers. *Biochim. Biophys. Acta*, 1469, 159–195.

(40) Jendrasiak, G.L., Smith, R.L., (2001). The effect of the choline headgroup on phospholipid hydration. *Chem. Phys. Lipids,* 113, 55–66.

(41) McIntosh, T.J., Simon, S.A., Needham, D., Huang, C.H., (1992). Interbilayer interactions between sphingomyelin and sphingomyelin cholesterol bilayers. *Biochemistry,* 31, 2020–2024.

(42) Koynova, R., Tenchov, B. (2001). Interactions of surfactants and fatty acids with lipids. *Curr. Opin. Colloid Interface Sci.*, 6, 277–286.

(43) Fernández, M.S., González-Martínez, M.T., Calderón, E. (1986). The effect of pH on the phase transition temperature of dipalmitoylphosphatidylcholine-palmitic acid liposomes. *Biochim. Biophys. Acta*, 863, 156–164.

(44) Abraham, W., Downing, D.T. (1991). Deuterium NMR investigation of polymorphism in *stratum corneum* lipids. *Biochim. Biophys. Acta*, 1068, 189–194.

(45) Bouwstra, J.A., Thewalt, J., Gooris, G.S., Kitson, N. (1997). A model membrane approach to the epidermal permeability barrier: an X-ray diffraction study. *Biochemistry*, 36, 7717–7725.

(46) Brief, E., Kwak, S., Cheng, J.T.J., Kitson, N., Thewalt, J., Lafleur, M. (2009). Phase behavior of an equimolar mixture of N-palmitoyl-D-*erythro*-sphingosine, cholesterol, and palmitic acid, a mixture with optimized hydrophobic matching. *Langmuir*, 25, 7523–7532.

(47) Scheffer, L., Solomonov, I., Weygand, M.J., Kjaer, K., Leiserowitz, L., Addadi, L. (2005). Structure of cholesterol/ceramide monolayer mixtures: implications to the molecular organization of lipid rafts. *Biophys. J.*, 88, 3381–3391.

(48) Goni, F.M., Alonso, A. (2009). Effects of ceramide and other simple sphingolipids on membrane lateral structure. *Biochim. Biophys. Acta*, 1788, 169–177.

4. Study of the miscibility of cholesteryl oleate in a matrix of ceramide, cholesterol and fatty acid

The co-authors of the work presented in this Chapter had the following contributions:

- J.A. Hamilton supervised the ^{13}C MAS NMR work at the Department of Biophysics of the Boston University,
- K.J. Hallock optimized the setup and helped with the ^{13}C MAS NMR measurements,
- S.S. Funari is the beamline scientist of A2 of Hasylab at DESY, optimized the experimental setup for our measurements, made the preliminary SAXS and WAXS conversion, and helped with the SAXS interpretation,
- W.L.C. Vaz co-supervised the initial steps of the study of the miscibility of cholesteryl oleate with ceramides.

It was published as:

Souza, S.L., Hallock, K.J., Funari, S.S., Vaz, W.L.C., Hamilton, J.A., Melo, E. (2011). Study of the miscibility of cholesteryl oleate in a matrix of ceramide, cholesterol and fatty acid. *Chem. Phys. Lipids*, 164, 664-671.

4.1. Abstract

Cholesteryl esters (CE) are not generally abundant but are ubiquitous in living organisms and have markedly different properties from cholesterol because of their acyl chain. The miscibility/immiscibility of CE with biological lipid structures is a key property for their functions. In this work we study the solubility of cholesteryl oleate (ChO) in a model of the *stratum corneum* lipid matrix composed of ceramide C16, cholesterol and palmitic acid in excess water. Experiments were done in conditions of fully ionized (pH = 9.0) and fully neutralized fatty acid (pH=4.0), and differential scanning calorimetry of the ternary mixtures with added ChO at pH = 9.0 clearly displayed a main transition with the same maximum temperature, peak shape, and enthalpy, suggesting that ChO was excluded from the remaining lipids. This technique is not conclusive at pH = 4.0 because the transitions of the lipid matrix and ChO overlap. The insolubility of ChO at both pH values is supported by X-ray diffraction. Adding the ceramide:cholesterol:fatty acid lipid mixture to ChO did not change the X-ray pattern of the mixture nor that of the ChO. To supplement the above physical techniques, we applied ^{13}C MAS NMR spectroscopy with C-13 carbonyl-labeled ChO. A single ^{13}C carbonyl peak from the ChO at 171.5 ppm was observed, indicating exposure to only one environment. The chemical shift was identical to pure ChO below and above the temperature of isotropic liquid formation. Taken together, our results lead to the conclusion that the solubility of ChO is negligible in the ceramide:cholesterol:fatty acid lipid mixture.

4.2. Introduction

Cholesteryl esters (CE), are a class of lipidic molecules often found in biological systems. In fact, cholesterol is transported in the blood stream, and

stored in living cells mainly in the form of esters. Most attention to the physical properties of CE has been focused on their bulk properties in the oily and fluid phase in lipoprotein cores and lipid-rich domains of plaques[1]. More recent studies have investigated whether and how these weakly polar lipids fit into membrane bilayers. Several cholesteryl esters have a very low solubility in phosphatidylcholine[2,3] and bovine brain sphingomyelin bilayers [4]. The CE have a precise conformation in the bilayer with the carbonyl at the aqueous interface, and their limited solubility in this conformation is diminished with high levels of cholesterol[4,5].

Much less attention has been paid to the interaction of cholesteryl esters with ceramides, alone or in lipid mixtures, in particular those found in the *stratum corneum* (SC). The SC protects mammalians from external xenobiotic aggression and restrains the loss of internal constituents. It is a composite structure mainly made of a network of interconnected dead hydrophilic cell bodies with the voids between them filled by lipids and water. The main lipid components are ceramides, cholesterol and long chain saturated fatty acids, roughly in 9:5:2 weight proportions[6].

Ceramide (CER) alone, or ceramide:cholesterol aggregates, form very rigid crystalline lamellar phases in equilibrium with low interbilayer water content[7,8]. Cholesterol (Ch) forms stoichiometric aggregates with N-palmitoyl-D-*erythro*-sphingosine (C16-Cer) in the L_C phase and is miscible with the L_α phase until at least 75 mol % in both cases[8], which is even higher than in phosphocholine bilayers ~50-60 mol %[9]. Another particularity of the ceramide-cholesterol systems is the difficulty to incorporate external components once formed, for example additional cholesterol. To incorporate Ch into CER C16 *in vitro*, it is mandatory that the mixture is made prior to the bilayer-assembling step[9,8].

Cholesteryl esters are considered by some investigators to be minor components of the SC, but several laboratories have found such esters to comprise as much as 18-19% by weight of the SC lipids (the sum of cholesteryl oleate (ChO), CER, Ch and fatty acid (FA))[10-12]. The origin of the CE found in the analysis of the SC lipids is not consensual. While some

sustain that they are sebum contaminants, eg.[13], others present experimental evidence that seem to support that they are constituents of the SC lipid matrix[12,14]. For the present study the origin of CE is irrelevant since, being in direct contact with the SC lipid matrix, only its solubility will dictate if it mixes with the remaining lipids.

In the present work we examine the solubility of cholesteryl oleate, in a system containing C16-Cer with cholesterol and palmitic acid, in molar proportions 44:38:18, composition hereafter designated as the CER:Ch:FA matrix. Cholesteryl oleate was chosen because it has been identified as the most abundant cholesteryl ester in the *stratum corneum*[12]. The particular proportion of ceramide, cholesterol and fatty acid used is approximately that found in the SC[6] and similar ternary mixtures have often been used as models to study the physical-chemical properties of the SC lipid matrix (for a review see ref. 15). Despite the importance of the information obtained with these systems they do not mimic the natural tissue due to three main reasons: *(i)* the ceramide is non-hydroxylated while in the SC ca. 70 wt.% of the ceramides are hydroxylated[6], *(ii)* the lipids in the SC are arranged in a thick phase (ca. 13 nm)[16-19] that is not observed with these mixtures, and *(iii)* the SC, as a multicomponent system, may not have the same mixing properties of a ternary mixture, e.g.[20]. Despite the enumerated limitations, including the use of a palmitoyl ceramide, which is not the more abundant component of the CER NS class (SC nomenclature), useful information can be obtained concerning ChO solubility with the system tested. The short chain length of the ceramide is probably not a concern since their properties do not depend significantly from the hydrophobic tail length[21]. Palmitic acid has been frequently used as a generic fatty acid and it is particularly adequate for our study due to the importance of using a chain length that matches the ceramide[22].

Our strategy was to use several biophysical methods to study this complex model system because one single analytical technique would be insufficient. In a ternary system, several phases may coexist and the solubility of ChO could differ from one phase to another. X-ray diffraction was used to discriminate

structures and potential structural alterations with CE, differential scanning calorimetry (DSC) was used to monitor changes in the thermotropic behavior of the components upon mixing, and ^{13}C NMR to discriminate if the carbonyl group reports different environments when alone and when the CER:Ch:FA lipid matrix is present.

Because the ionization state of the fatty acid could modify the physical-chemical properties of the lipid mixture as well as affect its capacity to incorporate ChO, we characterized the interaction of ChO with our model lipid system at both pH = 9.0 (fully ionized) and 4.0 (fully protonated). At pH 9.0 we took advantage of the formation of a single 2D lamellar crystalline phase for the mixture CER:Ch:PA in the 44:38:18 molar ratio, with the consequent congruent melting, that simplifies the detection of non-dissolved ChO. However, at pH 4.0 the scenario is more complicated and the analysis of the small angle X-ray scattering (SAXS) and wide angle X-ray scattering (WAXS) of the system reveals the presence of three coexisting phases at low temperature, two L_C and one L_α[41]. Published data of equimolar ternary mixtures based on bovine brain ceramide propose two rigid phases together with non-incorporated PA and Ch[23]. Other studies using synthetic non-hydroxy C16 ceramide report the coexistence of rigid and possibly liquid phases at pH = 5.2 [24]. The solubility is determined by the characteristics of the lipidic phases and since no other phases are observed at intermediate pH the conclusion attained for the two pH tested is valid for all the 4.0 to 9.0 pH range.

4.3. Materials and methods

General reagents

Ceramides used were obtained from Avanti Polar Lipids (Birmingham, AL, USA), a synthetic ceramide (2S, 3R, 4E)-2-hexadecanoylaminooctadec-4-ene-1,3-diol (N-palmitoyl-D-*erythro*-sphingosine), and a natural ceramide of egg origin (egg-Cer) which is 84% C16 non-hydroxylated ceramide according to

Avanti specification. Sodium azide, succinic and palmitic acids, cholesterol and cholesteryl oleate from Sigma (Sintra, Portugal), benzene was from Panreac (Barcelona, Spain), methanol and chloroform, both HPLC grade, sodium chloride, sodium hydroxide and disodium salt of ethylenediaminetetraacetic acid (EDTA) were from Merck (Darmstadt, Germany), and boric acid from Riedel-de-Haën, (Seelze, Germany). All chemicals were used without further purification. Water for buffer preparation was double distilled and further purified with an Elgastat UHQ-PS system (Marlow, U.K.). Buffers were borate for pH = 9.0 with 100 mM ionic strength (Na^+) and succinic acid for pH = 4.0 also 100 mM.

Synthesis of labeled ChO

^{13}C carbonyl-labeled ChO, was synthesized according to procedure of direct esterification developed by Sripada[25]. Following this method, cholesterol was condensed with [1-^{13}C]-oleic acid at 35-40 ºC in the presence of dimethylaminopyridine and dicyclohexylcarbodiimide (reagents from Aldrich, Steinheim, Germany) in anhydrous chloroform. The reaction was stopped after 1.5 hours, and the product purified by silica gel column chromatography and purity was verified by TLC. A single carbonyl carbon signal was observed by NMR for the pure ChO, as expected.

Preparation of dispersions

The molar proportion of ceramide, cholesterol and fatty acid we used, 44:38:18, was derived from the conversion of the weight percentages 57.3%CER:29.3%Ch:13.4%FA[11] into molar fractions based on the C24 chain ceramide and corresponding fatty acid. Among the large range of published compositions for the SC lipid matrix, we chose this composition on the basis of carefully reviewed data[6] showing that at least three independent research groups, using two different techniques, attained very similar compositions[10-12].

Determinations that appeared after the cited review that we are aware of[26,14,27], proposing relations of CER:Ch:FA of ca. 19:49:32, 38:34:28 and 48:22:30 respectively, are very disperse and do not change the conclusions presented by Wertz and Norlén. Except for DSC, in which egg ceramide was used, the experiments were done with synthetic C16 ceramide. Lipid stock solutions in benzene/methanol, 7:3 (v:v) were mixed in adequate amounts and allowed to equilibrate for 30 minutes with occasional vortexing. The solutions were frozen at –20 ºC for at least 2 hours and subsequently freeze-dried. To the resulting powder buffer at 98 ºC was rapidly added under vortexing, and the dispersion hydrated at 98 ºC for 30 min because our study required temperatures as high as 98 ºC and a low pH, we verified by TLC that the ceramide and ChO in our samples did not undergo hydrolysis.

This method of sample preparation revealed to avoid component separation that cannot be reversed after the hydration stage. It is known, and we have confirmed for our mixtures, that systems involving ceramides are prone to attain metastable states that are maintained without change at room temperature[28,29,7]. To work in equilibrium conditions, or at least conditions that do not evidence metastability in the thermograms and X-ray diffraction, we have previously found that relatively slow cooling rates (1.0 ºC/min) are needed after the annealing step. Before every measurement the sample temperature was raised until 96 ºC and slowly cooled until the temperature we intended as starting point for the experiment. After this treatment no exothermic signals are observed in the heating DSC, the X-ray diffractograms are reversible, albeit with hysteresis, and after being stored at room temperature for several weeks there is no modification in the sample X-ray profile. This is valid for the ceramide:cholesterol:fatty acid matrix, not for ChO, because ChO only attains its crystalline form if the samples are kept below 15 ºC for several hours, as explained in the Results section.

Differential scanning calorimetry

Thermograms were obtained in a microcalorimeter VP-DSC, MicroCal (Northampton, MA) with 5 x 10^{-3} mmol of total lipid, a heating rate of 1 ºC/min, and with subsequent cooling at the same rate unless otherwise stated. All illustrated thermograms are the second run or subsequent runs that were fully reproducible. Besides the expected differences in the first thermogram, we found that the characteristics of the microcalorimeter chamber associated to the low density of the lipid aggregates led to a decrease in the signal after the first scan. For each mixture, three distinctly prepared replicates were studied. Samples containing lumps of lipid floating in the buffer solution, as frequently observed for ceramide dispersions[30], were not used for quantification of the transition enthalpy. For ΔH^o determination, the amount of lipid present in the calorimeter chamber was quantified by ^{1}H-NMR. Transition temperatures are presented as T_m, the peak temperature.

Cholesterol and ChO quantification by ^{1}H-NMR for ΔH^o determination

Due to the characteristics of the samples we cannot ensure that a quantitative amount of lipid is transferred to the DSC compartment and a posterior analysis of the lipid content of the DSC chamber must be done. We assume, based on X-ray, TLC and the DSC itself, that despite the heterogeneous physical appearance of the samples they are homogeneous in which concerns composition and structure. After a DSC run all the lipid in the DSC chamber was removed, all solvent evaporated and the residue dissolved in chloroform and filtered through a 10.0 μm pore Teflon filter to remove the solid suspended particles of the borate buffer. Chloroform was substituted by a fixed amount of deuterated chloroform. Proton NMR spectra were acquired with a Bruker AMX 300 NMR spectrometer (Wissenbourg, France) operating at 300 MHz, with a delay time of 5 seconds. Cholesteryl oleate and cholesterol amounts were obtained using calibration curves obtained from standards of each component

for the peak located at respectively δ = 4.6 ppm and δ = 3.5 ppm. Once the amount of cholesterol is known, the relative content of ceramide and palmitic acid could be estimated considering that the original composition was maintained. The precision of method was found to be of 5%.

X-ray measurements

Small and wide angle X-ray scattering were measured at the Soft Condensed Matter beamline A2 at the storage ring DORIS III of the Deutsches Elektronen Synchrotron (DESY) using a setup allowing simultaneous collection in the wide and small angle regions[31]. The wavelength of the X-ray beam is 0.15 nm and the detectors were a Mar165 and a Gabriel-type gas detector, for SAXS and WAXS respectively. The samples were prepared as previously described for DSC, except that less than 0.3 ml of buffer was used. Hydrated lipid in a small volume of buffer was transferred to glass capillary tubes, 1.0 mm diameter with 0.01 mm wall (Markröhrchen, Germany), and then closed and annealed in a thermo-cryostat bath until 98 ºC using the protocol of the DSC measurements (1 ºC/min heating with subsequent cooling at the same rate).

The temperature controlled sample holder was continuously heated from 20 to 95 ºC at 1.0 ºC/min, and some samples subsequently cooled at the same scan speed. Every 120 s (ca. 2 ºC), a local shutter, normally closed to protect the sample, was opened for 20 s, during which data was continuously acquired. The temperature of the sample holder at the beginning of each data collection was automatically registered.

To convert channels into reciprocal distances, $s = 1/d$, where d stands for the distance between the active diffracting planes we used the patterns of rat tail tendon and tripalmitin as standards for the SAXS and WAXS regions, respectively (sample-SAXS detector distance of ca. 1.5 m).

MAS NMR

^{13}C NMR spectra were obtained on a Bruker AM-300 instrument (7.05 Tesla; 50.3 MHz for ^{13}C) equipped with a Bruker Solids Accessory Unit and a multinuclear magic angle probe (Billerica, MA, U.S.A.). The samples were spun at 3.5 KHz to eliminate side-bands. As the samples were too small (~25 mg) to fill the 7 mm rotor, small pieces of compacted Teflon were introduced into the rotor, to obtain an appropriate and balanced weight for the rotor to adequately spin. High-power (300 MHz) ^{1}H decoupling was applied during data acquisition. Chemical shift were calibrated to the 14.10 ppm signal of the terminal fatty acid methyl. NMR samples were prepared as those for DSC, except for the hydration buffer volume that was reduced, while ensuring that at least 30 waters per lipid molecule were present, an amount sufficient for complete hydration. In this way, the solid white lipid mass could be easily transferred to the NMR rotor eliminating the usual centrifugation step.

4.4. Results and discussion

To evaluate the solubility of ChO in the CER:Ch:FA matrix, we studied their mixtures to detect any ChO that might be unincorporated into the lipid mixture and possible changes in the properties of the CER:Ch:FA matrix due to the inclusion of ChO. To accomplish these objectives, the structure of the mixtures was analyzed by combined SAXS-WAXS, modification of the thermotropic behavior due to the presence of ChO was studied by DSC, and local interactions with the organized lipid environment were probed by ^{13}C MAS NMR.

DSC of CER:Ch:FA matrix with ChO at pH = 9.0

In Figure 4.1. we compare the heating thermogram of the CER:Ch:FA + 15 mol % ChO, with those of the CER:Ch:FA matrix and pure ChO, at pH = 9.0. In the presence of ChO the enthalpy and temperature of transition of the CER:Ch:FA matrix is maintained (ΔH^o (CER:Ch:FA) = 10.5 kJ mol^{-1}, T_m (CER:Ch:FA) = 81 ºC), which suggests that there is no incorporation of ChO into the CER:Ch:FA phase at this pH. In the same conditions, the temperature of the ChO endothermic transition, T_m (ChO) = 47 ºC, decreased slightly to 45 ºC, an indication that some component/s from the lipid matrix may contaminate the free ChO, however, within the experimental error, the transition enthalpy of ChO is maintained (ΔH^o (ChO) *ca.* 7 kJ mol^{-1}). Identical DSC experiments at pH = 4.0 are not conclusive because, as referred in the introduction, instead of a single L_C phase several phases are present and the CER:Ch:FA matrix transitions overlay the ChO peak.

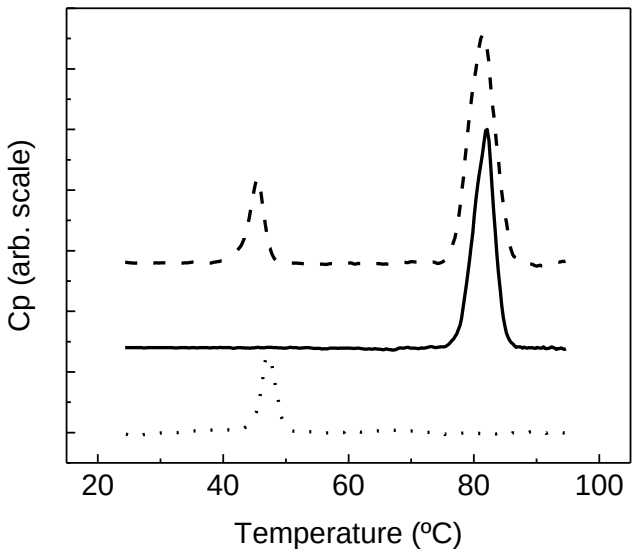

Figure 4.1. – Heating thermograms obtained at 1 ºC/min of: CER:Ch:FA matrix at pH = 9.0 (solid line), the same mixture to which 15% molar fraction of ChO was added (dashed line), and an aqueous suspension of ChO alone (dotted line).

Cholesteryl esters have complicated phase changes with several molecular organizations. Assignment of the endoenthalpic transition at 47 ºC to a particular phase transformation would aid in the interpretation of the X-ray data. Besides the usual crystalline and isotropic liquid phases, pure cholesteryl esters adopt metastable liquid crystalline structures known as the cholesteric and smectic arrangements as in Scheme 4.1.[32]. The molecular arrangement of the crystal is quite slow to attain when coming from any other state, isotropic, cholesteric or smectic, but the three liquid states interconvert with relative ease[32].

In Scheme 4.1. the kinetically hindered transitions are indicated by dashed arrows. Scheme 4.1. was proposed for pure ChO and our samples are dispersions in buffer. However only small differences are observed in the transition temperatures and the kinetics of conversion from isotropic liquid to cholesteric, and from this to the smectic form.

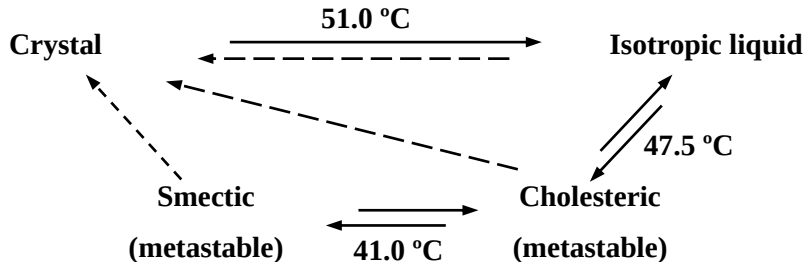

Scheme 4.1. - *Adapted from ref.*32.

The peak with T_m at 47 ºC observed in the heating run, Figure 4.1., must correspond to the transition of the pure ChO from a smectic organization to the isotropic liquid passing by the cholesteric intermediate. In fact the endoenthalpic transition obtained at 1 ºC/min is broad, and it unfolds into a double apex at ca. 43.5 and 44.7 ºC if the sample is scanned at 0.1 ºC/min (data not shown). We do not observe the melting of the crystal probably

because our samples are not kept at low temperature for long enough for re-crystallization before measurement.

CER:Ch:FA matrix with ChO at pH 4.0 and 9.0 – SAXS and WAXS

X-ray diffraction allows the analysis of mutual structural perturbations of the CER:Ch:FA matrix and ChO at both pH = 4.0 and 9.0. ChO that is unincorporated into the matrix can be detected by the appearance/disappearance of the characteristic diffraction peaks of each molecular arrangement in Scheme 4.1. The presence of crystalline ChO is revealed by the structured WAXS signal, while only a relatively broad band in wide angle is detected for the smectic, cholesteric and isotropic liquid. Owing to their layered structure, the crystal and the smectic are observed in small angle, whereas the arrangement characteristic of the cholesteric form does not present a particular X-ray diffraction[33].

For pH = 9.0 and at 20 ºC, the ternary mixture is organized in a crystalline lamellar phase, that melts to an inverted hexagonal phase at 88-90 ºC. The transition is observed simultaneously in the SAXS and WAXS regions ensuring that both signals have origin on the same phase (data not shown). To be noted that this is the transition observed at 81 ºC in DSC due to the use of the less pure egg-Cer. At pH = 4.0, and at 20 ºC, the mixture of ceramide, cholesterol and palmitic acid is organized in two lamellar crystalline phases, L_C, that coexist with a lamellar liquid crystalline phase, L_α. In Figure 4.3., panel II the region of the SAXS pattern for the first order peaks is shown for both pH values. At this pH several transitions are observed between 45 and 87 ºC, temperature above which no more crystalline phases are detected and the remaining lamellar liquid converts progressively into a isotropic fluid phase. The L_C phases are thermally connected with peak patterns in the wide-angle

region and the lamellar liquid crystalline phases accompanied by the characteristic wide band centered around 2.5 nm^{-1}.

Pure ChO dispersed in water should have the same behavior at pH = 4.0 and 9.0, and, we opted to study samples at pH = 9.0. In the wide angle region several reflections are observed, the more intense located at 2.06, 2.20, 2.27, 2.46 and 2.49 nm^{-1} that disappear between 47 and 51 ºC, Figure 4.2, corresponding approximately to the published value for the melting of the crystal to give the isotropic liquid (Scheme 4.1.). Existence of some kind of residual order in the chain packing in the isotropic liquid is revealed by a broad band centered at 5.0 Å. We do not observe the diffraction at s = 0.53 nm^{-1} (d = 18.7 Å) reported for the crystalline arrangement in monolayers type II[33], because it is out of the s-range sampled by our instrumental setup. In the subsequent cooling of the ChO sample a return to the crystalline form is not observed. Instead, a reflection in the small angle region, at s = 0.275 nm^{-1} (d = 3.64 nm) begins to appear when the temperature reaches 36 ºC, a reflection that expands with cooling, attaining 0.271 nm^{-1} (d = 3.69 nm) at 20 ºC, that we identify as the smectic state of ChO for which d = 3.55 nm has been reported[33,34]. The WAXS simultaneously acquired is not structured. This smectic phase, which appears in the cooling run with a delay of ca. 5 ºC relative to the observed transition, is metastable and the crystal only reappears if the system is cooled and maintained at low temperature for a much larger time than the duration of our experiment[32]. This metastability of the smectic phase results in a difference between the initial state of the samples in the DSC and X-ray experiments. While the samples for X-ray are kept at low temperature (4 ºC) before measurement, hence being mostly crystalline, those for DSC are only measured after a first heating and cooling in the calorimeter chamber, beginning as smectic in the second and subsequent scans.

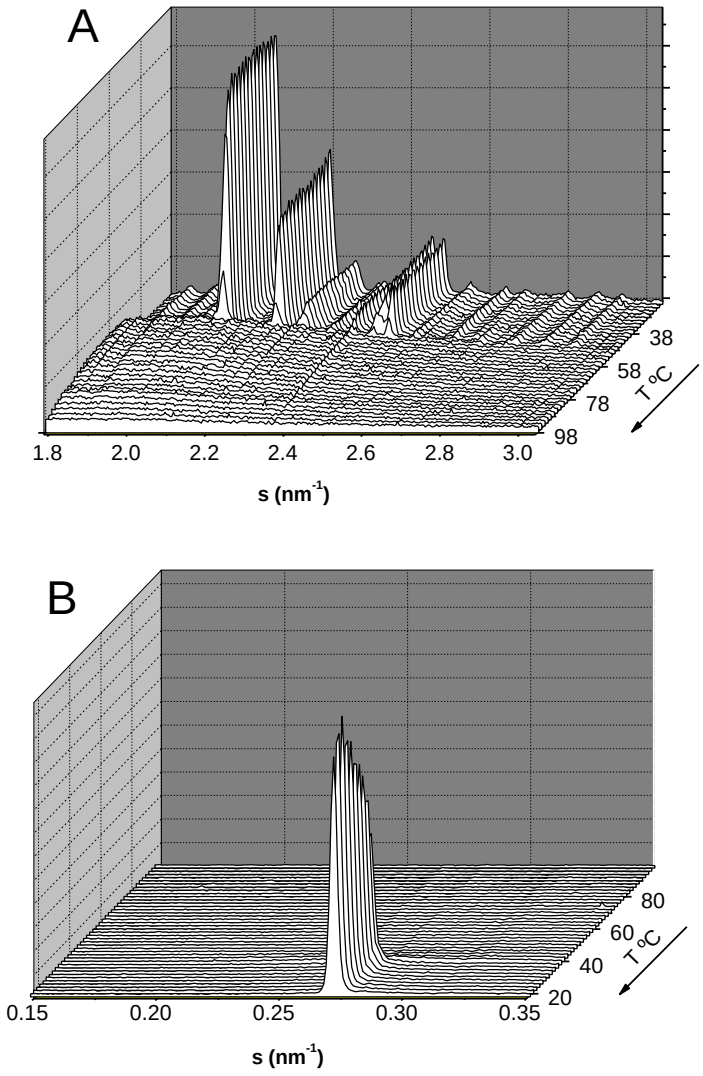

Figure 4.2. – Plots of the X-ray diffraction pattern of ChO in buffer at pH = 9.0. In the heating scan t (1 ºC/min; panel A), the melting of the crystalline form at ca. 49.5 ± 0.5 ºC is observed, while as explained in the text, no signal is visible in small angle. During the subsequent cooling of the same sample, also at 1 ºC/min, no structure appears in the WAXS but a strong diffraction in the SAXS, (panel B) is visible corresponding to the smectic state lamellar repeat distance.

When the CER:Ch:FA matrix is prepared in the presence of 15 mol% ChO, the original X-ray diffraction profile of the matrix is neither modified in spacing or in temperature behavior. Depending on the thermal history of the sample, different relative amounts of the smectic and crystalline ChO are detected. In these samples, the smectic is observable in SAXS as a single residual diffraction at 0.268 nm^{-1} that disappears between 31 and 37 ºC, where it is transformed into the cholesteric phase, which does not diffract. At the beginning of a T scan, most of the X-ray detectable ChO is in the crystalline form, as revealed by the strong characteristic peaks that do not overlap those from the CER:Ch:FA matrix appearing at 2.05, 2.19 nm^{-1}, Figure 4.3. panel I. These observations hold for both pH values tested. With increasing temperature, these reflections disappear between 43 until 47 ºC, as the isotropic liquid is formed. As in the case of the DSC results, the CER:Ch:FA matrix seems unperturbed by the presence of ChO in the medium; however, components of the lipid matrix act as impurities of the ChO, or at least interact with it sufficiently to lower its transition temperature a few degrees. We conclude that most of the added ChO remains excluded from the CER:Ch:FA matrix at both pH, but there is a possibility that a small fraction of ChO mixes with the other lipids without appreciably changing the WAXS pattern in the region sampled.

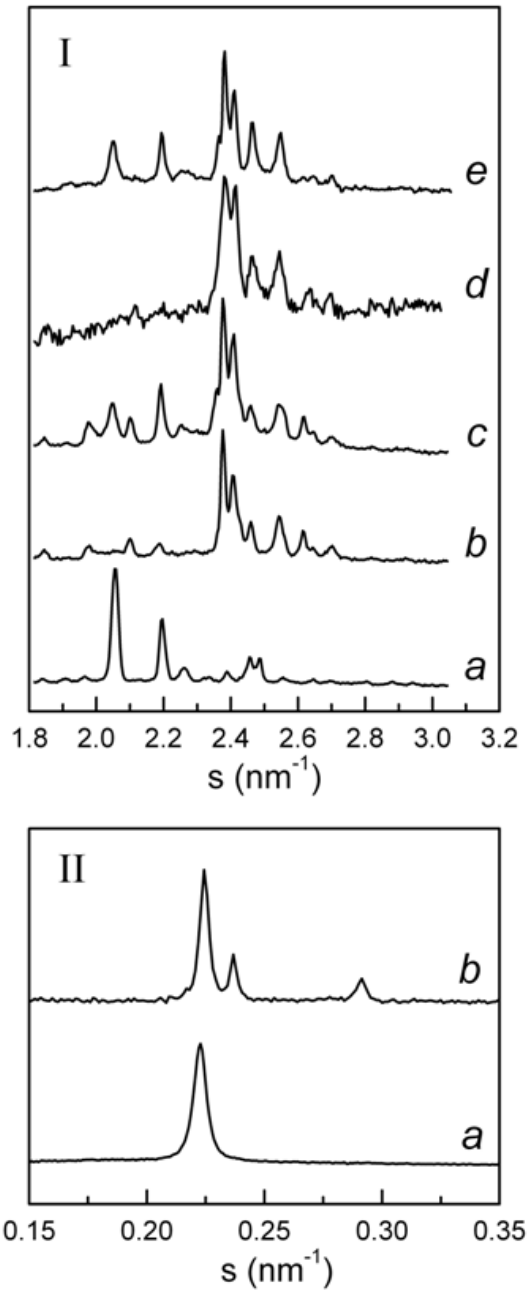

Figure 4.3. - In the panel I is shown the comparison of the wide angle X-ray diffraction patterns of ChO (*a*), CER:Ch:FA matrix at pH = 4.0 (*b*) and 9.0 (*d*) and CER:Ch:FA to which 15 mol% ChO were added at pH = 4.0 (c) and 9.0 (*e*). All the traces displayed were obtained at 20 ºC. In panel II the SAXS of the CER:Ch:FA matrix at pH = 9.0 (*a*) and 4.0 (*b*) at 20 ºC, showing the

single peak at 0.224 nm^{-1}, of the L_C phase at pH = 9.0, and the two new phases at pH = 4.0, one L_C and one L_α respectively at 0.289 and 0.235 nm^{-1}.

The WAXS signal of fluid pure ceramide C16 is compared in Figure 4.4. with those of ChO in the smectic, cholesteric and isotropic liquid forms. The trace of the ceramide, that peaks at 4.6 Å (s = 2.18 nm^{-1}), illustrates the typical fluid bilayer signal with an average chain distance[35] clearly smaller than that obtained for the less tightly packed ChO chains whose diffraction signal peaks at 5.1 Å (s = 1.97 nm^{-1}) irrespective from the liquid form presented by ChO. Therefore, the WAXS signal from liquid ChO is easily distinguished from that of a fluid lipid bilayer. Based on these results we may comment that the ChO found in the analysis of SC cannot be the main responsible for the SC lipid fluid phase signal underlying the WAXS peaks with maximum at 2.2 nm[19] observed in the intact SC.

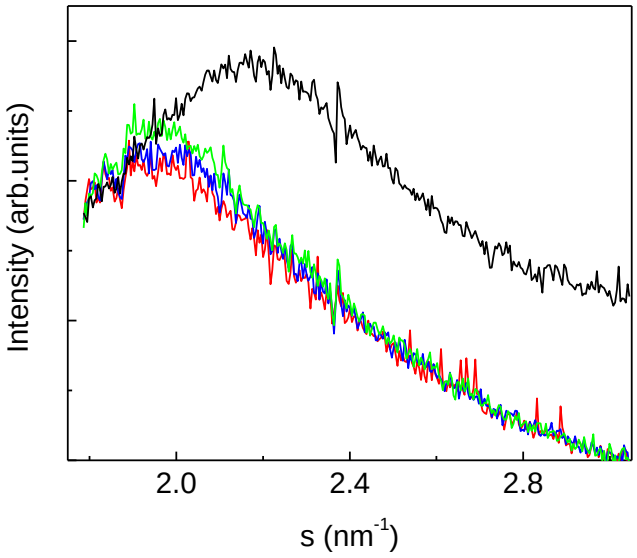

Figure 4.4. – WAXS signal for the fluid phase of pure CER 16 (—) at 98 ºC compared with those for ChO in the smectic (—), cholesteric (—), and liquid isotropic (—) phases at 30, 40 and 56 ºC, respectively.

CER:Ch:FA matrix plus ChO at pH = 4.0 and 9.0 – ^{13}C MAS NMR

In contrast to the preceding biophysical methods ^{13}C NMR spectroscopy provides information about the local environment and mobility of specie carbons, thus serving as a complementary method for our study. Previous ^{13}C NMR studies of the interaction of ^{13}C carbonyl labeled ChO with phospholipid dispersions proved to be able to discriminate the ChO molecules inserted in the bilayer from those coexisting as "pools" of free ChO[36]. The technique takes advantage of the upfield shift observed for the ^{13}C labeled carbonyl group of the ChO once inserted in the bilayer as a result of a folded configuration that exposes the carbonyl group to the water at the bilayer surface[36].

The spectrum of the CER:Ch:FA matrix containing 15 mol % unlabelled ChO at pH = 9.0 (Figure 4.5. trace *a*), reveals the expected peaks from the mobile acyl chain carbons of the constituent lipids, whereas the natural abundant ^{13}C carbonyl peaks from ceramide and palmitic acid are too broad to be seen. It was also verified that the carbonyl of the succinic acid used in the buffer of the samples at pH = 4.0 did not interfere with our measurements (data not shown). The broad peak at 111 ppm is from the Teflon that is used to fill the NMR rotor as explained in the Materials and Methods Section.

Figure 4.5. trace *b* shows the ^{13}C MAS NMR spectrum of the same matrix but with the addition of 4 mol% labeled ChO. The labeled carbonyl is revealed as a broad peak at 171.5 ppm. Upon increasing the temperature to 55 ºC, where the stable form of ChO is the isotropic liquid (Scheme 4.1.) the peak narrowed considerably but did not shift. (Figure 4.5., trace *c*).

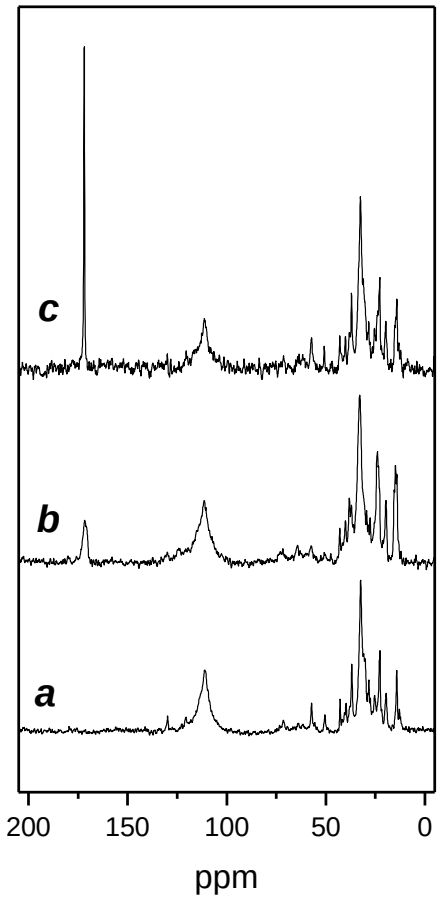

Figure 4.5. – In plots *a* and *b*: ^{13}C MAS NMR spectra at 75.47 MHz of the CER:Ch:FA matrix with 15 mol % unlabelled ChO, trace *a*, and of CER:Ch:FA matrix containing 4 mol % of ^{13}C carbonyl ChO, trace *b*, both in excess water at pH = 9.0. The spectra were acquired at room temperature. Spectra were obtained with a pulse interval of 6.3 s, and 8192 time domain points and processed with 10 Hz line broadening. In plot *c*, ^{13}C MAS NMR spectrum at 75.47 MHz of the previous CER:Ch:FA matrix containing 4 mol% of ^{13}C carbonyl ChO, at pH = 9.0. The spectrum was obtained at 55 ºC, a temperature above the ChO solid to isotropic liquid transition temperature. The instrumental conditions are the same as in plots *a* and *b*, except for the number of scans that was 3000.

When this sample was cooled to room temperature, the original spectrum (Figure 4.5. trace *b*) was replicated in all respects, especially the broad

carbonyl at 171.5 ppm (spectrum not shown). At both temperatures, when the amount of added ChO was increased to 8 mol%, the spectra were identical to those for the 4 mol% sample, except for an increased intensity of the carbonyl peak at 171.5 ppm)

The experiments above described for pH = 9.0 were repeated for the mixtures prepared at pH = 4.0 and 4 mol% labeled ChO and an identical behavior of the labeled ChO peak was observed.

In all spectra with labeled ChO the presence of a single absorption indicates that all ChO is in an identical environment[36]. Furthermore, the temperature dependence of the line width indicates that the ChO is present in a separate phase that melts from an ordered (liquid crystalline phase at room temperature to a disordered (isotropic liquid phase) at 55 ºC. When incorporated into the phosphatidylcholine bilayer[37], the peak intensity of the ChO inserted in the bilayer structure remained constant when the temperature was increased above the crystal to liquid isotropic transition[37]. The chemical shift of 171.5 ppm is significantly upfield from that for ChO incorporated into the liquid crystalline phase of the phospholipid bilayer (171.9), but close to that for phase separated ChO (171.4).

As final evidence for our conclusions above that most or all of the ChO is excluded from the CER:Ch:FA matrix, dry powdered ^{13}C labeled ChO was added *a posteriori* to the suspension of CER:Ch:FA containing 4 mol% ChO prepared in the usual way. Given the usual very slow kinetics of exchange of water-insoluble lipids between aggregates[38,39] this *a posteriori* added powdered ^{13}C labeled ChO would remain phase separated outside the CER:Ch:FA matrix in the course of the NMR experiment. The resulting ^{13}C spectrum was identical to previous spectra at room temperature, and heating to 55 ºC produced a single sharp peak as in Figure 4.5., trace *c*.

Further comments on the experimental results

It is to be noted that the CER:Ch:FA matrix at pH = 9.0 undergoes a congruent transition from an L_C to an H_{II} phase at 89 ºC (81 ºC with egg ceramide) easily observable and identified by X-ray[41]. Any departure from the 44:38:18 composition of the CER:Ch:FA matrix results in a more complex X-ray pattern due to other phases being present. This explains why in our samples one single endotherm is observed in DSC peaking at 81 ºC, allowing the identification of the separated ChO transition. The scenario is not so simple at pH = 4.0 where at low temperature two lamellar crystalline phases, one of nearly pure C16-Cer and other of CER:Ch, coexist with a liquid crystalline phase, which gives rise to a much more complex sequence of thermotropic events not allowing a straight conclusion about the presence of free ChO from DSC. However, the presence of 15 mol% of ChO does not affect neither the diffractions nor their thermotropic behavior.

It can be objected that it is very different to adjoin the ChO after *lamellae* formation, what will happen if ChO is originated in the sebum[13], or having it mixed since SC genesis[12,14]. Because of the known difficulty in adding new components to the already formed CER:Ch:FA structure sebum ChO will be much more difficult to be incorporated. Our solubility tests were done for the more unfavorable case by freeze-drying the samples with ChO already mixed with the remaining lipids.

Our experimental approach leave no doubt that ChO is excluded from the CER:Ch:FA matrix remaining in the system as a separated independent phase. However, a minor fraction of ChO is necessarily incorporated in the lipid matrix as a minor impurity, which is too small to be detectable by the methods used. The non-incorporated ChO is free in the system but is part of a chain of two equilibria: that of the partition to water (its water solubility), and the partition of the compound molecularly dispersed in water to the aggregate[40]. A more inclusive analysis of the solubility of ChO in the

CER:Ch:FA matrix could be done by the determination of those two equilibrium constants. However, pure ChO may be present in several metastable aggregated forms and is very insoluble in water making the solubility determination a quite difficult task. Moreover, it is technically difficult to obtain a partition constant between ChO in water and "dissolved" in the structures of the CER:Ch:FA matrix. A further difficulty is the slow kinetics expected for the incorporation of external molecules in the rigid ceramide structures making uncertain when the equilibrium is attained. All these limitations make this more educated approach unpractical, and overkill in view of our objectives.

4.5. Conclusions

In this work, we made a comprehensive analysis of the solubility of ChO in a particular mixture of ceramide C16, cholesterol and palmitic acid. Cholesteryl oleate was chosen to model of the class of the esters of cholesterol that exists in natural biological systems, and the mixture of ceramide, cholesterol and fatty acid as an attempt to model of the SC lipid composition. In previous works, other authors have shown that ChO miscibility with saturated and unsaturated phosphocholines and sphingomyelin is very low or negligible, the same occurring when those lipids are mixed with cholesterol[2,4,3].

In the DSC experiments, addition of 15 mol% ChO to CER:Ch:FA gave no detectable change in the thermotropic transitions of the CER:Ch:FA matrix, which measure the lipid bilayer organization at pH = 9.0. Simultaneous small and wide angle X-ray diffraction revealed no new molecular arrangements or structural distortion in samples at pH = 4.0 and 9.0 and temperatures between 20 to 98 ºC. ^{13}C-NMR permitted focus on the ChO and definitively showed that the environment of ChO was identical in the presence or absence of the CER:Ch:FA matrix. Moreover, the increase in the intensity of the ChO ^{13}C

carbonyl signal above the liquid crystalline to isotropic liquid transition temperature that is characteristic of pure ChO is observed in the mixtures.

All evidence taken together we conclude that the solubility of ChO in the CER:Ch:FA matrix under study is negligible at least until the main transition for a totally fluid phase that takes place well above the physiological temperature. The solubility is negligible at pH = 9.0, at which one single L_C phase is present. At pH = 4.0 where three phases are observed, one L_C of pure C16-Cer, another, also L_C, of C16-Cer:Ch, and an L_α that contains a mixture of C16-Cer, Ch and FA, ChO does not interact with the remaining lipids which means that it is insoluble in each of the three phases. Despite limitations that may be cited concerning the adequacy of our system to model the lipidic matrix of the *stratum corneum*, it seems very improbable that ChO is soluble in the *in vivo* structure.

The high concentrations of ChO determined by some authors[10-12] is evidence for its chemical presence in direct contact with the SC, whatever its origin. Either being part of the SC or penetrating *a posteriori* it will reside as a separated fluid phase in the *stratum corneum*. In this case, it could contribute to, but not being the principal origin of the fluid signal observed in the intact *stratum corneum*.

4.6. Acknowledgments

This work was financially supported by FCT – Fundação para a Ciência e Tecnologia, Portugal PTDC/QUI/68242/2006 and project II-20060163 EC from HASYLAB of DESY (Germany). S.L.S. is indebted to FCT, Portugal for Grant BD/6482/2001.

4.7. References

(1) Small, D.M. (1988). Duff,George,Lyman Memorial Lecture - progression and regression of atherosclerotic lesions - insights from lipid physical biochemistry. *Arteriosclerosis*, 8, 103-129.

(2) Janiak, M.J., Small, D.M., Shipley, G.G. (1979). Interactions of cholesterol esters with phospholipids - cholesteryl myristate and dimyristoyl lecithin. *J. Lipid Res.*, 20, 183-199.

(3) Salmon, A., Hamilton, J.A. (1995). Magic-angle spinning and solution C-13 nuclear magnetic resonance studies of medium- and long-chain cholesteryl esters in model bilayers. *Biochemistry*, 34, 16065-16073.

(4) Mackay, A.L., Wassall, S.R., Valic, M.I., Gorrissen, H., Cushley, R.J. (1980). H-2 and P-31-NMR studies of cholesteryl palmitate in sphingomyelin dispersions. *Biochim. Biophys. Acta*, 601, 22-33.

(5) Spooner, P.J.R., Hamilton, J.A., Gantz, D.L., Small, D.M. (1986). The effect of free-cholesterol on the solubilization of cholesteryl oleate in phosphatidylcholine bilayers - a C-13-NMR study. *Biochim. Biophys. Acta*, 860, 345-353.

(6) Wertz, P.W., Norlén, L.P.O. (2004). "Confidence intervals" for the "true" lipid composition of the human skin barrier? In Skin, Hair, and Nails. Forslind, B., Lindberg, M., Eds., Marcel Dekker, New York, pp. 85-106.

(7) Shah, J., Atienza, J.M., Duclos, R.I., Rawlings, A.V., Dong, Z.X., Shipley, G.G. (1995). Structural and thermotropic properties of synthetic C16-0 (palmitoyl) ceramide - Effect of hydration. *J. Lipid Res.*, 36, 1936-1944.

(8) Souza, S.L., Capitan, M.J., Alvarez, J., Funari, S.S., Lameiro, M.H., Melo, E. (2009). Phase behavior of aqueous dispersions of mixtures of N-palmitoyl

ceramide and cholesterol: a lipid system with ceramide-cholesterol crystalline lamellar phases. *J. Phys. Chem. B*, 113, 1367-1375.

(9) Huang, J.Y., Buboltz, J.T., Feigenson, G.W. (1999). Maximum solubility of cholesterol in phosphatidylcholine and phosphatidylethanolamine bilayers. *Biochim. Biophys. Acta*, 1417, 89-100.

(10) Bonte, F., Saunois, A., Pinguet, P., Meybeck, A. (1997). Existence of a lipid gradient in the upper *stratum corneum* and its possible biological significance. *Archives of Dermatological Research*, 289, 78-82.

(11) Norlen, L., Nicander, I., Rozell, B.L., Ollmar, S., Forslind, B. (1999). Inter- and intra-individual differences in human *stratum corneum* lipid content related to physical parameters of skin barrier function *in vivo*. *J. Invest. Dermatol.*, 112, 72-77.

(12) Wertz, P.W., Swartzendruber, D.C., Kathi, C.M., Downing, D.T. (1987). Composition and morphology of epidermal cyst lipids. *J. Invest. Dermatol.*, 89, 419-424.

(13) Elias, P.M. (2005). *Stratum corneum* defensive functions: an integrated view. *J. Invest. Dermatol.*, 125, 183-200.

(14) Pappinen, S., Hermansson, M., Kuntsche, J., Somerharju, P., Wertz, P., Urtti, A., Suhonen, M. (2008). Comparison of rat epidermal keratinocyte organotypic culture (ROC) with intact human skin: lipid composition and thermal phase behavior of the *stratum corneum*. *Biochim. Biophys. Acta*, 1778, 824-834.

(15) Kessner, D., Ruettinger, A., Kiselev, M.A., Wartewig, S., Neubert, R.H.H. (2008). Properties of ceramides and their impact on the *stratum corneum* structure: a review - part 2: *stratum corneum* lipid model systems. *Skin Pharmacol. and Physiol.*, 21, 58-74.

(16) Bouwstra, J.A., Gooris, G.S., Vanderspek, J.A., Bras, W. (1991). Structural investigations of human *stratum-corneum* by small-angle X-ray-scattering. *J. Invest. Dermatol.*, 97, 1005-1012.

(17) Elias, P.M. (1991). Epidermal barrier function - intercellular lamellar lipid structures, origin, composition and metabolism. *J. Control. Rel.*, 15, 199-208.

(18) Swartzendruber, D.C., Wertz, P.W., Kitko, D.J., Madison, K.C., Downing, D.T. (1989). Molecular-models of the intercellular lipid *lamellae* in mammalian *stratum-corneum*. *J. Invest. Dermatol.*, 92, 251-257.

(19) White, S.H., Mirejovsky, D., King, G.I. (1988). Structure of lamellar lipid domains and corneocyte envelopes of murine *stratum-corneum* - an X-ray-diffraction study. *Biochemistry*, 27, 3725-3732.

(20) Janssens, M., Gooris, G.S., Boowstra, J.A. (2009). Infrared spectroscopy studies of mixtures prepared with synthetic ceramides varying in head group architecture: coexistence of liquid and crystalline phases. *Biochim. Biophys. Acta*, 1788, 732-742.

(21) Chen, H.C., Mendelsohn, R., Rerek, M.E., Moore, D.J. (2000). Fourier transform infrared spectroscopy and differential scanning calorimetry studies of fatty acid homogeneous ceramide 2. *Biochim. Biophys. Acta*, 1468, 293-303.

(22) Chen, X., Kwak, S.J., Lafleur, M., Bloom, M., Kitson, N., Thewalt, J. (2007). Fatty acids influence "solid" phase formation in models of *stratum corneum* intercellular membranes. *Langmuir*, 23, 5548-5556.

(23) Bouwstra, J.A., Thewalt, J., Gooris, G.S., Kitson, N. (1997). A model membrane approach to the epidermal permeability barrier: an X-ray diffraction study. *Biochemistry*, 36, 7717-7725.

(24) Brief, E., Kwak, S., Cheng, J.T.J., Kitson, N., Thewalt, J., Lafleur, M. (2009). Phase behavior of an equimolar mixture of N-palmitoyl-D-*erythro*-sphingosine, cholesterol, and palmitic acid, a mixture with optimized hydrophobic matching. *Langmuir,* 25, 7523-7532.

(25) Sripada, P.K. (1988). Synthesis of single-C-13-labeled and double-C-13-labeled cholesterol oleate. *Chem. Phys. Lipids*, 48, 147-151.

(26) De Paepe, K., Weerheim, A., Houben, E., Roseeuw, D., Ponec, M., Rogiers, V. (2004). Analysis of epidermal lipids of the healthy human skin: factors affecting the design of a control population. *Skin Pharmacol. Physiol.*, 17, 23-30.

(27) Merle, C., Laugel, C., Chaminade, P., Baillet-Guffroy, A. (2010). Quantitative study of the *stratum corneum* lipid classes by normal phase liquid chromatography: comparison between two universal detectors. *J. Liquid Chromatogr. Relat. Technol.*, 33, 629-644.

(28) Lafleur, M. (1998). Phase behavior of model *stratum corneum* lipid mixtures: an infrared spectroscopy investigation. *Can. J. Chem.*, 76, 1501-1511.

(29) Rerek, M.E., Chen, H.C., Markovic, B., van Wyck, D., Garidel, P., Mendelsohn, R., Moore, D.J. (2001). Phytosphingosine and sphingosine ceramide headgroup hydrogen bonding: structural insights through thermotropic hydrogen/deuterium exchange. *J. Phys. Chem. B*, 105, 9355-9362.

(30) Holopainen, J.M., Lemmich, J., Richter, F., Mouritsen, O.G., Rapp, G., Kinnunen, P.K.J. (2000). Dimyristoylphosphatidylcholine/C16:0-ceramide binary liposomes studied by differential scanning calorimetry and wide- and small-angle X-ray scattering. *Biophys. J.*, 78, 2459-2469.

(31) Funari, S.S., Barcelo, F., Escriba, P.V. (2003). Effects of oleic acid and its congeners, elaidic and stearic acids, on the structural properties of phosphatidylethanolamine membranes. *J. Lipid Res.*, 44, 567-575.

(32) Small, D.M. (1970). The physical state of lipids of biological importance: cholesterol esters, cholesterol, triglyceride. In Surface chemistry of biological systems. Blank, M., Ed., Plenum Press, New York, pp. 55-84.

(33) Small, D.M. (1986). Handbook of lipid research. The physical chemistry of lipids, vol.4., Plenum Press, New York, pp. 395-473.

(34) Ginsburg, G.S., Small, D.M. (1981). Physical-properties of cholesteryl esters having 20 carbons or more. *Biochim. Biophys. Acta*, 664, 98-107.

(35) Small, D.M. (1986). Handbook of lipid research. The physical chemistry of lipids, vol. 4, Plenum Press, New York, pp. 475-522.

(36) Hamilton, J.A., Small, D.M. (1982). Solubilization and localization of cholesteryl oleate in egg phosphatidylcholine vesicles - a C-13 NMR-study. *J. Biol. Chem.*, 257, 7318-7321.

(37) Hamilton, J.A., Fujito, D.T., Hammer, C.F. (1991). Solubilization and localization of weakly polar lipids in unsonicated egg phosphatidylcholine - a C-13 MAS NMR-study. *Biochemistry,* 30, 2894-2902.

(38) Estronca, L.M.B.B., Moreno, M.J., Vaz, W.L.C. (2007). Kinetics and thermodynamics of the association of dehydroergosterol with lipid bilayer membranes. *Biophys. J.*, 93, 4244-4253.

(39) Feigenson, G.W. (1997). Partitioning of a fluorescent phospholipid between fluid bilayers: dependence on host lipid acyl chains. *Biophys. J.*, 73, 3112-3121.

(40) Melo, E., Freitas, A.A., Chang, Y.W., Quina, F.H. (2001). On the significance of the solubilization power of detergents. *Langmuir*, 17, 7980-7981.

(41) Souza, S.L., Valério, J., Funari, S.S., Melo, E. (2011). The thermotropism and prototropism of ternary mixtures of ceramide C16, cholesterol and palmitic acid. An exploratory study. *Chem. Phys. Lipids*, 164, 643-653.

5. Final Discussion

The work presented concentrates in the study of the physical-chemical properties, with particular attention to the structural characterization of the aggregates formed by N-palmitoyl-D-*erythro*-sphingosine (C16-Cer), a synthetic N-sphingosyl ceramide, and of its mixtures with cholesterol (Ch), palmitic acid (PA), and Cholesteryl Oleate (ChO).

In our studies, we have observed that both C16-Cer, and their mixtures with cholesterol, palmitic acid and cholesteryl oleate, are systems prone to become trapped in metastable states. Other authors had previously reported this behavior and some of them advocate the need of stabilization periods of the order of few months[1]. Consequently, a careful heating, cooling protocol has to be used in the preparation of C16-Cer and their mixtures to achieve the equilibrium state for subsequent characterization studies. We determined that after hydration above the C16-Cer main phase transition, a cooling rate of 1ºC/min was slow enough to achieve the equilibrium state, or at least a state without evidence of metastability.

When C16-Cer was prepared in excess water, at 20 ºC it was arranged in a lamellar crystalline (L_C) state, with a lamellar repeat distance of 4.46 nm. Several reflections in the wide angle region were detected, that could be fitted in a hexagonal lattice with $a = b = 4.87$ Å and $c = 45.5$ Å. The wide angle information was insufficient to permit an unequivocal deduction of the lattice, and an acceptable fit could also be obtained for an orthorhombic lattice with $a = 4.22$ Å, $b = 3.93$ Å, $c = 45.5$ Å, with $\alpha = \beta = \gamma = 90^o$. Consequently, the C16-Cer phase is in a perpendicular chain arrangement. With the increase of temperature, a main phase transition was observed at $T_m = 93$ ºC, with a $\Delta H^o = 71.9$ KJ.mol^{-1}. The X-ray profile of the C16-Cer melted phase showed a very broad small angle X-ray diffraction band located at 0.317 nm^{-1} (3.15 nm), associated with a broad wide angle band centered at 2.2 nm^{-1} (0.45 nm), characteristic of stacked melted hydrocarbon chains. The melted C16-Cer

does not maintain the typical lamellar structure, even if some meso-order still exists. During subsequent cooling, a thin fluid structure with a lamellar repeat distance of 3.42 nm was detected at 82 ºC, before conversion to the low temperature C16-Cer L_C phase, and the question remains if this is not the stable lamellar arrangement of the L_α structure.

A possible direction for future work could be the test of the hypothesis that N-sphingosyl ceramides are arranged in an extended conformation. This arrangement has been observed for phytosphingosine ceramides[2,3], even when those ceramides were prepared in the presence of water[4]. Furthermore, this packing form is able to explain the interlamellar repeat distance of 4.46 nm detected in our C16-Cer mesophases. It also explains the quite small lamellar repeat distance of 3.15 nm observed for a lamellar fluid phase of C16-Cer detected when cooling the sample from 98 ºC, if we consider that the C16-Cer molecules are packed in an extended conformation with interpenetrated chains. If this hypothesis is correct, water is not present between the several *lamellae*, and the C16-Cer mesophases we used are not hydrated, a hypothesis we have raised along the presented work. It is suggested that the molecular packing of C16-Cer is obtained by single crystal studies, in order to establish if an extended conformation is observed for N-sphingosyl ceramides. Also, the absence or presence of water between the *lamellae* of C16-Cer after the hydration step should be verified.

Below the main phase transition temperature, N-sphingosyl ceramides adopt the lamellar crystalline state, in contrast with the majority of other double chain amphiphilic lipids that adopt a lamellar gel state (L_β).The crystallinity and the considerably higher transition temperatures of the N-sphingosyl ceramides can be rationalized as the result of stronger head-group interactions. In fact, the amide head-group of N-sphingosyl ceramide mesophases, establish strong H-bonds as become evident by FTIR studies[5,6]. In addition, N-sphingosyne ceramide head-groups have a much smaller dipole moment compared to phosphatidylcholines, reducing their headgroup repulsions. The calculated

dipolar moment for N-sphingosyl ceramide was ca. 2.5 Debye, whereas glycerol-3-phosphocholine head-groups gave a dipolar moment of ca. 17 Debye.

Several mixtures of C16-Cer with cholesterol, in all the relative molar proportions were characterized and the correspondent binary phase diagram in excess water derived, refer to Figure 2.5, pg. 86. From the phase-diagram, it became clear that cholesterol is only residually miscible with ceramide in the solid state, in the sense of the formation of a random dispersion of the components, instead forming mixed crystalline compounds with ceramide. The diagram obtained was of the eutectic type for molar fractions of C16-Cer above 40 mol %. While studying the mixtures to derive the phase diagram, we detected by powder pattern X-ray diffraction, two crystalline compounds of ceramide and cholesterol. One with lamellar repeat distance of 3.50 nm and an estimated C16-cer:Ch molar ratio of 2:3, compatible with a tetragonal lattice $a = b = 6.96$ Å, $c = 35.6$ Å and $\alpha = \beta = \gamma = 90^{o}$. A second structure with a lamellar repeat distance of 4.24 nm, and an estimated C16-Cer:Cholesterol molar ratio of 1:3 was also detected. For this compound, the wide angle X-ray diffraction peaks did not allow the deduction of the correspondent lattice. To the best of our knowledge, this is the first direct experimental evidence of the existence of laterally organized stoichiometric aggregates with amphiphilic lipid bilayer forming lipids and cholesterol. Crystalline compounds of ceramide and cholesterol, have previously, been observed in monolayers[7]. This finding reopens the controversy about the existence of organized clusters induced by cholesterol, known as “cholesterol-lipid condensed complexes” in lipid bilayers. Some authors propose the formation of reversible “complexes”, of phospholipids with cholesterol. Others reject this hypothesis, explaining the physical-chemical properties and structural organization of phospholipids-cholesterol mixtures in alternative ways. The identification of stoichiometric aggregate structures of ceramide and cholesterol also strengthens the

proposal of the existence of laterally segregated domains of ceramide in the cell membrane, named “ceramide-rich domains”[8].

In a subsequent study, we added palmitic acid to a mixture of C16-Cer and cholesterol in excess water, and studied the thermotropic and prototropic behavior of a set of ternary mixtures, but not to a detail of a phase diagram. The purpose was to explore the phase transitions, and the main phases, refer to Figure 3.7, pg. 122 and Figure 3.8, pg. 126 that condense our main observations. For the mixtures at pH ≤ 7.0, and for the molar composition of C16-Cer:Ch:PA of 44:38:18, a coexistence of lamellar crystalline phases with liquid lamellar phases was observed at 20 ºC. When intact *stratum corneum* is characterized by powder pattern X-ray diffraction, reflections with origin in both crystalline and lamellar fluid lipid arrangements are detected[9]. Ceramides and their mixtures form crystalline phases, but the question about the origin of the *stratum corneum* (SC) fluid lipid phase remains open. The knowledge of the origin of this fluid phase is important both for the fundamental understanding of the structure of the SC lipid matrix, and the design of enhancer strategies for drug delivery systems through the skin. In fact substances would tend to permeate the skin through fluid regions. Our simple ternary model, at pHs values similar to the physiologic, also contains coexisting crystalline and liquid lamellar phases. Despite the divergences that can be raised concerning our simple mixture with intact *stratum corneum* lipid matrix, the coexistence of crystalline and fluid phases at physiological pH values can be a characteristic of ternary mixtures composed of ceramide, cholesterol and long chain fatty acids.

At pH = 9.0, the formation of an inverted hexagonal phase was observed for some mixtures. This contrast with the behavior of the mixtures that were totally or partially neutralized, in which melting of the low temperature phases always originated fluid lamellar phases. For the mixtures with the molar composition of C16-Cer:Ch:PA of 44:38:18 at pH ≤ 7.0, the liquid lamellar phase/s gave origin at higher temperatures to a isotropic fluid. The formation of inverted hexagonal

phases seems to be characteristic of mixtures of ceramide, cholesterol and fatty acid at high temperatures, as other authors have previously detected such structures in this type of mixtures[10,11,12]. Although long chain fatty acids are known to induce inverted hexagonal phases in phosphatidylcholine bilayers[13], our mixtures contain in addition to the ceramide, cholesterol, and therefore we cannot at this moment rationalize this observation.

In the ternary systems studied, palmitic acid was found to be soluble at least until 60 mol % in the ceramide, cholesterol mixtures at pH = 9.0, whereas segregated co-existing neutral PA could be detected for the samples containing already 18 mol % of the acid, when the mixtures were prepared at pH = 4.0.

The ternary mixture with molar composition of C16-Cer:Ch:PA of 44:38:18 at pH = 9.0 showed by DSC, one unique phase transition, relatively narrow, and symmetric, typical of a pure substance. The X-ray characterization of this mixture confirmed the organization in a single phase at 20 ºC that melted at 88-90 ºC, to a single fluid inverted hexagonal phase. We interpreted these experimental results, together with other lines of evidence, as suggesting that this specific ternary mixture forms a stoichiometric aggregate. The attributed stoichiometry would be C16-$Cer_5Ch_4PA_2$. The lamellar repeat distance of this compound was 4.46 nm, identical to the lamellar repeat distance of pure C16-Cer, and with the experimental detection conditions used, the wide angle reflections observed for the ternary mixture, were identical to several reflections of C16-Cer. It should also be noted that the lamellar repeat distance of the ternary compound is invariable with pH which is hard to understand except if these layers do not include water. However, we are not able with just the present data to give a complete explanation of this invariability.

Ceramides seem to be prone to form stoichiometric aggregates. It might be interesting to understand the physical reasons that determine this behavior. A possible approach can be the study and determination of additional phase

diagrams of other ceramide types, with a different head-group architecture - number and position of hydroxylations - and acyl chain length with cholesterol. Note however that, the detection of several ceramide stoichiometric aggregates can be simply the result of the preference for the adoption of the L_C state by ceramides and their mixtures at room temperature, in contrast with other more well characterized amphiphilic lipids such as phosphatidylcholines, that frequently remain trapped in the rigid L_{β}' state. In fact, it is possible that compound structures are also abundant in mixtures of phosphatidylcholines with other lipids, but have never been detected due to the difficulties to attain the L_C state.

Having characterized the phases that compose the system of C16-Cer, cholesterol, palmitic acid in the same molar proportions reported for the *stratum corneum* lipid matrix, we tested in this simple mixture, the solubility of cholesteryl oleate at both full ionization, pH = 9.0, and full protonation, pH = 4.0. It is known that the miscibility of cholesteryl esters with both saturated and unsaturated phosphatidylcholines, and sphingomyelin is reduced or negligible. This immiscibility is also observed when these systems include cholesterol[14,15,16]. With the combination of several techniques such as DSC, powder pattern small and wide angle X-ray diffraction, and magic angle spinning ^{13}C NMR, it was established that the solubility of ChO in the C16-Cer:Ch:PA mixture was negligible in all the system phases at both pH values. From the previous characterization of the C16-Cer, cholesterol, palmitic acid ternary system, no additional phases were found at intermediate pH values. We can therefore conclude that ChO is insoluble in the C16-Cer:Ch:PA mixture at all the pHs values that range from 9.0 to 4.0.

It was also observed in the mixtures, that part of the segregated cholesteryl ester remained in the fluid state at physiological temperatures. Nevertheless, the wide angle reflection of fluid cholesteryl oleate was not identical to the reflection of fluid lipid in intact *stratum corneum*. With the appropriate reserves in which concerns extrapolation of information obtained with our model mixture

to intact *stratum corneum*, we can suggest that ChO is not the principal origin of the fluid lipid signal observed in this tissue.

We hope that the effort made represents a valid contribution to a more systematized study of the physical-chemical properties of the mesophases formed by ceramides and their mixtures.

5.1. References

(1) Brief, E., Kwak, S., Cheng, J.T.J., Kitson, N., Thewalt, J., Lafleur, M. (2009). Phase behavior of an equimolar mixture of *N*-Palmitoyl-D-*erythro*-sphingosine, cholesterol, and palmitic acid, a mixture with optimized hydrophobic matching. *Langmuir*, 25, 7523-7532.

(2) Dahlén, B., Pascher, I. (1972). Molecular arrangements in sphingolipids: crystal structure of N-Tetracosanoylphytosphingosine. *Acta Crystallogr. B*, 28, 2396-2404.

(3) Pascher, I., Sundell, S. (1992). Molecular arrangements in sphingolipids: crystal structure of the ceramide N-(2D,3D-dihydroxyoctadecanoyl)-phytosphingosine. *Chem. Phys. Lipids*, 61, 79-86.

(4) Raudenkolb, S., Wartewig, S., Neubert, R.H.H. (2003). Polymorphism of ceramide 3. Part 2: a vibrational spectroscopic and X-ray powder diffraction investigation of N-octadecanoyl phytosphingosine and the analogous specifically deuterated d35 derivative. *Chem. Phys. Lipids*, 124, 89-101.

(5) Rerek, M., Chen, H.C., Markon, C.B., van Wych, D., Garidel, P., Mendelsohn, R., Moore, D.J. (2001). Phytosphingosine and sphingosine ceramide headgroup hydrogen bonding: Structural insights through thermotropic hydrogen/deuterium exchange. *J. Phys. Chem. B*, 105, 9355-9362.

(6) Moore, D., Rerek, M., Mendelsohn, R. (1997). FTIR spectroscopy studies of the conformational order and phase behaviour of ceramides. *J. Phys. Chem. B*, 101, 8933-8940.

(7) Scheffer, L., Solomonor, I., Weygand, M.J., Kjaer, K., Leiserowitz, L., Addedi, L. (2005). Structure of cholesterol/ceramide monolayer mixtures: implications to the molecular organization of lipid rafts. *Biophys. J.*, 88, 3381-3391.

(8) Stancevic, B., Kolesnick, R. (2010). Ceramide-rich platforms in transmembrane signaling. *FEBS Letters.*, 584, 1728-1740.

(9) White, S., Mirejovsky, D., King, G. (1988). Structure of lamellar lipid domains and corneocyte envelopes of murine *stratum-corneum* – an X-ray-diffraction study. *Biochemistry*, 27, 3725-3732.

(10) Kitson, N., Thewalt, J., Lafleur, M., Bloom, M. (1994). A model membrane approach to the epidermal permeability barrier. *Biochemistry*, 33, 6707-6715**.**

(11) Bouwstra, J.A., Gooris, G.S., Dubbelaar, F.E.R., Ponec, M. (2000). Phase behavior of skin barrier model membranes at pH 7.4. *Cell. Mol. Biol.*, 46, 979-992**.**

(12) Abraham, W., Downing, D. (1991). Deuterium NMR investigation of polymorphism in *stratum-corneum* lipids. *Biochim. Biophys. Acta*, 1068, 189-194.

(13) Koynova, R., Tenchov, B. (2001). Interactions of surfactants and fatty acids with lipids. *Curr. Opin. Colloi Interface Sci.*, 6, 277-286.

(14) Janiak, M., Small, D., Shipley, G. (1979). Interactions of cholesterol esters with phospholipids – cholesteryl myristate and dimyristoyl lecithin. *J. Lipid Res.*, 20, 183-199.

(15) Mackay, A.L., Wassall, S.R., Valic, M.I., Gorrissen, H., Cushley, R.J. (1980). H-2 and P-31-NMR studies of cholesteryl palmitate in sphingomyelin dispersions. *Biochim. Biophys. Acta*, 601, 22-33.

(16) Salmon, A., Hamilton, J. (1995). Magic-angle spinning and solution C-13 nuclear magnetic resonance studies of medium- and long-chain cholesteryl esters in model bilayers. *Biochemistry*, 34, 16065-16073.